DESIGN GUIDELINES TO PREVENT DOWNDRAUGHT

Effective measures to assure thermal comfort near glass façades

Suzan Timmers

Graduation Project - Part II

Photograph cover: S. Timmers

DESIGN GUIDELINES TO PREVENT DOWNDRAUGHT

Course:	7SS37 Graduation Project
Name:	Suzan Timmers
Student ID:	0589484
Chairman:	prof.dr.ir. J.L.M. Hensen
Supervisor:	dr.ir. M.G.L.C. Loomans ir. E.S.M. Nelissen ir. L. Schellen
Department:	Physics of the Built Environment Department of Architecture, Building and Planning Eindhoven University of Technology
Date:	May 23th , 2011

Preface

The report in front of you is to finish my graduation project of the Mastertrack “Physics of the Built Environment” at the Eindhoven University of Technology.

More than one year ago, Elphi Nelissen told me about her assumption that because of fear for downdraught energy could be wasted. This immediately took my attention, and together with PhD-research of Lisje Schellen about thermal comfort in non-uniform environments I could create and interesting graduation project. Looking back, it was an ambitious project in which many (new) things are learned. The project contained amongst others, a literature study, measurements, statistical processing, simulations with Matlab, CFD-simulations, and writing reports. Also different engineering agencies showed their interest and I was able to join the KenWIB project (Kenniscluster Energieneutraal Wonen in Brainport). Time was always the challenging factor in this project, but in the end I’m pleased with this result, although many more research related to downdraught is possible.

I also want to thank a lot of people that supervised and helped me. First I want to thank my committee, consisting of prof.dr.ir. J.L.M. Hensen, dr.ir. M.G.L.C. Loomans, dr.ir. W.D. van MarkenLichtenbelt, ir. L. Schellen, and ir. E.S.M. Nelissen.
Also the staff members of the laboratory of the unit BPS need to be thanked for their help during the measurements: ing. J. Diepens, G. Maas, W. van Bommel, H. Smulders, P. Cappon, and ing. M. van Aarle. Special thanks go to dr.ir. P. Steskens for teaching the first CFD skills and to B. Kingma MSc. for improving the program ThermoSEM again and again.
During this project I got the support of the KenWIB project. Prof.dr.ir. W.F. Schaefer let me participate in the project, in which I was also able to organize a studytrip to Freiburg with other students and business people. I want to thank KenWIB and dr.ir. E. Blokhuis, especially for the experimental subject payment.
Gratitude also goes to all experimental subjects that participated in this research. Without them, the project was impossible. So, thank you Alexander, Bart, Dolf, Joris, Loek, Marco, Maurice, Patrick, Ruben, Tom, and William!
And of course all other people that are involved in this graduation research and have been of importance are thanked this way.

Suzan Timmers
May, 2011

Summary

Consulting engineers are in search for applicable design guidelines to prevent downdraught in new-built and renovated buildings. Downdraught is the air flow close to a cold surface, resulting from density differences between warm and cold air (buoyancy forces). Assuming a conservative design in practice, there is a possibility of wasting materials and energy. Next to that, it is difficult or even impossible to predict the airflow in a room due to downdraught. The same counts for assessing such a non-uniform environment in terms of thermal comfort.

As a result, the focus in this research is on downdraught and effective measures to assure thermal comfort near glass façades. The project starts with a literature study related to downdraught. After that, measurements are done in the climate chamber at the TU/e to calibrate a CFD model. With experimental subject measurements relevant thermal comfort models are validated. Subsequently, variants are simulated with the calibrated CFD model and assessed by a thermal comfort model. In the end, a start is made on composing design guidelines.

The main research questions in this project are:

1. What is the definition of downdraught?
2. How can thermal comfort in relation to downdraught be predicted correctly?
3. What are possible design guidelines to predict downdraught?

Based on the results, the following overall conclusion can be drawn. No problems regarding downdraught (natural convection from a cold vertical surface) exist in a standard office, based on the experimental subject results. By not fearing downdraught, energy and materials can be saved in the built environment (such as dwellings). However, with calibrated CFD simulations it turned out that an increased floor temperature can worsen the occurring downdraught (increased air velocity). This indicates that radiators or convectors cannot simply be replaced by floor heating to prevent downdraught.
The outcome of the PMV model corresponds to the thermal sensation votes of the subjects. ISO 7730 is found best to assess downdraught situations, where the rule of thumb to prevent downdraught is very conservative. More research is needed to find the thermal comfort limit (i.e. maximum air velocity combined with radiation asymmetry) to compose design guidelines. Important parameters for the guidelines are window height, temperature difference between the window and indoor air, and floor temperature. To compose more extended design guidelines more simulation variants are still needed.

Samenvatting

Adviseurs zijn op zoek naar geschikte ontwerprichtlijnen om koudeval te voorkomen, zowel in nieuwbouw als bij renovaties. Koudeval is de luchtstroming bij een koud vlak die ontstaat door dichtheidsverschillen tussen warme en koude lucht. De mogelijkheid bestaat dat in de praktijk materiaal en energie verspild worden, uitgaande van conservatief ontwerp uit angst voor koudeval. Daarnaast is het moeilijk om de luchtstroming t.g.v. koudeval te voorspellen. Hetzelfde geldt voor het thermisch comfort van een dergelijk niet-uniforme omgeving.

De focus in dit project ligt dus op koudeval en maatregelen om thermisch comfort nabij de gevel te garanderen. Het project is gestart met een literatuur studie. Daarna zijn er metingen verricht in de klimaatkamer om een CFD model te kalibreren. Met proefpersoonmetingen zijn de relevante thermische comfortmodellen gevalideerd. Vervolgens zijn enkele varianten gesimuleerd met het gekalibreerde model en beoordeeld door een thermisch comfortmodel. Uiteindelijk is een start gemaakt met het samenstellen van ontwerprichtlijnen.

De drie hoofdonderzoeksvragen in dit project zijn:

1. Wat is de definitie van koudeval?
2. Hoe kan thermisch comfort in relatie tot koudeval correct voorspeld worden?
3. Wat zijn mogelijke ontwerprichtlijnen om koudeval te voorspellen?

Op basis van de verkregen resultaten kan een algemene conclusie getrokken worden. In een standaard kantoor ontstaan er volgens de proefpersonen geen klachten door koudeval (natuurlijke convectie door een koud vlak). Door niet bang te zijn voor koudeval kunnen energie en materialen bespaard worden in de gebouwde omgeving (zoals woningen). Met het gekalibreerde CFD model bleek echter dat een verhoogde vloertemperatuur de koudeval kan verslechteren (hogere luchtsnelheden nabij de vloer). Dit geeft aan dat radiatoren en convectoren niet simpelweg vervangen kunnen worden door vloerverwarming.
Daarnaast komt het resultaat van het PMV model overeen met de thermische sensatie van de proefpersonen. ISO 7730 is het beste gebleken om koudeval situaties te beoordelen, terwijl de vuistregel ter voorkoming van koudeval erg conservatief is. Meer onderzoek is nodig naar een correcte comfort limiet die in ontwerprichtlijnen gebruikt kan worden (bijv. een maximale luchtsnelheid samen met een stralingsasymmetrie). Belangrijke parameters voor ontwerprichtlijnen ter voorkoming van koudebal zijn raamhoogte, temperatuurverschil tussen het raam en de binnenlucht en de vloertemperatuur. Meer simulatievarianten zijn nodig om complete ontwerprichtlijnen op te stellen.

Table of contents

Part I
Introduction

Consulting engineers are in search for applicable design guidelines to prevent downdraught. As a result, the focus in this research is on downdraught and effective measures to assure thermal comfort near glass façades. In this first part of the report an overview of the total graduation project and some background information regarding downdraught are given.

Chapter 1
Introduction

In this chapter the relevance of the project, the problem definition, the project objective, the research questions, and the methodology are presented. This report is the second part of the project and treats measurements and simulations, the first part is about the literature study and reported in Timmers (2010).

1.1 Relevance of the project

The total graduation project has a practical as well as scientific relevance. Furthermore, the project can be linked with more popular terms like sustainability, energy efficiency, zero-energy buildings, cost reduction, and thermal comfort.

Practical relevance

It is assumed by Nelissen consulting engineers that (too) often radiators or convectors are installed beneath windows because of fear for downdraught. Energy and materials can be saved if no heating is needed or when downdraught can be prevented by using Low Temperature Heating (LTH) systems. [Source: Nelissen 2010] It is also desired by consulting engineers to verify an existing rule of thumb considering current technologies. The rule of thumb (chapter 2.2) or design guidelines can be used for new developments, but also for renovation projects. For existing window heights and with current glazing types it may be possible to replace radiators by LTH-systems that save energy and eventually also money. In that case, design guidelines can play an important role for example to make Eindhoven a zero-energy city, the intention of the community Eindhoven to be reached by 2040.

Scientific relevance

The scientific relevance is related to thermal comfort prediction in combined non-uniform situations and to prediction/simulation of indoor air flow due to natural convection.
According to Olesen et al. (2002) it is unclear how to predict thermal comfort in combined non-uniform situations, such as downdraught situations. In fact, draught and radiation occur simultaneously, where the standards (ISO 7730) only treat them separately. It also has to be determined whether draught, radiation asymmetry, or a combination of both is the main comfort problem. Additionally, van Marken-Lichtenbelt et al. (2007) and de Dear (2011) showed the importance of simulating thermophysiological responses, i.e. by ThermoSEM (chapter 4.2), to predict thermal alliesthesia (unpleasant or pleasant experience depending on the subject's internal state) and thermal comfort for individuals.
It is also relevant to be able to predict or simulate the indoor air flow due to natural convection correctly to assess different situations or solutions. This is difficult, especially close to human beings and windows. As a result, very few downdraught researches are available that study multiple parameters at the same time or take human beings into account. Heiselberg et al. (1995) showed that downdraught problems can be reduced by using the structural system of the window or the window bay as an obstacle. With more knowledge on the air flow, passive solutions to downdraught can be developed.

1.2 Problem definition

In this paragraph the problem definition is given. This definition is directly deduced from the relevance of the project.

The main problem concerning downdraught is that consults are often given with the use of an existing rule of thumb or the experience of the engineer. Assuming a conservative design, there is a possibility of wasting materials and energy if no validated rule of thumb or design guidelines are available. Besides this, it is difficult or even impossible to predict the airflow in a room due to downdraught. The same counts for assessing such non-uniform environment in terms of thermal comfort. To assess the combined effect of different developments on downdraught a correct simulation model and thermal comfort model are needed.

1.3 Objective of the project

The objective is the basis of the methodology of the total project. It is deduced from the problem definition and relevance as well.

The main objective is to compose design guidelines to predict downdraught. With design guidelines downdraught can be prevented and an energy-saving, comfortable indoor climate for occupants of new-built or renovated buildings can be created. A last remark is that the design guidelines should be easy to use to ensure its practical applicability.

A definition of downdraught is needed to reach the main objective of this project. This definition consists of objective parameters like air velocity and a (subjective) thermal comfort assessment. First it is determined what the effect of downdraught is on male, young-adults in an office environment. This can be extended to other groups of people with different activities and/or own system control in further research. Subsequently, several variants can be simulated and assessed with the definition for downdraught. In the end, consulting engineers can give founded advices with the composed design guidelines and energy can be saved. If necessary, complex situations can be simulated.

1.4 Research questions

Within this graduation project, there are three main research questions that are subdivided in sub questions. The questions that are shown in this paragraph are those remaining after the literature study.

1. What is the definition of downdraught?
    - How can downdraught be defined in terms of air velocity, air direction, air temperature, turbulence intensity and other parameters?
    - Because of what parameters are people thermally dissatisfied in case of a cold vertical surface and low temperature heating / no heating?
    - What is acceptable or unacceptable for people in case of a cold vertical surface and low temperature heating / no heating in a room?

2. How can thermal comfort in relation to downdraught be predicted correctly?
    - In what way can global and local thermal comfort in downdraught situations be predicted with the Standards (EN-NEN-ISO 7730)?
    - To what extent can (local) thermal comfort in downdraught situations be predicted with the outcome of the thermophysiological model ThermoSEM?

3. What are possible design guidelines to predict downdraught?
    - How accurate can downdraught cases be predicted?
    - To what extent is the existing rule of thumb sufficient to predict downdraught?

1.5 Project methodology

In this paragraph the methodology that is going to be used during the total graduation project is explained (shown in figure 1.1). The methodology starts with a question from consulting engineers, requiring scientific research to be answered. This project contributes to the question of Nelissen consulting engineers and to the PhD research of ir. L. Schellen.

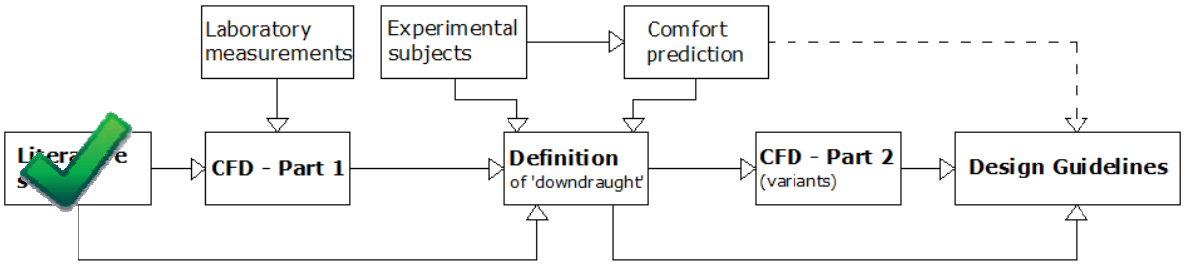

Figure 1.1 Schematic overview of the graduation project

- **Literature study**
  In October 2010, part 1 of this graduation project (literature study) was completed by Timmers (2010) presenting answers to some of the research questions. This report (part 2) focuses on measurements in the climate chamber and CFD simulations.

- **Calibration of a CFD model**
  A 3D CFD-model of the climate chamber will be calibrated with measurements. “Fluent” is used to perform CFD simulations.

- **Thermal comfort prediction (with experimental subjects)**
  With 10 male subjects, the existing thermal comfort models will be validated to decide on what model predicts comfort best in downdraught situations. Those measurements are also needed to determine when downdraught is acceptable and when it is not.

- **Simulation of variants in CFD**
  Different, complex variants will be designed and simulated with the calibrated CFD model. The parameters in the variants are the heating system, window surface temperature, and window height. The number of variants that can be simulated is restricted due to the extensive computational time required per simulation.

- **Composition of design guidelines**
  With the calibrated CFD model (simulation of variants) and a thermal comfort prediction model (assessment of variants) design guidelines can be composed. Those possible design guidelines can be used by engineers, for new developments as well as for renovation projects. In this way the graduation project focuses on research but also on consultancy.

Chapter 2
Downdraught

In this chapter the most important findings in literature concerning downdraught are shown. Mainly the conclusions of existing experimental and numerical downdraught studies are treated. Also the definition of downdraught and the rule of thumb are given. Finally, several downdraught solutions are shown. For the complete literature study is referred to: Timmers, Design guidelines to prevent downdraught – part 1 (TU/e).

2.1 Introduction on downdraught

In case of downdraught the layer of air close to cold surfaces (i.e. windows) is cooled by convection. The density of cold air is higher than that of warm air, which causes the layer to flow downwards due to gravity (buoyant forces). In this project, the term “downdraught” is used for such buoyancy driven flows. If the cold air downstream close to the surface is not compensated by a warm air upstream, it can end up in the living area and can cause discomfort. [Aarts et al., 2005] [Heiselberg, 1994]
Since convection is more important to transmit heat compared to radiation, downdraught can be compensated by warm air coming from high temperature heating systems like radiators or convectors (figure 2.1). Nevertheless, the focus during this research is on LTH-systems (based on radiation) because of its energy saving potentials. [Eijdems et al.]

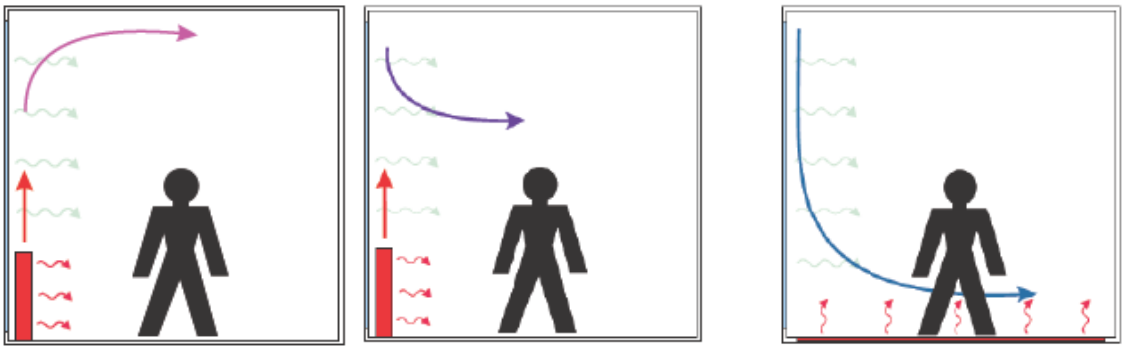

Figure 2.1 Difference between radiator heating (left) and floor heating (right)

Two possible thermal comfort problems in relation to cold windows that play a role in this project are cold radiation asymmetry and downdraught. [Huizenga et al., 2006]
Radiation asymmetry is influenced by the window surface temperature, posture of the human being, and human factors like clothing and metabolism. Huizenga et al. (2006) stated that radiation heat exchange is a significant factor that influences thermal comfort because the body is affected asymmetrically and some body parts may become cooler than others.
In turn, according to an occupant survey 30% of the people is bothered by downdraught when Low Temperature Heating (LTH) systems are applied. [de Vries and Silvester, 2000]

2.2 Rule of Thumb

To prevent (thermal comfort) problems near cold vertical surfaces a rule of thumb has been created by Olesen (1995) in which a maximum accepted air velocity of 0.18 m/s in the living area is assumed. The rule of thumb is still in use by engineers and relates the thermal resistance of the glass to the maximum allowed height of the glass surface.

- $\mathbf{U_{glass} \cdot h \leq 4.7}$

If a maximum allowed air velocity of 0.15 m/s is considered, the rule of thumb changes to:

- $\mathbf{U_{glass} \cdot h \leq 3.2}$

According to the rule of thumb no problems occur with glazing heights up to three meters if double glazing with gas filling is used. [TVVL, 2008]

2.3 Downdraught solutions

One of the passive solutions to prevent downdraught is lowering the U-value of the window. This can be done by a second skin façade which is expensive and requires maintenance. Another passive possibility is to increase the thermal performance of the window using multiple layers of glass or a gas filling. Passive solutions are preferred over active ones like electrical heating of the glass, since active measures increase the energy consumption.
However, research done by Heiselberg et al. (1995) showed that for window heights above standard room height downdraught problems cannot be avoided by only decreasing the U-value of the window. In that case, the window frames can contribute to a solution because of the influence on the airflow pattern (see paragraph 2.4). Also perforation of the window bay as well as a vertical barrier with perforation in front of the window can take away draught complaints. [Prendergast et al., 2004]
Another possibility to reduce downdraught problems is floor heating with a higher density close to the cold surface. Nevertheless, results of a simulation study performed by Richter (2003) showed little effect on the radiant asymmetry and the Draught Rate. The occurring surface temperatures can be seen in figure 2.2.

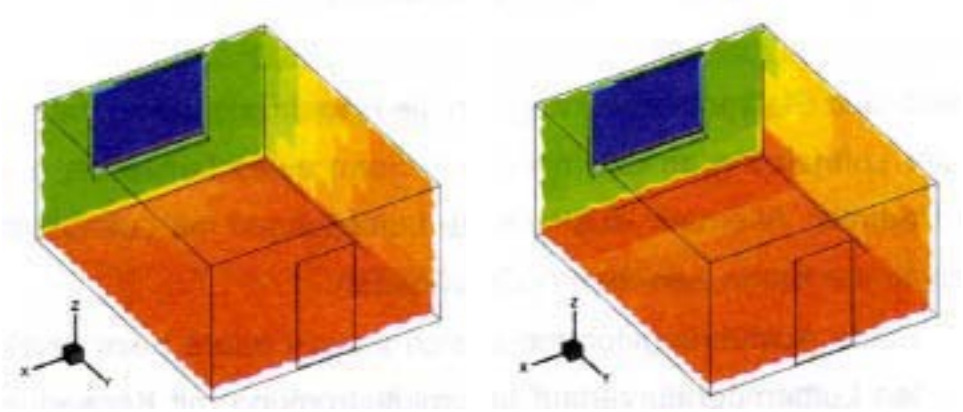

Figure 2.2 Effect of dense floor heating(right) on surface temperatures [Richter, 2003]

2.4 Experimental and numerical downdraught studies

In the past, a few experimental and numerical studies have been done to gain more insight in the flow principles of downdraught and the effect of several solutions. Heiselberg (1994) developed four expressions for maximum air velocity and minimum air temperature that occur in the flow above the floor in the occupied zone. Those functions are related to the distance from the cold wall (x) and based on climate chamber measurements.

- $v_{max} = 0.055 \cdot \sqrt{\Delta T \cdot h}$ if x < 0.4 meters
- $v_{max} = 0.095 \cdot \frac{\sqrt{\Delta T \cdot h}}{x+1.32}$ if 0.4 < x < 2.0 meters
- $v_{max} = 0.028 \cdot \sqrt{\Delta T \cdot h}$ if x > 2.0 meters
- $T_f = T_{in} - (0.3 - 0.034x) \cdot \Delta T$

Those equations are checked by Manz and Frank (2004) and showed good agreement with CFD simulation results for an empty room. The equations are also modified for a furnished room with internal heat sources and can be found in literature.

Heiselberg (1995) also researched the influence of the window frame and window bay on the boundary layer flow. The structural system can act as an obstacle. When a recirculation zone is created below the obstacle, the comfort conditions improve, because of a lower air velocity and temperature difference between glass surface and living area. The critical width (the flow changes from reattachment to separation) of an obstacle is hard to determine. However, if the width of the obstacle is smaller than the critical width, the flow reattaches to the surface and a recirculation zone is created, see figure 2.3. Only with turbulent boundary layers the critical width is realistic in practice (0.15–0.30 meters). To create turbulent conditions a large distance between the obstacles is needed (>2 meters).

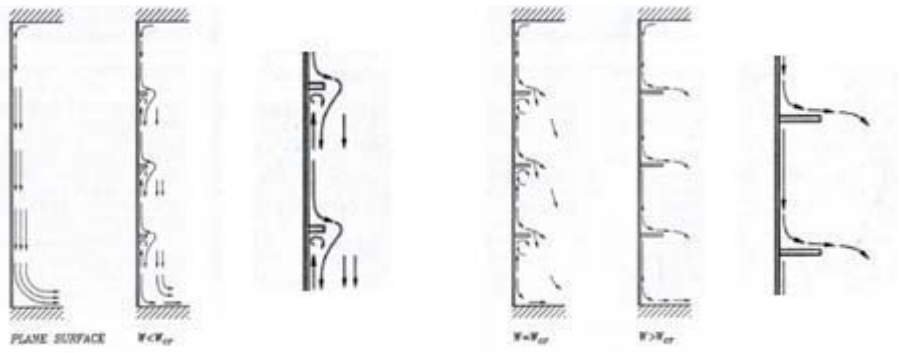

Figure 2.3 Flow principals of the boundary layer around obstacles [Heiselberg et al., 1995]

The performed researches give the overall statement that with window heights up to 2.5 meters no problems related to downdraught occur when insulating glass is used, even when the location of the person is 0.6 to 1 meter from the window. The allowed temperature difference between the room and the window is 2.5°C. Next to that, the air flow pattern is influenced significantly by furniture, HVAC systems, internal heat loads, and window bays.

Additionally some shortcomings of the experimental and numerical studies can be pointed out. Firstly, only draught is taken into account and no radiation asymmetry is considered while it is not clear what the exact comfort problem is. Only the Draught Rate or a maximum air velocity (0.15-0.18 m/s) is used to draw conclusions and thermal comfort is not considered as an additional aspect, for example with experimental subjects.
Furthermore, in almost all studies only two to three meter high windows are researched, while it is expected that higher windows, which appear in practice, cause more problems.

Overall, from literature can be concluded that in case of a cold window two main thermal comfort problems can occur: radiant asymmetry and downdraught. A rule of thumb exists to predict downdraught and to prevent (thermal comfort) problems. However, the question is to what extent this rule of thumb is able to predict downdraught correctly. Besides this, several solutions for downdraught are available but the effect of it on downdraught needs more research. In this project the main focus is on window heights above standard room height and on thermal comfort prediction in downdraught situations, because those are the shortcomings in existing downdraught studies. For that reason, experimental subjects play an important role during this research but also CFD simulations are needed to predict several situations. In the end, the objective is to compose design guidelines that prevent downdraught and create an energy-saving, comfortable indoor climate.

Part II

Downdraught and thermal comfort

In previous downdraught studies the assessment is based on a maximum allowed air velocity or the Draught Rate. During this research experimental subjects are used to determine their response to downdraught environments and to validate the relevant thermal comfort models. In this second part of the report, the best way to assess downdraught in terms of thermal comfort will be established.

Chapter 3

Experimental subject measurements

As indicated before, experimental subject measurements are used to determine human responses to downdraught situations. In this chapter the measurement setup (methodology) is treated and the experimental subject measurement results are discussed. Prior to that, relevant literature related to thermal comfort of human beings is shown.

3.1 Introduction

In this paragraph first a short introduction related to 'thermal comfort' is given, followed by an explanation of the human response to the environment and the establishment of thermal comfort. For the complete literature study is again referred to Timmers (2010).

3.1.1 Thermal comfort

People's health and productivity and also building energy consumption can be influenced by thermal comfort. [Schellen, 2007] According to ASHRAE 55 (2004), thermal comfort is defined as: *"that condition of mind which expresses satisfaction with the thermal environment and is assessed by subjective evaluation"*. Thermal comfort is also referred to as thermal neutrality, which is a situation in which a person would prefer neither warmer nor cooler surroundings. Thermal comfort can be divided into whole-body comfort and local thermal comfort (comfort or discomfort to specific areas of the body).

To quantify and assess thermal comfort the Bedford comfort scale (1936) is available, including the preference of the subject. However, more often the seven-point thermal sensation scale (1966) is used, in which a neutral sensation is given a value of zero. Both scales can be seen in figure 3.1. [Parsons, 2003] Sensation describes the magnitude and sign (warm versus cool) of the experience, whereas comfort qualitatively describes the pleasantness of the stimulus (like versus dislike). [de Dear, 2011]

Fanger (1970) linked the outcome of the sensation scale to a PPD (predicted percentage dissatisfied). However, it is still not clear how thermal sensation relates to thermal comfort.

Bedford comfort scale		Thermal sensation scale	
Much too warm	7	Hot	+3
Too warm	6	Warm	+2
Comfortably warm	5	Slightly warm	+1
Comfortable	4	Neutral	0
Comfortable cool	3	Slightly cool	-1
Too cool	2	Cool	-2
Much too cool	1	Cold	-3

Figure 3.1 Thermal Comfort (TC) scale and Thermal Sensation (TS) scale

3.1.2 Thermophysiological responses

Core temperature in human beings is maintained between narrow limits by internal heat production and countermeasures of the thermoregulatory system like shivering and changes to skin blood flow (vasomotion). Thermoreceptors detect the human's thermal state. Cold receptors are closer to the skin surface and more densely distributed than warm receptors, resulting in regionally different thermal sensitivity of the skin. [Hensel, 1981] According to Huizenga et al. (2004) the human body is more protective against cold than heat. Additionally, large temperature differences between the upper and lower part of the body or between dorsal and frontal side may be uncomfortable.

Research by Fobelets (1987) showed that in environments with air velocity and radiation asymmetry local skin temperatures decrease because blood vessels vasoconstrict. Also the neck is most sensitive to draught. More recent research with human beings in non-uniform environments is done by Zhang et al. (2010-part II). It is observed that people do not react identical on warm and cold conditions. The back, chest, and pelvis are dominant at influencing overall thermal sensation and comfort and have a preference for warmth. Next to that, the overall thermal state of the body influences the sensitivity to local thermal sensation. When the feet were cooled or warmed when the whole body was respectively warm or cold, it was perceived as comfortable. [Zhang et al., 2004] Wang et al. (2007) concluded that in offices often the extremities (hand and feet) become cold and removing that discomfort has a strong effect on overall thermal sensation and comfort.

Based on literature, the research questions that are of importance during this chapter are:

- Because of what parameters are people thermally dissatisfied in case of a cold vertical surface and low temperature heating or no heating?
- What is acceptable / unacceptable in case of a cold vertical surface and a LTH-system?

3.2 Methodology

In this paragraph the measurement protocol is reported. First the measurement facility and cases are shown after which the experimental subjects, parameters of interest and related equipment are explained with the measurement planning included.

3.2.1 Climate chamber

At the laboratory of the unit Building Physics and Systems at the Eindhoven University of Technology (TU/e) a unique thermophysiological test room is realized in November 2010, shown in figure 3.5. The climate chamber has the same dimensions as a standard office room: 3.6 x 5.4 x 2.7 m³ (W x L x H). The construction consists of 100 mm well insulated walls and can be compared a cold-storage chamber.

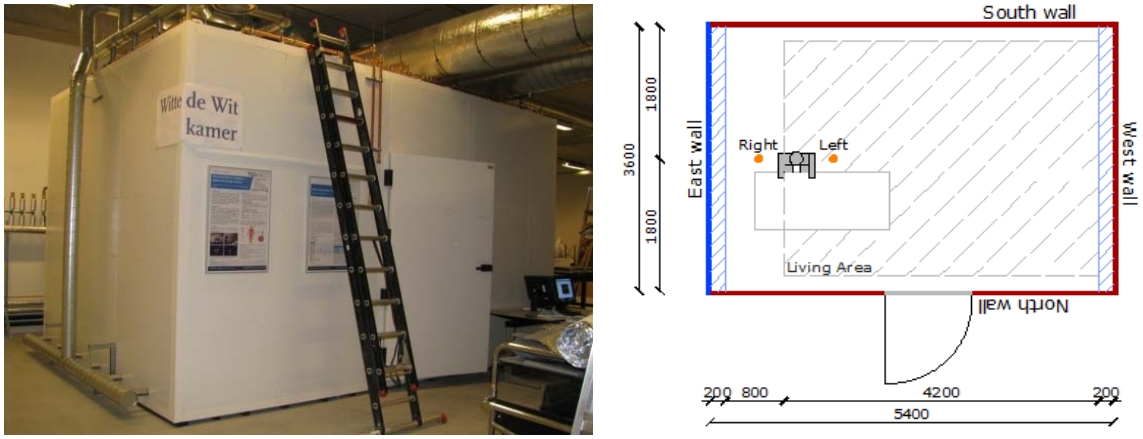

Figure 3.5 Photograph of the climate chamber at the TU/e (left) and floor plan (right)

In the climate chamber all four walls, the floor, and the ceiling can be given a temperature in the range of 11°C - 35°C by connecting the aluminum profiles (figure 3.6) to the warm or cold water circuit. The water is cooled by the aquifer system on the campus of which the temperature range may differ over the time of the year.

Along the short edges of the chamber four ventilation boxes (200 x 3600 x 200 mm³) are installed, as shown in figure 3.7. The boxes can both be used as inlet and exhaust and the size of the ventilation opening can be adjusted. The maximum volume rate of the system is 170 l/s (612m³/h). The ventilation air temperature can also be set and the air can be humidified. [Schellen et al., 2010]

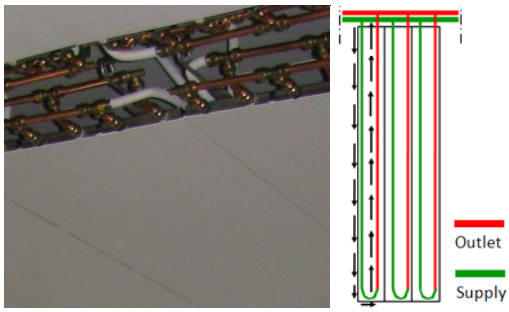

Figure 3.6 Aluminum profiles

Figure 3.7 Ventilation boxes and close-up

3.2.2 Cases

Two downdraught cases are composed to research the effect of floor heating on human responses. To create downdraught, the east wall (3.6 x 2.7 m^2) temperature is designed at 13°C being the lowest possible temperature with the aquifer system. It is also chosen to put the experimental subjects in a worst case situation. For the same reason, the person is placed one meter from the cold wall, which is also the beginning of the living area.
It is not desired that the ventilation influences the experimental subjects (downdraught research); therefore an inlet air temperature close to room air temperature is chosen with the lowest flow rate possible (approximately 150 m^3/h), using the ventilation box at the top.

Both cases have the same operative temperature of 21.5°C and can therefore be compared at comfort level. The difference between the cases is that Case I has one cold wall and all other five walls have the same temperature ("uniform") and Case II has one cold wall, a warm floor and the other walls are free floating ("non-uniform"). More information on the cases can be found in table 3.1, figure 3.8, and the heat balance is reported in Appendix 1.

Table 3.1 Measurement cases

	Case I	Case II
East wall temperature [°C]	13.4	13.4
Floor temperature [°C]	23.2	24.4
Rest wall temperature [°C]	23.2	22.6
Inlet air temperature [°C]	21.9	21.6
Inlet air velocity [m/s]	1.2	1.2
Internal heat load - convection [W]	168	168

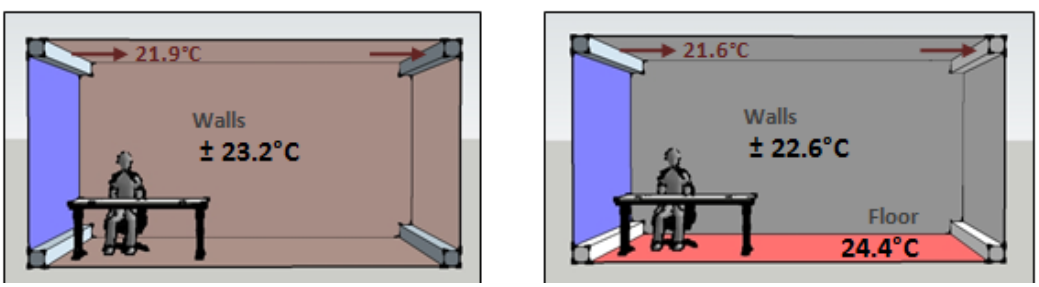

Figure 3.8 Measurement cases: Case I (left) & Case II (right)

3.2.3 Experimental subjects

Ten healthy male subjects between 18 and 30 years old participated in the research. According to the power calculation, ten people are enough for a paired T-test. Prior to the measurements, information about the objective and actual measurements is distributed and a consent form is signed by each subject, as shown in Appendix 2 (in Dutch).

Before entering the climate chamber, several body characteristics are measured. An overview of the characteristics of ten experimental subjects is given in table 3.2. The used equations to calculate BMI, skin area, and fat percentage based on BMI and skin folds can be found at the end of Appendix 5. All measurements are done based on the guidelines of Lohman et al. (1988). From the waist to hip ratio can be concluded how the fat is distributed over the body. In this case, the fat is mainly present at the hips and thighbones and not at the abdomen.

Table 3.2 Body characteristics of the participating experimental subjects

Variable	Mean	Std. Dev.	Minimum	Maximum
Age	**23.5**	1.7	20	26
Height [cm]	**185.0**	6.1	177.0	197.0
Skin area [m²]	**2.0**	0.1	1.8	2.2
Weight [kg]	**77.7**	8.8	67.5	91.2
Waist to Hip ratio [-]	**0.87**	0.04	0.81	0.92
Skin folds [mm]	**44.1**	13.8	21.3	73.0
BMI [kg/m²]	**22.6**	1.6	21.4	25.9
Fat percentage (Skin folds) [%]	**16.8**	3.9	8.7	23.5
Fat percentage (BMI) [%]	**16.4**	2.0	14.5	20.2

Metabolism and clothing affect thermal comfort and responses and therefore both are kept constant between all experimental subjects. During this project an office space is researched in which human beings perform sedentary activity corresponding to 1.2 met or 70 W/m². In addition, all subjects wear a standard clothing assemble consisting of a shirt, cardigan, and a pair of trousers made of 100% cotton. This is completed with own underwear, socks and shoes that did not cover the ankles. Based on ISO-9920 the summarized clo-value of these clothes is 0.85 clo. Together with the chair of 0.15 clo, the total clothing insulation becomes 1.0 clo. More information about metabolism and clothing can be found in Appendix 5.

3.2.4 Parameters and measurement instruments

To study the effect of downdraught on human beings, several physical and physiological parameters need to be measured and thermal comfort need to be determined. In this paragraph those parameters with the used equipment are treated and the questionnaire is shown. In Appendix 4 an overview of all instruments, loggers and connections can be found.

Physical parameters

At the left and right side of the person, at 0.2m distance, the air velocity and air temperature are measured. At that distance, the sensors are out of the natural convection boundary layer around the human being. As can be seen in figure 3.9, the sensors are located at 0.1m, 0.6m, 1.1m and 1.7m height based on ISO 7726. The same parameters are also measured as close as possible to the inlet, to monitor the inlet conditions.

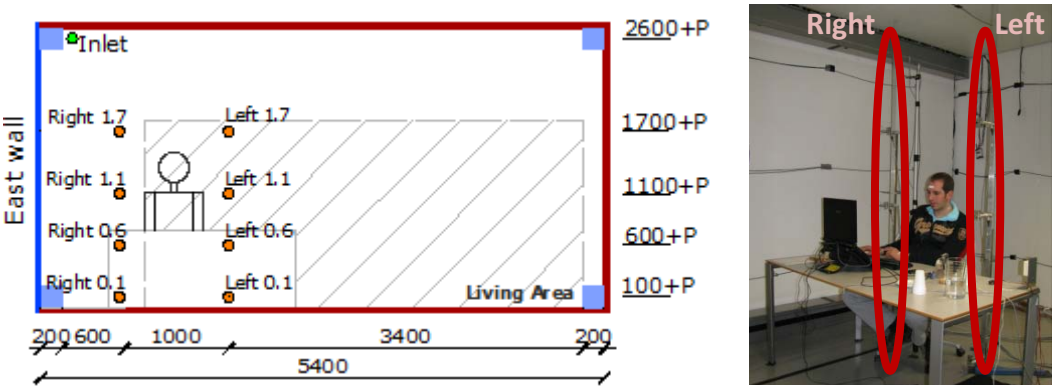

Figure 3.9 Cross section and picture of the measurement positions

Background information on the used sensors can be found in Appendix 5 including related equations and calibration data. The main instruments are:

- Dantec: Air velocity (in the range of 0.05 - 1.0 m/s) and Turbulence Intensity (calculated)
- NTC Thermistor (with radiant strip): Air temperature
- Humidity sensor: Relative humidity
- Copper U-thermistor: Surface temperature and mean radiant temperature (calculated)

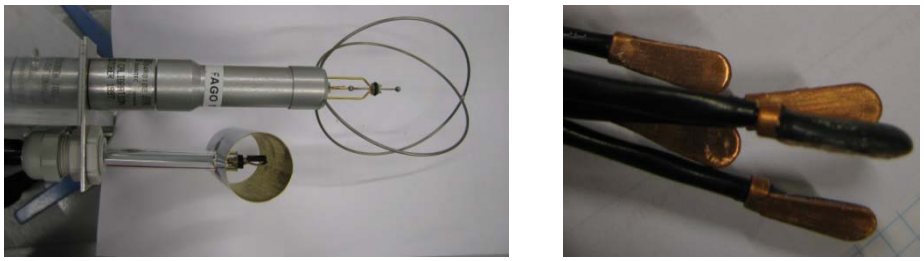

Figure 3.10 Dantec, NTC, and Humidity sensor (left) and copper U-thermistors (right)

Physiological parameters

The first physiological parameter is the core temperature. It is measured by a non-digestible HQ Inc. thermometer pill (figure 3.11) taken orally. During the experiment the capsule is in the stomach and intestine and every minute the core temperature is logged.
Skin temperature is measured at 24 positions at the skin using iButtons (wireless, Ø 16mm), see figure 3.12. The difference between the left and right side of the body can be researched that way, but also the effect of vasomotion on thermal comfort. The mean skin temperature can be calculated from positions 1 to 14, see also Appendix 6. [ISO 9886, 2004]

Figure 3.11 Core and skin temperature sensor

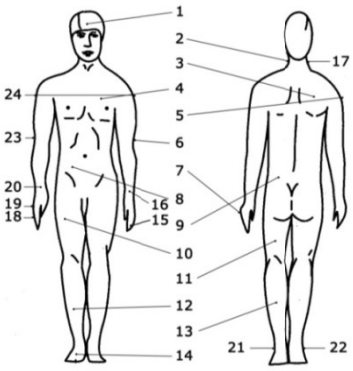

Figure 3.12 Skin temperature positions

Questionnaire

Thermal comfort and sensation votes are often obtained by questionnaires. One drawback is that the answer can be influenced by numerous factors like stress level or annoyance. During this research an existing questionnaire is used, developed by Schellen (2010). The complete questionnaire can be seen in Appendix 3.

Every experimental subject can fill out the questionnaire on his own laptop, via an internet application made by the University of Denmark. The application can be reached at: http://www.ie.dtu.dk/tue2010. One questionnaire takes around 12 minutes.
In the questionnaire the Thermal Sensation scale is used to assess whole body sensation and local thermal sensation of fifteen body parts. A visual analogue scale (VAS) is used for that, of which an example (in Dutch) can be seen in figure 3.13. Also whole body and local thermal comfort are asked, using a Likert scale (also shown in figure 3.13). In addition, acceptability and preference are included in the questionnaire. Two other questions focus on noticed air movement. To finish the questionnaire a productivity test of 10 minutes has to be made, consisting of adding numbers or typing a text.

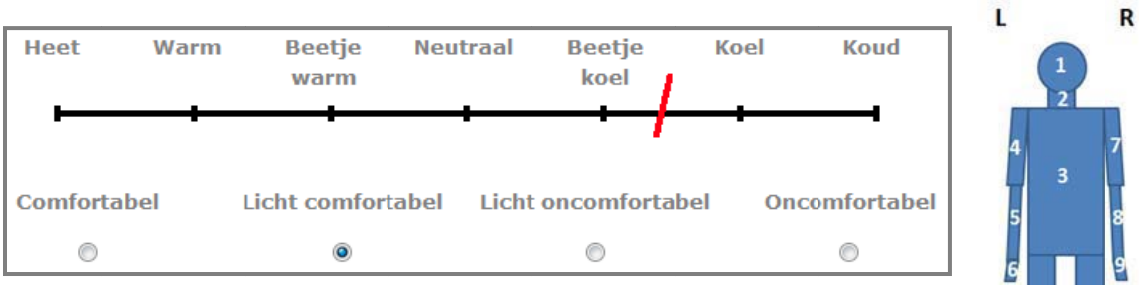

Figure 3.13 VAS-scale (above) and Likert-scale (below)

Overview

To conclude, an overview of the parameters and equipment is given, based on ISO 7726 and calibration data. In Appendix 4 all used instruments and connections can be found and Appendix 5 contains background information of the used instruments.

Table 3.3 Overview of equipment

Variable	Unit	Range	Accuracy	Uncertainty	Interval [s]	Sensors
Air temperature	°C	10-40	±0.5	0.2°C	60	9 NTC
Air velocity	m/s	0.05-1.0	±(0.05+ 0.05v_a)	10%	1/10	9 Dantec
Surface temperature	°C	0-50	±1.0	0.2°C	60	54 U-therm.
Relative humidity	%	0-100	-	3.5%	60	9 sensors
Skin temperature	°C	-10 - 65	-	0.121°C	60	24 iButtons
Core temperature	°C	-	-	-	60	1 pill
Comfort & Sensation	-	-	-	-	1800	17 quest.

3.2.5 Measurement planning

The last part of the methodology consists of a planning. The used checklist can be found in Appendix 6 and in Appendix 7 the planning for a whole day is shown.
The experimental subjects are exposed to two downdraught cases over a time period of four hours. Half of the group is participating in the morning, the other half in the afternoon. Every 30 minutes a subject has to fill out a questionnaire, expressed in the timeline in figure 3.14.

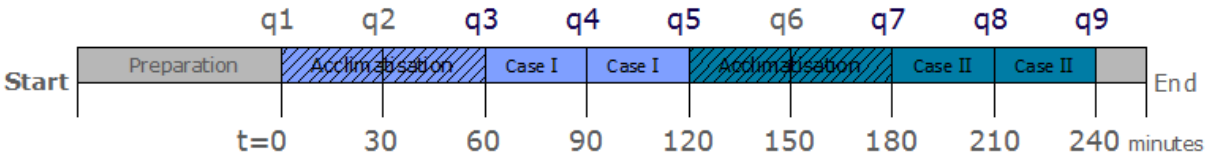

Figure 3.14 Measurement timeline for two cases (q = questionnaire)

Before continuing with the results, an overview of Case I and Case II is given by the use of infrared pictures. The sequence of the cases could not be varied, because Case II has free floating walls. To expose all subjects to the same conditions the free floating temperature must always come from the same temperature (Case I).


t=60 (Case I)


t=120 (Case I)

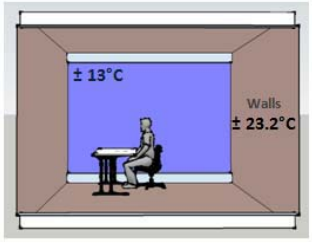

Designed Case I

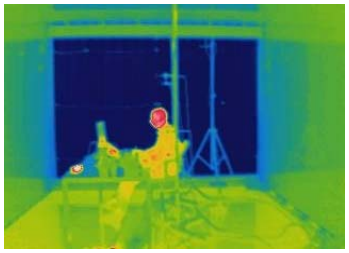
t=180 (Case II)


t=240 (Case II)

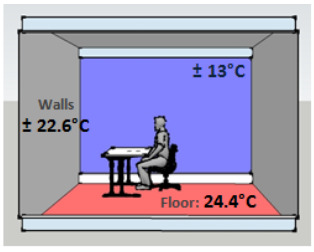

Designed Case II

3.3 Results

The measurements are processed and also a statistical analysis is performed. Therefore, a summary of the cases and an overview of the measurement results are shown in this paragraph. Finally, the results of the statistical analysis are given.

3.3.1 Case summary

First an overview of the measured cases is given in table 3.4. An attempt is made to keep the cases (surface temperatures, inlet conditions, etc.) as constant as possible to reproduce the same cases for all experimental subjects. However, this turned out to be difficult for the window surface temperature and the relative humidity. A comparison of the environmental conditions for all subjects can be seen in figure 3.15 and figure 3.16.

Table 3.4 Case summary (mean, minimum, maximum and standard deviation per case)

	Case I				Case II			
Variable	**Mean**	Min.	Max.	Std	**Mean**	Min.	Max.	Std
Surface temp. window [°C]	**13.7**	13.1	14.3	0.44	**13.7**	13.0	14.5	0.56
Surface temp. floor [°C]	**23.0**	23.0	23.1	0.03	**24.3**	24.1	24.5	0.10
Surface temp. wall west [°C]	**23.2**	23.2	23.3	0.05	**22.7**	22.5	22.9	0.12
Operative temperature [°C]	**21.6**	21.5	21.7	0.08	**21.8**	21.6	22.0	0.16
Mean air temperature [°C]*	**22.1**	22.0	22.2	0.08	**22.2**	22.0	22.5	0.15
Mean air velocity [m/s]*	**0.07**	0.07	0.09	0.01	**0.09**	0.07	0.12	0.02
Mean turbulence intensity [%]*	**25.9**	23.7	28.6	1.64	**25.9**	23.8	27.8	1.28
Mean relative humidity [%]*	**46.9**	37.0	55.4	6.27	**47.7**	38.2	55.3	6.00
Temperature Gradient [°C]*	**1.4**	0.9	1.5	0.17	**0.8**	0.7	0.9	0.09
Radiation Asymmetry [°C]	**6.1**	5.7	6.4	0.27	**6.1**	5.6	6.5	0.31

* Mean calculated over two tripods

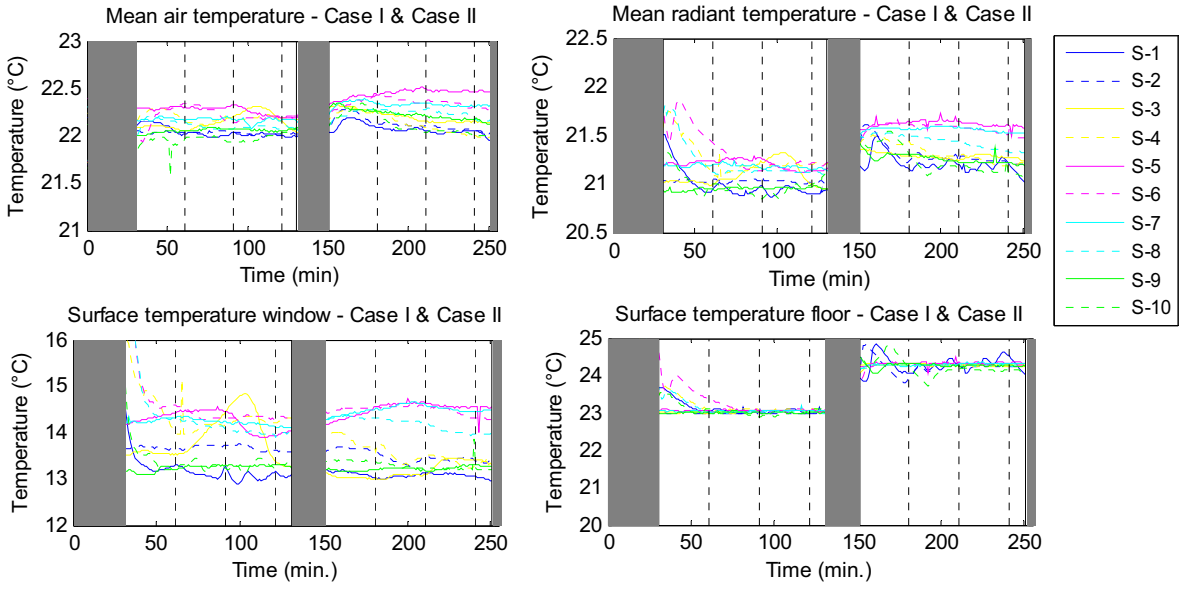

Figure 3.15 Mean air, mean radiant, and window and floor surface temperature (S = Subject number)

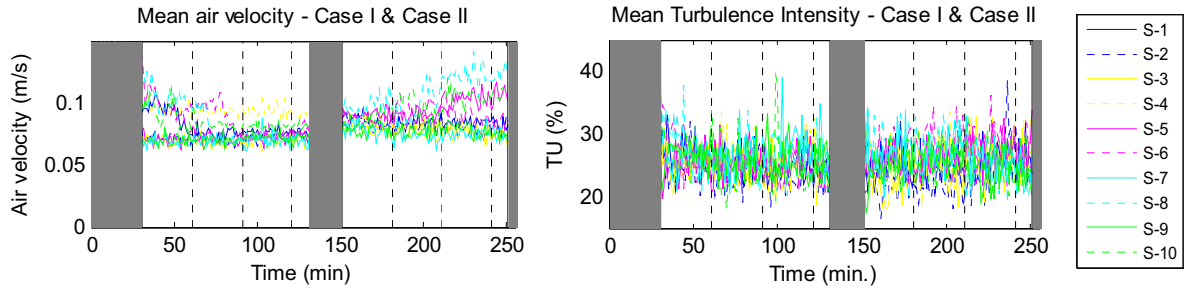

Figure 3.16 Mean air velocity and turbulence intensity in the room (S = Subject number)

It is evident that the surface temperatures remain between narrow limits when those are connected to the warm water circuit (like the floor, figure 3.15). However, the cold water temperature depends on the aquifer system and the designed 13°C could not always be reached. As a result, subject 3, 5, 6, 7, and 8 had a window temperature of above 14°C. This higher temperature immediately affected the mean radiant temperature and also the mean air temperature in the room. In figure 3.16 the mean air velocity in the room is given for every experimental subject showing variations between subjects. The air velocity fluctuated a lot, resulting in turbulence intensities between 20% and 30%. More case results for the experimental subjects can be found in Appendix 8.

3.3.2 Measurement results

In this paragraph the results will be explained for only one experimental subject since these are comparable for other subjects, as can be seen in Appendix 9. The physical measurement results are treated, but also the physiological results like measured skin temperatures and vasomotion. Finally, a trend line of thermal sensation and comfort votes is shown.

Physical measurement results

The air temperature at four sensors at the left and right side of the person (figure 3.9) is shown in the graph of figure 3.17. It is clear that the air temperature remains constant during the measurement period, which indicates a heat balance. Figure 3.17 also shows the expected temperature gradient in the room. The two sensors closest to the floor (solid blue and red line) measured the lowest temperatures in the room. This shows that downdraught is occurring. During Case II the lowest temperature has increased because of a higher floor temperature, which also decreases the vertical temperature gradient.

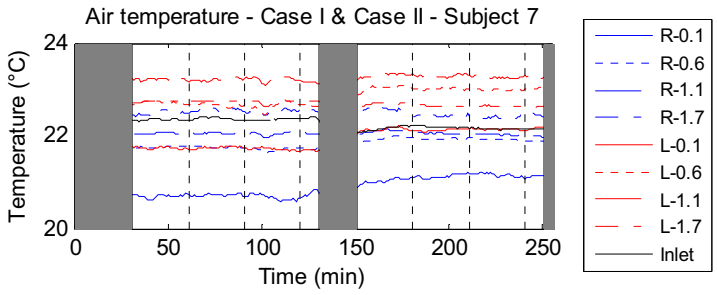

Figure 3.17 Room (eight sensors) and inlet air temperature

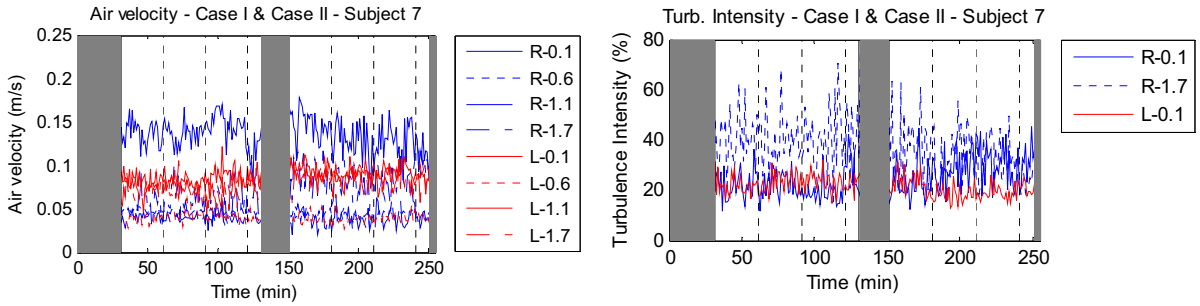

Figure 3.18 Air velocity at eight sensors & Turbulence Intensity for three sensors

The air velocity sensors are located at the same positions as the temperature sensors. The 10 hertz measurement results are averaged over a minute and used to draw the graphs in figure 3.18. Again the two solid lines (two sensors at 0.1 meters above the floor) show the highest air velocity due to downdraught. This effect is mainly visible for the blue line, because the subject disturbs the flow field which lowers the air velocity at the left side of the person. In the rest of the room very low air velocities occur that are out of the measurement range of the Dantec. This also results in high turbulence intensities, shown for three sensors in figure 3.18. The turbulence intensity is calculated by dividing the standard deviation by the mean air velocity of a minute. For the sensors close to the floor the turbulence intensity remains at a 20% level because of the higher air velocities.

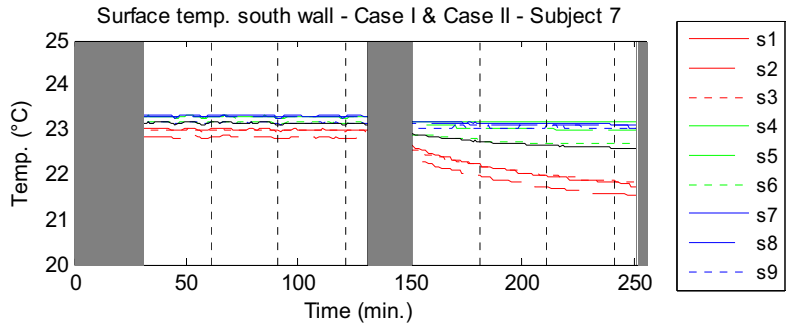

Figure 3.19 Surface temperature of the south wall measured by 9 sensors

The surface temperature is measured by nine equally distributed sensors. In Case II free floating walls are present of which one is the south wall. When the warm water circuit is turned off the wall keeps its temperature and is mostly cooled by the cold east wall. This can be seen in figure 3.19: the three red lines are the three sensors closest to the cold wall. This also means that the walls have an anisotropic temperature distribution during Case II.

Physiological measurement results

Eight of the skin temperature measurements can be seen in figure 3.20. In all of the cases the skin temperature at the right side of the body (facing the cold wall) is lower than that at the left side of the body. In Appendix 8 also the mean skin temperature per subject is shown. The mean skin temperature remains constant during the cases, but the skin temperature differs between the individuals (min. 32°C to max. 33.5°C).

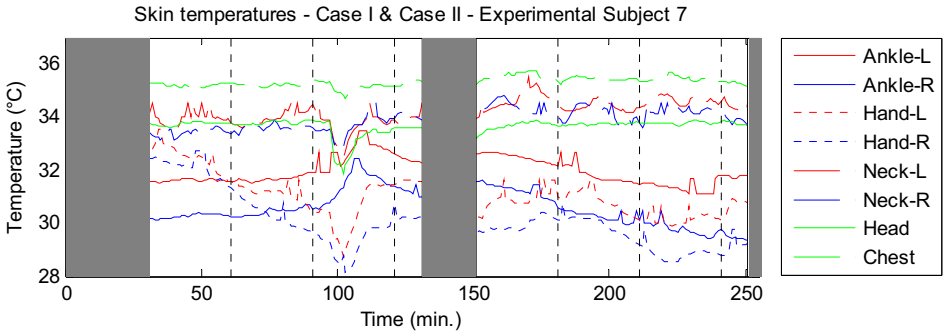

Figure 3.20 Skin temperature for eight different body parts

In figure 3.20 can also be noticed that for example the left and right ankle describe the same trend during the case. This is valid for all left and right body parts. The chest temperature remains constant, because this body part is close to the core of the human body.
Figure 3.21 shows that the mean proximal temperature (calculated from the chest, shoulder, back, and abdomen) remains more constant than the mean distal temperature (calculated from feet, ankles, fingers, hands, and head).

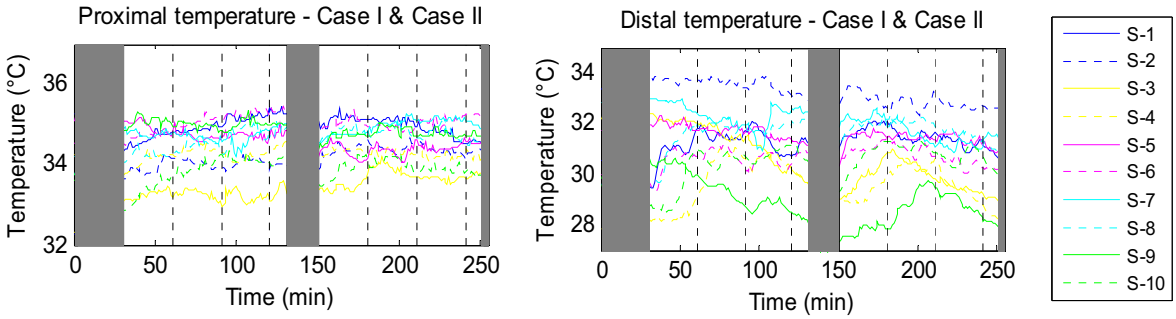

Figure 3.21 Mean proximal and distal temperatures per subject (S = subject number)

Finally, the temperature difference between the lower arm and finger tip is a measure for vasomotion. A negative number indicates vasoconstriction, while a positive number means vasodilatation. In figure 3.22 the results for the left hand and right hand are shown. Again, the trend between left and right is the same. Most of the time, the hands are vasodilatated, while subject 3, 4, and 9 react the opposite way (individual differences).

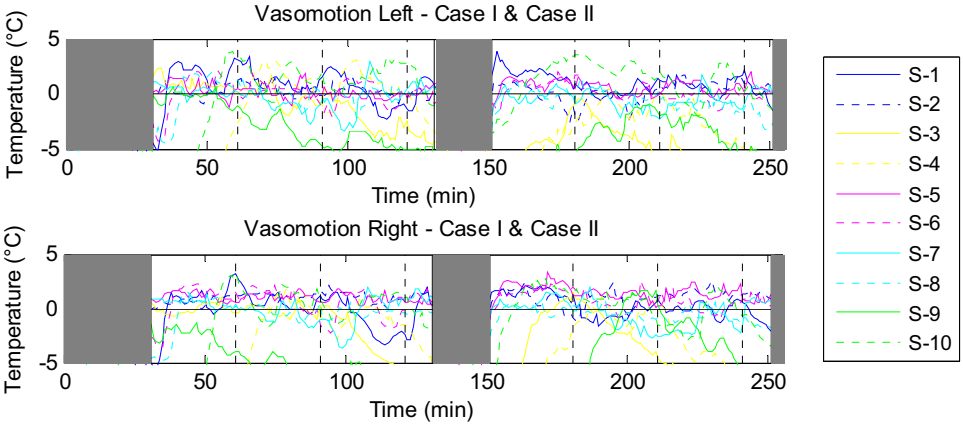

Figure 3.22 Vasomotion for the left and right hand per subject (S = subject number)

Thermal comfort and sensation measurement results

To end this subparagraph, a trend line is made of the thermal comfort and thermal sensation votes in time. For every subject a single graph is made, shown in Appendix 8. Two of those graphs can be seen in figure 3.23. Thermal sensation is a score on the thermal sensation scale (between -3 and 3) indicating a cold or warm feeling. Thermal comfort is rated by comfortable (C), slightly comfortable (SC), and slightly uncomfortable (SU). Most of the time, the thermal comfort line follows the thermal sensation line. On the other hand, when the thermal sensation of subject 9 lowered, comfort decreased and when he got a warmer feeling comfort increased again.

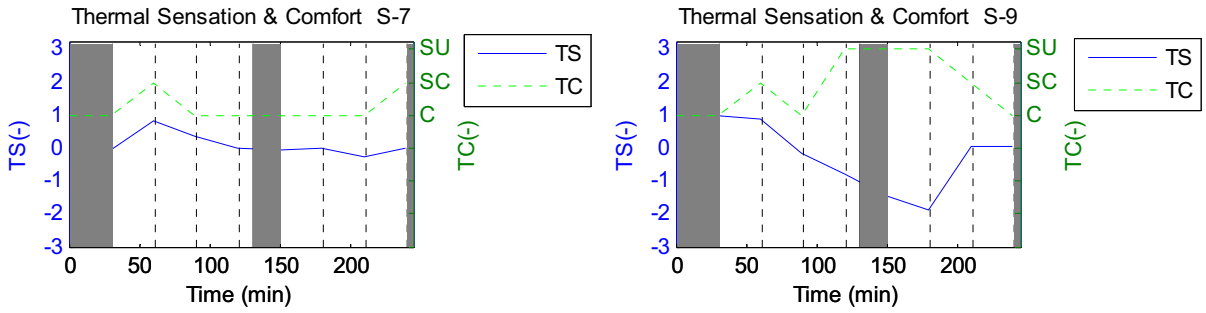

Figure 3.23 Thermal comfort and sensation votes in time of subject 7 and subject 9

3.3.3 *Statistical analysis*

The choice of an analysis method (frequencies, differences, or relations) is based on the used scales and the number of variables. [de Heus et al.,2008] [Baarda et al., 2006] In this sub-paragraph the statistical results are treated combined with a statistical introduction on the obtained data. For more background information is referred to Appendix 10.

Statistical introduction

Before starting the analysis the dataset has to be reduced. When several parameters are added together in one variable, the main question is to what extent all parameters measure the same effect. This internal consistency can be determined by Cronbach's α. An acceptable value is 0.7 or higher. [Field, 2009] In table 3.5 the alphas for the interesting variables in this research are shown. Also environmental parameters are included in the dataset to find its effect on TS-votes. An overview of the total dataset can be found in Appendix 12.

Table 3.5 Cronbach's alpha of several dataset variables

Dataset Variable	α	Dataset Variable	α
Mean skin temperature	0.715	Neck temperature	0.808
Change of skin temperature	-	Hand temperature	0.923
Mean distal temperature	0.858	Feet temperature	0.909
Mean proximal temperature	0.430	Left / right side temperature	0.738
Mean vasomotion	0.941	Mean thermal sensation	0.913

To check whether the obtained data of a small sample is normally distributed the kurtosis and skewness values need to be inspected. Deviation from the normal distribution can be found in lack of symmetry (skew) and pointyness (kurtosis). SPSS produces the values of skewness, kurtosis, and their standard errors of which the Z-value can be calculated.

$$Z_{skewness} = \frac{\text{Skewness}}{\text{S.E.of skewness}} \quad \text{and} \quad Z_{Kurtosis} = \frac{\text{Kurtosis}}{\text{S.E.of kurtosis}}$$

If the Z-value is larger than 1.96, the data is normally distributed. In the composed dataset for this research the data is not normally distributed, except for the thermal sensation votes. Therefore, non-parametric tests are used.

As a final remark, often a significance level of $p<0.05$ is adopted. This shows whether a null hypothesis is rejected or in other words: the probability that the distribution depends on coincidence is smaller than 5%. [Montgomery et al., 2004] [Baarda et al., 2006]

Frequency analysis

The experimental subjects completed four questionnaires per case. Most of the questions are asked at nominal and ordinal level and can be processed by frequency calculations. The first two questionnaires are in the acclimatization period and are not taken into account during the analysis. The final two are used to calculate frequencies, of which the main results can be seen in figure 3.24. All the frequency results can be found in Appendix 11.

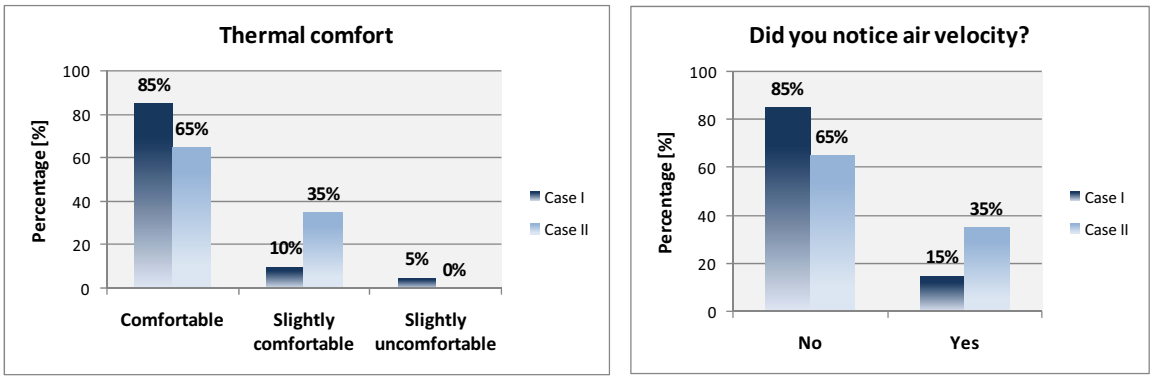

Figure 3.24 Frequency results of thermal comfort and noticed air velocity

The results show that Case I and Case II both are comfortable (one slightly uncomfortable vote). Both cases are also acceptable and no change is preferred. From the body parts only the feet, right and left lower arm and right and left hand are sometimes uncomfortable. Air velocity is more noticed in Case II than in Case I but in both cases no change is preferred. One remarkable result is that most of the time the air velocity is felt at the head.

The whole body Thermal Sensation is measured at an interval scale, which means a mean and standard deviation can be calculated. For Case I the TS-mean = 0.10 (Std.Dev.=0.365) and for Case II the TS-mean = 0.11 (Std.Dev.=0.471). In figure 3.25 the histogram with corresponding values is shown.

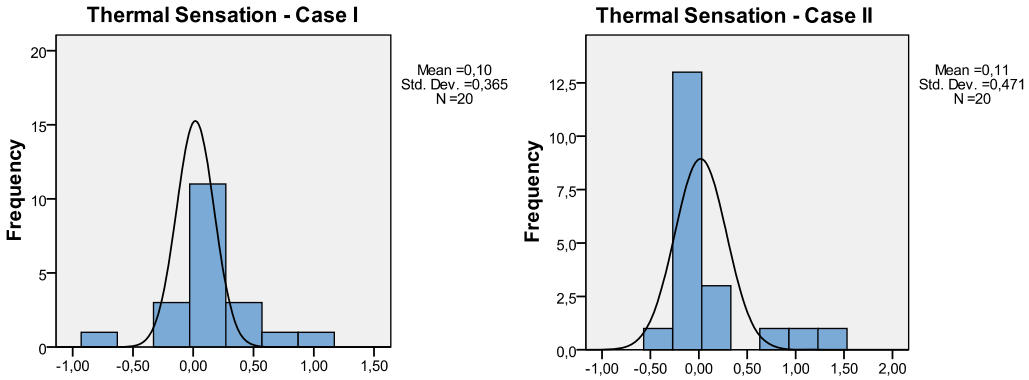

Figure 3.16 Frequency results of the thermal sensation votes

Differences analysis

In this research the Wilcoxon signed-rank Test is used to indicate the differences between Case I and Case II. This is a non-parametric test in which the differences are ranked. In the test, two hypotheses are formulated:

- Null hypothesis (mean difference between paired observations is zero) $\mu_d = 0$
- Alternative hypothesis (things are different from each other) $\mu_d < 0$ or $\mu_d > 0$

A two-tailed probability smaller than 0.05 ($p < 0.05$) is accepted as statistically meaningful: the two groups are significantly different and the null hypothesis (H_0) will be rejected. [Field, 2009] [Montgomery et al., 2004]

All results of this test are shown in Appendix 12, but the significant outcome of the Wilcoxon signed-rank Test can be found in table 3.6. Also the thermal comfort and thermal sensation are shown, because this project is about thermal comfort in downdraught situations.

Table 3.6 Wilcoxon signed-rank Test results

Variable	Asymp. Significance	Relation
Thermal Sensation	0.397	Case I = Case II
Thermal Comfort	0.705	Case I = Case II
Air temperature (mean)*	0.000	Case I < Case II
Temperature Gradient	0.005	Case I > Case II
Air velocity (mean)	0.037	Case I < Case II
Radiant temperature	0.007	Case I < Case II
Surface temp. floor	0.005	Case I < Case II
Operative temperature	0.009	Case I < Case II
Distal skin temperature	0.017	Case I > Case II
Skin temperature – Head*	0.002	Case I > Case II
Skin temperature - Foot	0.007	Case I > Case II
Mean skin temperature	0.037	Case I > Case II
Change of distal temp. in time	0.037	Case I > Case II

** This significance is only found with three questionnaires in the dataset instead of one*

The results show that the Thermal Comfort and Thermal Sensation votes do not differ between the cases while the environmental variables are significantly different. Additionally, by changing the floor temperature (the intended manipulation), also the mean radiant temperature, air temperature, and operative temperature changed. Furthermore, only the skin temperature of the right foot, mean distal temperature and the mean skin temperature are different between the cases. However, those differences caused no change in TC or TS. The last observation is that Case I is lower in environmental temperatures, but the skin temperatures are always higher.

Relations analysis

To indicate a relationship between two non-normally distributed variables of a small sample, Kendall's tau is used. The value is in the range of -1 to +1, and the closer to one the better the relation. Conclusions about causality cannot be drawn from correlation coefficients, only relations are shown. [Field, 2009]

In this project is focused on the assessment of a downdraught situation. For that reason, only correlation coefficients between Thermal Sensation and other variables of the dataset are evaluated. This way, important elements of thermal comfort models can be found.
In table 3.7 the significant results of the Kendall's tau (correlation coefficients) are shown. The final three questionnaires of both cases are used to find a single correlation between TS and mean skin temperature. This does not mean no other correlations exist, but in this experiment those could not be found. Even significant parameters in literature, like core temperature or the change of skin temperature in time, did not show a correlation to TS.

Table 3.7 Significant correlation coefficients (Kendall's tau) with Thermal Sensation

Variable	Correlation coefficient	Significance
Mean skin temperature	0.208	0.025

Since no significance is found by the use of correlation coefficients, a linear mixed model is applied, although this is a parametric model. The fixed factors in the model are the case number and questionnaire number to correct for repeated measures. The random factor is the experimental subject. [West et al., 2007] One of the results with dependent variable TS and covariate mean skin temperature can be seen in table 3.8. With a significance of 0.211 ($p>0.05$) there is no relation. The only significant parameter found influencing TS during this experiment is the temperature difference between the left side and the right side of the body. In Appendix 12 all the linear mixed model results can be found.

Table 3.8 Linear mixed model; Dependent variable= TS_wholebody

Variable	Significance	Variable	Significance
Case	0.697	Case	0.966
Questionnaire	0.855	Questionnaire	0.625
Mean skin temperature	0.211	Temp. diff. Left-Right	0.012

3.4 Discussion and conclusion

In this paragraph the measurements and statistical results are discussed. Also the climate chamber and the cases will be treated. Finally, a conclusion regarding the relevant research questions is drawn.

Discussion

The results show an increased air velocity and related decreased air temperature close to the floor. This indicates that all experimental subjects are exposed to downdraught during the measurements in the climate chamber. Nevertheless, no air velocity around the feet is noticed by the subjects. Most of the time, the air velocity is felt at head level or at uncovered body parts where the measured air velocities are very low. It has to be noted that air velocities below 0.05 m/s cannot be measured by the Dantec.

The physiological results show that the core temperature is not affected by the cold wall, but the skin temperatures are. The right side of the body is always cooler than the left side. However, the left and right body parts show the same trend. In addition, individual differences in for example mean skin temperature are noticed and the skin temperatures of extremities fluctuate more to regulate heat exchange with the environment. In the comparison between the subjects it has to be noted that not all subjects are exposed to the same cases. The east (cold) wall varied in temperature (standard deviation > 0.5°C), because the cold water temperature depended on the aquifer system. For reproducibility an active cooling system is recommended. Furthermore, the anisotropic temperature distribution of the walls in Case II is ignored and the mean temperature of the wall is used in the remainder of the project because it is not expected to influence (thermophysiological) responses. In addition, because the ventilation box was located against the cold wall the inlet air temperature setpoint had to be 24.5°C to reach the intended 21.6°C inlet temperature in the climate chamber.

In the statistical analysis is found that Case I and Case II do not differ in Thermal Sensation votes, based on the Wilcoxon signed-rank test. However, the cases significantly differ in environmental conditions. The differences are small because a constant air temperature and operative temperature are desired and a heat balance has to be obtained. With the additional limitation of having only two water temperatures (already used for the wall of 13°C and floor heating in Case II), the remaining walls can only be free floating. Since the subjects need to be exposed to the same conditions, the free floating temperature has to come from the same value. For that reason, Case I is always followed by Case II.
The same statistical test also shows a difference between skin temperatures for both cases. The measured skin temperatures are always higher in Case I than in Case II, while the environment of Case I has lower temperatures. This can indicate that people are still cooling down by the cold wall or the reaction of the skin temperatures on the environment is

delayed by more than two hours (case duration). At least it shows that time plays an important role in thermal comfort prediction. Despite all differences between the cases, none of the subjects experienced it as uncomfortable.

The linear mixed model is used to find correlations between the various parameters within this project. However, for the two found correlations the question is whether it is a significant result or just coincidence due to the size of the dataset. To improve the method presented in this report a larger difference between the cases should be designed (one manipulation, which is hard to obtain in the built environment) or the number of participants should be increased. The sample size consisted of ten men (n=10), resulting in no normal distributed data and therefore less common non-parametric tests were needed for the analysis. Besides this, a repeated measurements method had to be applied.

Despite the unclear relations in this research, Zhang et al. (2010-part II) observed a dominant influence of the back, chest, and pelvis on thermal sensation. Also overall thermal state of the body influences the sensitivity to local thermal stimuli. [Zhang et al., 2004] This is also observed in this research. The whole body stays comfortable, while some body parts like feet and hands are sometimes uncomfortable. Also de Dear (2011) indicates the effect of for example local skin temperatures or change of skin temperature in time on whole body thermal comfort and sensation. He points out the importance of an individual simulation model of the human regulatory response with a comfort prediction included. Also in this research the individual differences are noticed.

Conclusion

In this conclusion an answer is given to the two relevant research questions in this chapter. Based on the performed measurements, also a first definition of downdraught can be given. Downdraught is an increased air velocity (between 0.15 and 0.20 m/s) and decreased air temperature close to the floor. An increased floor temperature increases the air velocities and decreases the vertical temperature gradient in the room. It did not have any influence on the Thermal Sensation or Thermal Comfort votes of people.

- *Because of what parameters are people thermally dissatisfied in case of a cold vertical surface and low temperature heating or no heating?*

Whether radiation asymmetry or draught is the main comfort problem could not be indicated by the measurements. In practice, it is more likely that higher air velocities occur (compared to the climate chamber) due to increased window heights than larger radiation asymmetries (because a window surface temperature of 13°C only occurs in the Dutch climate with single glazing). If there are still problems with downdraught other research can focus on air velocities around the feet. However, the effect of radiation asymmetry in time should also be considered.

- *What is acceptable / unacceptable in case of a cold vertical surface and a LTH-system?*

Based on the results of this chapter no indication of what is unacceptable for people can be given, because no such votes occurred in the experiments. It can be concluded that in a room with one cold wall (13.0°C – 14.0°C), an air temperature between 22.0°C and 22.5°C and a mean radiant temperature in the range of 21.0°C and 21.5°C no complaints occur due to downdraught (with a maximum air velocity of 0.2 m/s around the feet). One remarkable result is that when air velocity is felt, it is felt at the head and never around the feet because socks and shoes are worn.
From the calculated frequencies can be seen that all subjects accepted the situation and called it comfortable. Additionally, when thermal sensation moves to neutral, comfort increases and comfort decreases when thermal sensation moves away from neutral. When thermal sensation remains constant, thermal comfort does also remain constant.

Chapter 4
Thermal comfort prediction models

The experimental subject measurement results are also used to validate relevant thermal comfort models. It might be possible that the Standards (ISO 7730) and the Comfort Zones graphs are insufficient to predict thermal comfort in combined non-uniform environments and a new model or method is desired. In this chapter the main findings in literature related to the relevant thermal comfort models are shown. It is followed by simulation results of ThermoSEM. In the end, the actual validation of thermal comfort models is given.

4.1 Introduction on thermal comfort models

The relevant thermal comfort models for downdraught situations, ISO 7730 and the Comfort Zone graphs, are shortly explained in this paragraph. For more information is referred to Timmers (2010). In this project adaptability of people is not considered. The relevant research questions in this chapter are:

- In what way can global and local thermal comfort in downdraught situations be predicted with the Standards (EN-NEN-ISO 7730)?
- To what extent can (local) thermal comfort in downdraught situations be predicted with the outcome of the thermophysiological model ThermoSEM?

4.1.1 Standards (ISO 7730)

The standard ISO 7730 sets requirements for whole-body and local thermal (dis)comfort of healthy men and women in moderate thermal indoor environments, mainly offices.

The whole body comfort index is the Predicted Mean Vote (PMV) composed by Fanger (1970). The main variables of the model are air temperature, mean radiant temperature, clothing insulation, and metabolic rate. Using figure 4.1 the PMV can be converted to a Predicted Percentage Dissatisfied (PPD).
Local thermal discomfort can be caused by radiant asymmetry (ΔT_{pr}) from a cold wall, by warm floors (T_{fl}), as well as by too large temperature differences between head and feet ($\Delta T_{a,v}$) and draught. Equations are available that express the Percentage Dissatisfied (PD). Another local thermal discomfort parameter is draught, defined as unwanted cooling of the body by air movement. The Draught Rate predicts the percentage of people bothered by draught, using air velocity, air temperature, and turbulence intensity. [EN-NEN-ISO 7730]

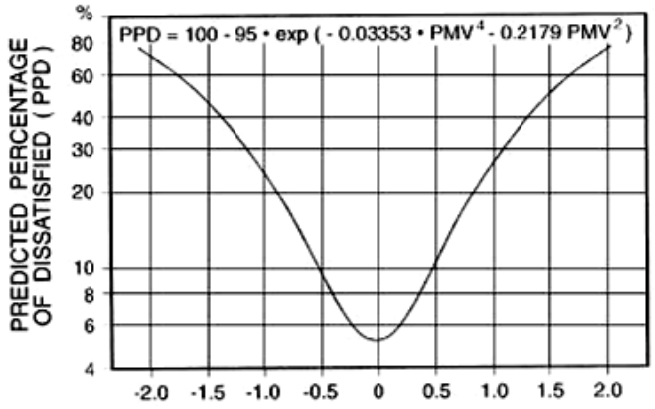

Figure 4.1 Relation between Thermal Sensation and PPD

Shortcomings

Despite its common use in Europe, ISO 7730 has some drawbacks. First, a total Percentage Dissatisfied caused by overall and local thermal comfort combined is unpredictable. [Olesen and Parsons, 2002] The constraint of the PMV is that it is based on a uniform environment and comfort for a large group is calculated instead of individuals. However, the PMV model is widely studied, tested and validated. [Timmers, 2008]
The local discomfort equations are based on sedentary people with summer clothing and close to thermal neutrality. Besides, local thermal discomfort is only treated separately in the standards while it can occur at the same time. Berglund (1987) and Toftum (2002) showed that discomfort due to draught is independent of radiant asymmetry and vertical air temperature differences. The effect of those parameters is additive. Sensation of draught also depends on activity level, clothing insulation, and overall feeling, all factors that are not included in the Draught Rate. [Toftum et al. 1996] Based on this, the accuracy of the rule of thumb is questionable because it only uses a maximum allowed air velocity as comfort criterion. Griefahn et al. (2002) modified the Draught Rate equation, as can be seen below, and included metabolic rate (M) and external work (W).

$$PD = (t_{sk} - t_a)(v_a - 0.05)^{0.6223} (3.143 + 0.37 \cdot v_a \cdot TU)(1 - 0.0061 (M - W - 70))$$
with $t_{sk} = 32.3 + 0.079 \cdot t_a - 0.019 (M - W)$

4.1.2 Comfort Zones (Nilsson)

According to earlier research performed by Timmers (2008) the only other relevant model to predict thermal comfort in combined non-uniform situations is the 'Comfort Zones graph'.

The Comfort Zones graphs (included in the car industry standards) use the whole-body equivalent temperature and the local equivalent temperatures to assess an environment. The equivalent temperature is defined as the temperature of a homogenous space in which a person has the same heat loss as under the actual (inhomogeneous) circumstances (see figure 4.2). [Nilsson and Holmer, 2003]
The relation between local equivalent temperatures and thermal comfort for 18 segments is shown in figure 4.3. In the graph, a neutral (-0.5<MTV<0.5), just comfortable (-1.0<MTV<-0.5 and 0.5<MTV<1.0) and uncomfortable (MTV<-1.0 or MTV>1.0) zone is created. The Mean Thermal Votes also correspond to a Percentage Dissatisfied (PD) as shown is figure 4.3. The whole body and local equivalent temperatures both have to be in the "cold / hot but comfortable" zones. [ISO DIS 14505 – part 2] [ISO DIS 14505 – part 4] [Nilsson, 2004]

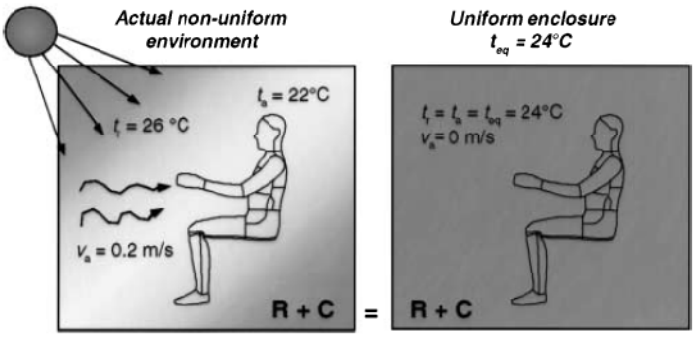

$$T_{eq} = \frac{h_r \cdot t_r + h_c \cdot t_a}{(h_r + h_c)} = t_s - \frac{R+C}{h_r + h_c}$$

Figure 4.2 Equivalent temperature [Nilsson, 2004]

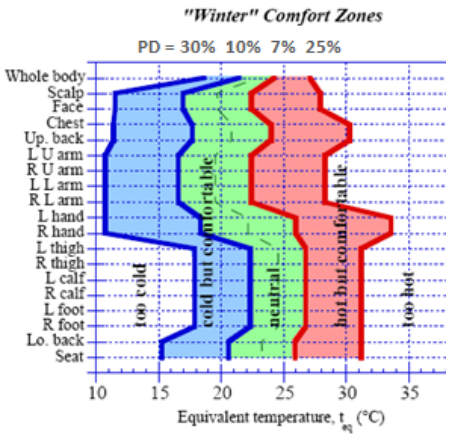

Figure 4.3 Comfort Zones graph

Shortcomings

Also the Comfort Zones graph has some limitations, though the method looks promising (a single graph for a non-uniform environment).
For designing the graphs, Nilsson (2004) used the Mean Thermal Vote scale instead of the Thermal Sensation scale, but also determined the relation between MTV and PD. The main limitation of the model is the use of equivalent temperatures. The needed radiative and convective heat transfer coefficients are hard to determine or additional simulations are needed, i.e. by CFD or ThermoSEM. De Dear et al. (1997) established the whole-body radiative coefficient (4.5 W/m²K) and the convective coefficient (3.3 W/m²K). However, the found values in literature are very diverse. In Appendix 14 the coefficients per body part according to de Dear et al. (1997) can be found together with equations to calculate the whole body heat transfer coefficient. Clothing surface heat transfer per segment is difficult to measure and no reports are found in literature.

4.1.3 ThermoSEM

A computer simulation of the human thermoregulatory system is a valuable tool to predict physiological responses for different situations. The Fiala model (1998) simulates the human body and heat transport mechanisms within the body and its periphery by an interacting passive and active system. This model is validated against a wide range of indoor climate conditions and showed good agreement. [Schellen, 2007] [Fiala et al.,1999]
Because of growing interest in 'personalized' models predicting thermal behavior of specific groups like elderly or individuals, the Fiala model was changed to ThermoSEM (2007). The human body is modeled with one spherical and 18 cylindrical body elements consisting of several tissue layers and sectors. The model is still in development. [van Marken Lichtenbelt et al., 2004] [van Marken Lichtenbelt et al., 2007] In this project this model is validated and its usefulness in thermal comfort prediction is assessed.

4.2 ThermoSEM simulations

In this paragraph the simulation results of ThermoSEM are compared to measurements to assess the performance of the latest version of the program (March 2011). First the applied method is shown, followed by the results and a discussion afterwards.

4.2.1 Method

In ThermoSEM, a man is implemented with 1.86 m² body surface area, of 73.5 kg, and with 14.4% fat. The possibility to vary those values is not yet implemented in the graphical user interface (GUI). Therefore, it is chosen to compare the simulation results to those of the experimental subject closest to the "standard man": subject 8. Also the results of all subjects are averaged to compare with the outcome of ThermoSEM.

In table 4.1 the input in ThermoSEM is shown, as well as in Appendix 15. The input consists of the air temperature, air velocity, and relative humidity at three levels in height. Also the temperature of six surrounding surfaces can be given. It is possible to give a transient input (every time step another value) instead of a constant value, but the climate chamber cases are steady and it makes a maximal difference of 0.13°C in the output, see table 4.2.

Table 4.1 Input ThermoSEM (deduced from the measurements)

Variable	Case I	Case II
Air temperature	22.0 °C	22.1 °C
Air velocity	0.08m/s	0.08 m/s
Wall temperature (window) Wall temperature (floor)	13.7 °C 23.0 °C	13.7 °C 24.3 °C
Relative Humidity	47 %	47 %
Metabolism	1.2 met	1.2 met
Clothing	Winter (1 clo)	Winter (1 clo)
Posture	Sitting	Sitting

Table 4.2 Comparison between constant input and transient measured input in ThermoSEM

Input	Mean skin temperature Case I	Mean skin temperature Case II
Constant input (after 100 min.)	32.47	32.32
Transient input (after 100 min.)	32.34	32.34

After 900 time steps the solution is converged and the simulated skin temperatures are constant. The core temperature, the mean skin temperature of the whole body, and the skin temperature of 17 body parts (Comfort Zones graph) are compared to measurements.

4.2.2 Results

Two results are treated in this subparagraph. First, the mean skin temperature (of 14 body parts) is assessed in time. In the graph of figure 4.4 the mean skin temperature of subject 8 in time is shown. The Root Mean Square (RMS) for the difference between simulations and measurements is for Case I 0.92°C and for Case II 1.08°C. However, it turned out that the skin temperature of the foot is extremely underestimated (by 5°C) and this temperature is included in the mean skin temperature calculation. When the foot temperature is removed from the average, the Root Mean Square (RMS) for Case I is 0.54°C and for Case II it becomes 0.71°C.

Also the trend of the skin temperature is followed by the simulation. In the measurements, the mean skin temperature of Case II is in the end lower than the mean skin temperature of Case I. This is also visible in the simulation results.

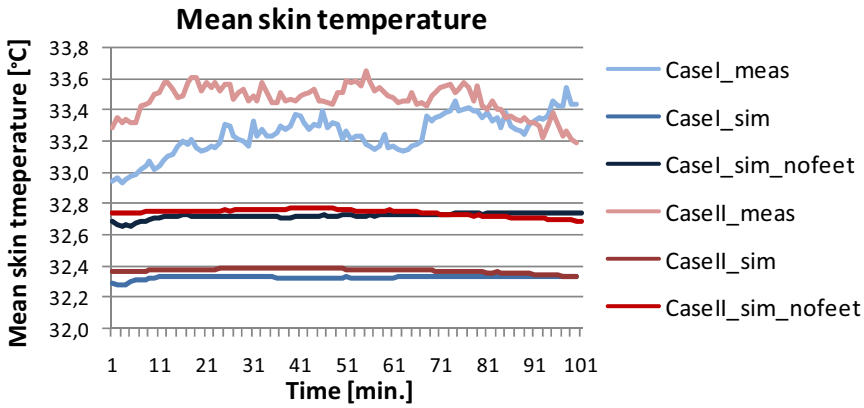

Figure 4.4 Comparison of measured and simulated mean skin temperature of subject 8

Second, the simulated and measured skin temperatures (averaged over all subjects) are compared for Case II. The results for Case I and for subject 8 are comparable (Appendix 16). In figure 4.5 the comparison for the core and skin temperatures of 15 body parts is shown. The core temperature (maximum difference 0.3°C) and the mean skin temperature (maximum RMS = 1.8°C) show good agreement. The foot, left upper arm, and lower back differ more than 2.0°C, without those body parts the maximum RMS becomes 0.9°C.

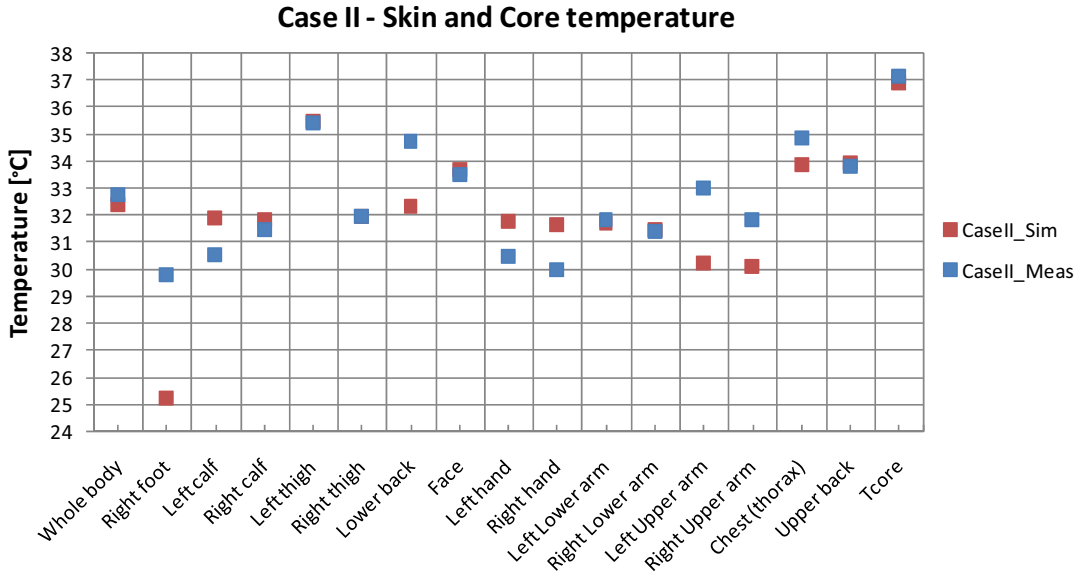

Figure 4.5 Comparison of measured and simulated core/skin temperatures (average of all subjects)

4.2.3 Discussion

In this paragraph only ThermoSEM is discussed. The RMS of the mean skin temperature in this project is better than 1.3°C found by van MarkenLichtenbelt et al. (2007). The skin temperatures of separate body parts sometimes deviate from the measured values, but the maximum RMS is still 1.8°C. When one individual is considered (for example subject 8), the RMS of skin temperatures increases to 2.2°C. But still the difference is often below 1.0°C. The largest deviation is found for the foot temperature. The foot temperature is measured at the top of the foot. In that way the subjects still could wear their own shoes. However, the measured temperature is not at the extremity. Next to that, the higher air velocities only occur at foot level and the cooling is perhaps overestimated with ThermoSEM. Furthermore, the model predicts the trend and core and skin temperatures close to reality for those downdraught situations.

For this project, the output in terms of heat transfer coefficients and heat fluxes is used. It is assessed whether it is useful in thermal comfort prediction, using the output to calculate equivalent temperatures.

4.3 Validation of thermal comfort models

The two relevant thermal comfort models, ISO 7730 and the Comfort Zones graphs, are validated in this paragraph. The method and results are shown and finally the validation is discussed. The conclusion regarding the research questions is given in paragraph 4.4.

4.3.1 Method

The method consists of three parts. First the whole body comfort index (PMV) is considered, followed by the local comfort criteria. Finally, the Comfort Zones graph is assessed.

The predicted mean vote (PMV) is compared to the actual mean vote (AMV) of the subject to test the PMV-equation of Fanger in downdraught situations. For every case, the final three questionnaires are taken into account to calculate the mean AMV and its standard deviation.

For all local thermal discomfort parameters the percentage dissatisfied is calculated. This includes draught, the radiation asymmetry, the vertical temperature gradient, and the floor temperature. It is also compared to the thermal comfort votes of the subjects.

To assess the Comfort Zones graph, the equivalent temperatures have to be calculated and the subject votes for every body part have to be located in a "comfort zone".
The subject votes have to be compared to the predicted comfort in the Comfort Zones graph. The mean AMV for all subjects is around zero for all body parts and Nilsson included a neutral line in the Comfort Zones graph. This way, the body parts can be placed in the "neutral green zone" by using the AMV of the subjects.
To calculate the equivalent temperatures, the skin temperature and related heat flux, resulting from ThermoSEM, can be used or environmental parameters. Also the (radiative and convective) heat transfer coefficients are needed. De Dear (1997) measured the coefficients, but those can also be found in the output of ThermoSEM (based on Fiala). A comparison between those heat transfer coefficients is made, shown in table 4.3.

Table 4.3 Heat transfer coefficients (hr + hc) of de Dear and ThermoSEM (Fiala)

Body part	de Dear	ThermoSEM
Whole body	7.8	-
Scalp	7.6	8.6
Face	7.6	8.6
Chest (thorax)	6.4	6.0
Upper back	7.2	6.7
Lower back	7.2	6.8
Left Upper arm	8.2	7.6
Right Upper arm	8.2	7.5
Left Lower arm	9.0	7.7
Right Lower arm	9.0	7.8
Left hand	8.4	7.5
Right hand	8.4	7.6
Left thigh	8.3	7.3
Right thigh	8.3	7.2
Left calf	9.4	7.8
Right calf	9.4	7.9
Left foot	8.4	8.4
Right foot	8.4	8.6

4.3.2 Results

The results are divided in three parts, as explained in the method part. Only the relevant graphs are presented in this report, other results can found in Appendix 16.

ISO 7730 - Whole body comfort

With the PMV (Predicted Mean Vote) the whole body comfort of people is predicted. Both cases are designed at PMV = 0, and consequently no complaints are expected. However, the question is whether the PMV of Fanger predicts comfort correctly in non-uniform situations, such as those downdraught situations. Therefore, a comparison is made between the PMV and AMV of every subject for Case I and Case II, see figure 4.6.

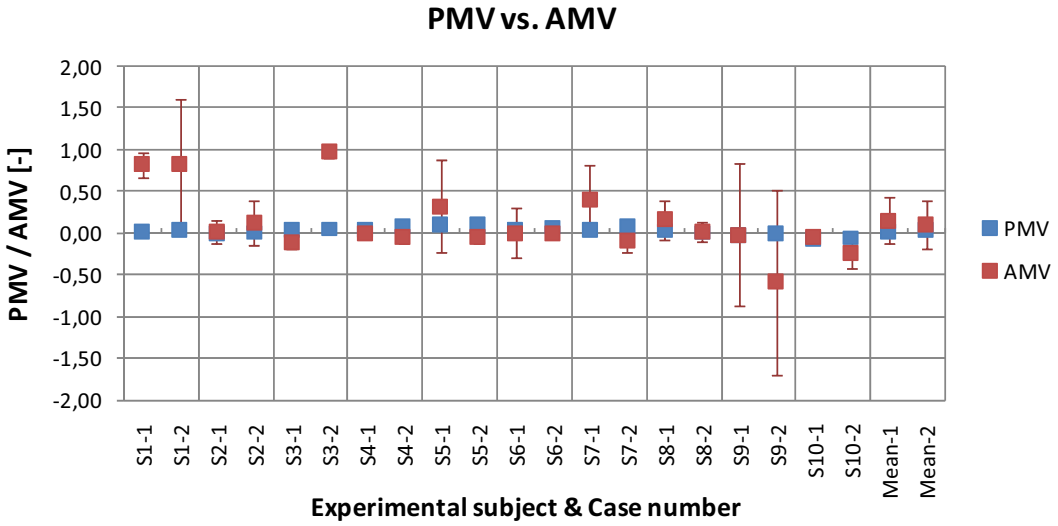

Figure 4.6 Comparison of the Predicted Mean Vote (PMV) and Actual Mean Vote (AMV)

From the results can be seen that the PMV predicts the Actual Mean Vote well. In only two cases the AMV is above the PMV. When looking at the average of all subjects, the PMV and AMV are the same. One outstanding result is that the votes of Case II often are lower than those of Case I while statistically seen Case II is warmer (table 3.6).
Also the percentage dissatisfied is calculated, shown in table 4.4. The mean PMV scores result in a predicted percentage dissatisfied (PPD) of 5% for both cases.

Table 4.4 Predicted Percentage Dissatisfied

	Case I	Case II
Mean PMV (-)	0.02	0.04
PPD (%)	5%	5%

ISO 7730 - Local body comfort

Also the four local body comfort equations, as given in ISO 7730, are assessed. This is difficult because a percentage dissatisfied outcome has to be compared with the outcome of ten subjects. Nevertheless, the predicted results for all subjects are shown in table 4.5.

Table 4.5 Predicted Percentage Dissatisfied [%] due to local thermal discomfort

	Case I			Case II		
	Mean	Min.	Max.	Mean	Min.	Max.
Draught Rate	4.2	3.6	6.0	5.6	4.2	9.2
Vertical Air Temp. Difference	1.1	0.7	1.2	0.7	0.6	0.7
Warm floor	5.6	5.6	5.6	5.6	5.6	5.7
Radiation Asymmetry – cold wall	1.1	1.0	1.2	1.1	0.9	1.2
Total sum	11.9	11.2	13.2	13.0	11.6	16.4

As can be seen in table 4.5 the predicted percentages dissatisfied due to local thermal discomfort is very low (<6%). According to Berglund, the percentages can be added, which brings the percentage dissatisfied to 13%. During the measurements, the subjects did not complain about the situation.

Because it is expected that draught plays an important role in downdraught situations, the Draught Rate is also calculated for the area around the feet and with the adjusted equation of Griefahn et al. The results are presented in figure 4.7. The equation of Griefahn et al. lowers the PD due to an increased metabolic rate. In the area close to the feet the Draught Rate increases to 9%, which is still below the limits (20%) indicated by ISO 7730.

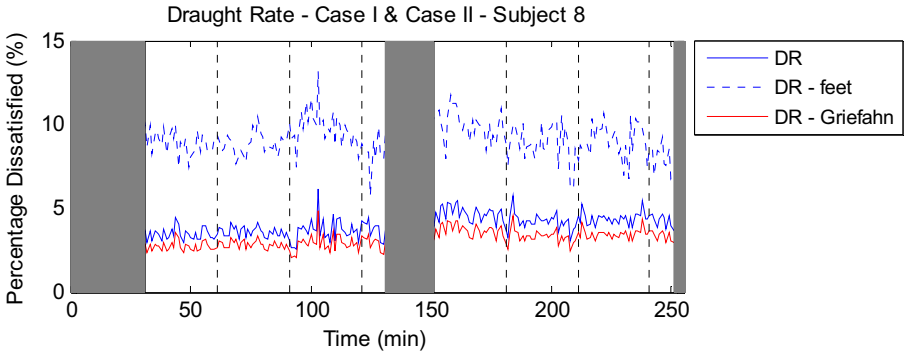

Figure 4.7 Draught Rate – in the room, around the feet, and the Griefahn et al. equation

Comfort Zones graph (Nilsson)

The other model that is assessed is the Comfort Zones graph of Nilsson (2004). In the first graph of figure 4.8, the averaged subject votes are drawn. All votes for the body parts and whole body were in the green “comfortable” zone around the neutral line. The remaining graphs show the predicted comfort (black line) based on a different equivalent temperature calculation. First the outcome of ThermoSEM is used (skin temperatures), in the lower two graphs the mean radiant temperature and air temperature are used with different heat transfer coefficients (htc). The choice of the coefficients of de Dear or ThermoSEM does not influence the equivalent temperatures. When the environmental parameters are used all parts are still in the green “comfortable” zone, but those do not follow the neutral line. With the outcome of ThermoSEM, the right side of the graph (arms and chest) is slightly overestimated in the red “warm but comfortable” zone.

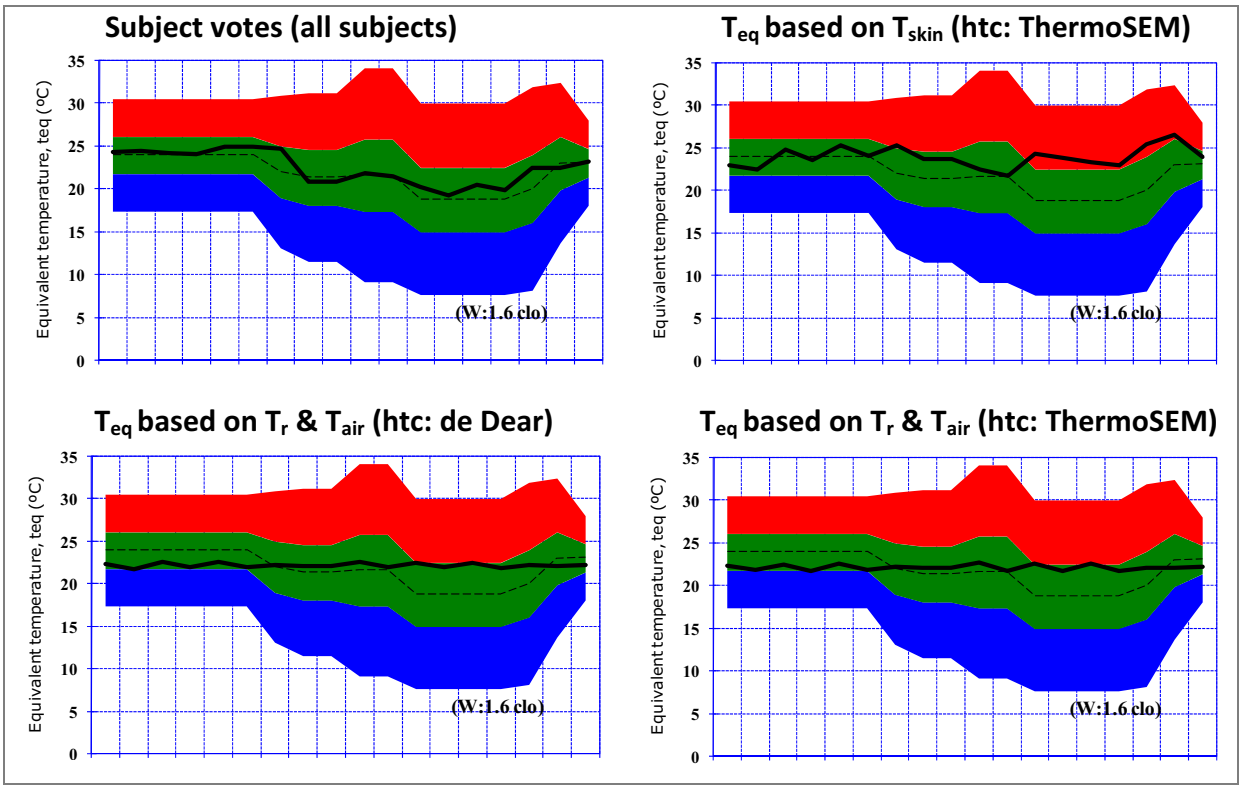

Figure 4.8 Comfort Zone graphs (subject votes and prediction with different calculation methods)

4.3.3 Discussion

In this discussion the validation of the relevant thermal comfort models is discussed. Mainly ISO 7730 is treated, with inclusion of literature. Furthermore, the potential of the Comfort Zones graph is explained.

The whole body comfort model (PMV of Fanger) is a good predictor of thermal comfort in the researched downdraught cases, although literature shows that the model is best applicable in uniform cases. The non-uniform cases in this study are designed at PMV = 0, but it is recommended to research the PMV model also for the total range (-3 to 3).
The AMV values of Case II are often below those of the colder Case I. This is also noticed during the statistical analysis, in which the skin temperatures were lower in Case II. People are probably still being cooled by the cold wall, indicating that time plays a role in comfort prediction due to radiation asymmetry.

Also the local thermal comfort models of ISO 7730 are assessed. According to Berglund (1987) and Toftum (2002), all local effects are additive. In this case, the models result in a total PPD of 12% for Case I and 13% for Case II due to local effects. In this research, a low number of people voted for an uncomfortable situation as well. The remark is that only ten subjects are used. Therefore, the local thermal comfort models are difficult to validate. For example, a percentage dissatisfied of 12% with ten people cannot be measured reliable.

For the same reason it is unclear from this research how reliable the Draught Rate is. The percentage dissatisfied around the feet is 9% but with the socks, shoes, and trousers worn during winter it is questionable if it will ever be noticed (at least not in this research). Furthermore, the Draught Rate is designed for draught at the neck and the average in the room (4 - 6%) is too low to be noticed by the subjects and to validate the model.

In ISO 7730, limits for every discomfort parameter are given. In this research, two cases are used that are still below those limits. Because no complaints did rise, it is suggested to design two different, more extreme, cases on comfort level to validate thermal comfort models like the standards. As said by Olesen and Parsons (2002) there is no method for combining the percentages dissatisfied people due to whole body and local comfort to give a prediction of the total number of people rating an environment unacceptable. In this research, the additive value for local and whole body comfort is 17% for Case I and 18% for Case II. However, only 5% of the subjects voted Case I uncomfortable and for Case II no uncomfortable votes occurred (figure 3.24). Since all cases are accepted this shows that summing the percentages is not allowed. Future research has to establish another, correct way to predict the total percentage dissatisfied.

With the Comfort Zones graph it is difficult to obtain a comparable comfort prediction. This is due to different calculation methods for the equivalent temperatures. Theoretically, the outcome should not change using different calculation methods, but because of all assumptions (for example different heat transfer coefficients) it does. The subjects also voted a thermal sensation around zero for a body part, but indicated the same body part as uncomfortable. This combination is not possible in the Comfort Zones graph. Consequently, more research on the relation between sensation and comfort is needed.

4.4 Conclusion

The answers on the relevant research questions in this chapter are given in this paragraph. A short final conclusion on the use of thermal comfort models in the rest of this project is given subsequently.

- *In what way can global and local thermal comfort in downdraught situations be predicted with the Standards (EN-NEN-ISO 7730)?*

The PMV of Fanger is a good predictor of thermal comfort in the downdraught situations tested in this project. Also the local thermal comfort equations predicted a low number of dissatisfied people, which is also the case with the subjects. However, as explained in the discussion, this can be deceptive, based on the low number of participants. In this project, with the downdraught cases, ISO 7730 is a sufficient predictor of thermal comfort of people.

- *To what extent can (local) thermal comfort in downdraught situations be predicted with the outcome of the thermophysiological model ThermoSEM?*

At this moment, ThermoSEM predicts skin temperatures correctly within a RMS of 1.8°C. Nevertheless, a link between the outcome of ThermoSEM (consisting of skin temperatures, heat fluxes and heat transfer coefficients) is needed to predict thermal comfort. The only relevant existing model is the Comfort Zones graph, containing the comfort for the whole body and 17 body parts. This way, it is also possible to look at the effect of local stimuli which is an advantage regarding the Standards (ISO 7730). However, calculating the correct equivalent temperatures turned out to be difficult. It can be concluded that more research is needed to link the outcome of ThermoSEM to a thermal comfort prediction. Furthermore, the Comfort Zones graphs look promising but are not very user-friendly.

Within this project ISO 7730 will be used to assess a downdraught situation, being the best prediction model at the moment. The graphs of Nilsson will be used to get an impression of local effects (by using ThermoSEM) but not to draw conclusions regarding thermal comfort.

Part III

Downdraught prediction with CFD

This third part of the report treats the Computational Fluid Dynamics (CFD) simulations that are performed to predict downdraught flows. With a calibrated CFD model and a thermal comfort prediction model, several variants can be compared and assessed. The focus in the variant study is on window height above standard room height, because this is a shortcoming of existing downdraught studies.

Chapter 5

Calibration of the CFD model

Before the variant study can be done, it is essential to know the reliability of the CFD model. As a result, the 3D model of the climate chamber is calibrated by air temperature and air velocity measurements. In this chapter the calibration method is explained with a discussion of the results. Prior to that, an introduction on CFD is given.

5.1 Introduction on CFD

Fluid dynamics can be considered as fluid flows in motion, based on the conservation laws: conservation of mass, momentum, and energy. Resulting flows can be laminar or turbulent (unstable with irregular fluctuations). Generally, it is impossible to find analytical solutions. Numerical simulations (CFD) can be used to find solutions for more complicated cases such as downdraught situations. For more background information is referred to literature, since fluid dynamics is a very complicated and extensive specialism. [van Heijst, 2007]

Natural convection

With CFD simulations downdraught (air temperature and velocity) can be simulated. It is a natural convection problem of which the velocity profile is shown in figure 5.1. The velocity in the boundary layer equals zero at the surface because of the no-slip condition. After that, it increases until a maximum is reached and at a certain distance (δ) the velocity returns to zero. It is proven to be difficult to predict flow characteristics of natural convection flows correctly. To describe the natural convection flow, the boussinesq approximation is used in which density variations are neglected except for the buoyancy forces. [Loomans, 1994]

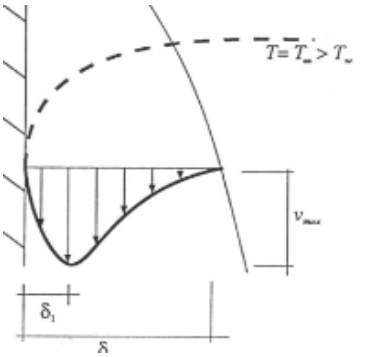

Figure 5.1 Natural convection velocity profile

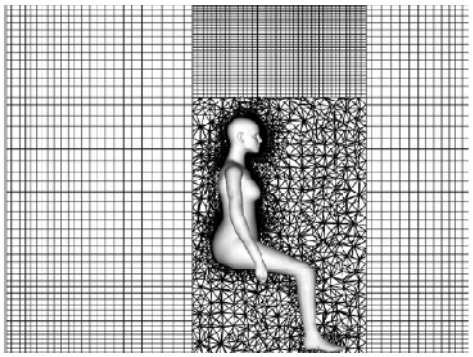

Figure 5.2 Two types of meshes

CFD model

To perform a CFD simulation, an indoor environment has to be divided in control volumes (cells). The accuracy of the solution and computing time highly depend on the number of those cells. A mesh can be structured or unstructured (figure 5.2). Often cells are distributed irregularly, with more cells at places where the flow varies the most. Near the wall a special treatment is needed, such as the wall function method or low-Reynolds-number-modeling. In complex 3D flows, wall functions are often the only possibility to perform the simulation with. Wall functions are used when $y^+ > 30$ and low-Reynolds-number-modeling when $y^+ < 5$. The y^+ value is a dimensionless number representing the distance between the wall and the first grid point and depends on the occurring flow characteristics. Also a grid sensitivity study has to be done by refining the grid to obtain a grid independent solution. [Blocken, 2008] It is possible to put a person or heat source in the model. Topp et al. (2002) concluded that the amount of detail only has an influence in the near region of the simulated person. Boundary conditions like heat fluxes, wall temperatures, or inlet and outlet characteristics can be specified in the CFD program.

Turbulence modeling

The most applied method for indoor air flow is RANS (Reynolds Averaged Navier-Stokes) in which turbulence is modeled with often the k-ε model or the k-ω model. The k-ε model is based on transport equations for turbulent kinetic energy (k) and its dissipation rate (ε) and in the k-ω model turbulence frequency (ω) plays an important role. Stamou et al. (2006) showed that all models predict the main features sufficiently. However, the RNG k-ε model is more accurate than the standard k-ε model and the SST k-ω model simulates buoyancy-driven flows better. Nevertheless, the performance of a turbulence model is problem dependent and there is no universally preferable turbulence model. [Zhang et al., 2007]

CFD simulations

Simulations are preferred above full-scale measurements because different situations can be modeled, it is less expensive, and results are more detailed. With CFD, for every grid point the value of the variables (i.e. air velocity) is calculated by discretization equations. However, to obtain reliable results, calibration with experimental results is needed. [Loomans, 1998]

Finally, an unsteady calculation (time dependent solution) must be performed to reduce convergence problems. At the time the value of a variable remains constant or the residual norm becomes smaller than the set limit, the solution is called converged. This way the iteration-convergence error is minimized. [Blocken, 1998] [Hsieh et al., 2004]

The main research question that is going to be answered in this chapter is also related to an important remark of Manz (2003). He states that the user's knowledge and experience with CFD simulations influences the accuracy of the simulations. Therefore, the question is:

- How accurate can downdraught cases be predicted with CFD?

With the calibration measurements, also the next question can be answered:

- How can downdraught be defined in terms of air velocity, air direction, air temperature, turbulence intensity and other parameters?

5.2 Methodology

In this paragraph two methodologies are treated. First the calibration measurements are explained and subsequently the simulation methodology. Both methods are required to calibrate a CFD model and to minimize physical modeling errors. The calibration results are shown in the next paragraph.

5.2.1 Calibration measurements

One of the objectives of the calibration measurements is to gain more insight in the flow pattern in case of downdraught. However, the main goal is to collect measurement data of the flow in the room and of the boundary conditions to calibrate the CFD model. In this paragraph the measurements are explained in terms of cases, equipment, grid and planning.

Climate chamber cases

A CFD model of the 3.6 x 5.4 x 2.7 m^3 climate chamber at the TU/e (described in paragraph 3.2.1) is created. The same cases as for the experimental subjects are used for calibration measurements. Those cases can be found in paragraph 3.2.2. For completeness, the composed cases are shown again in figure 5.3.

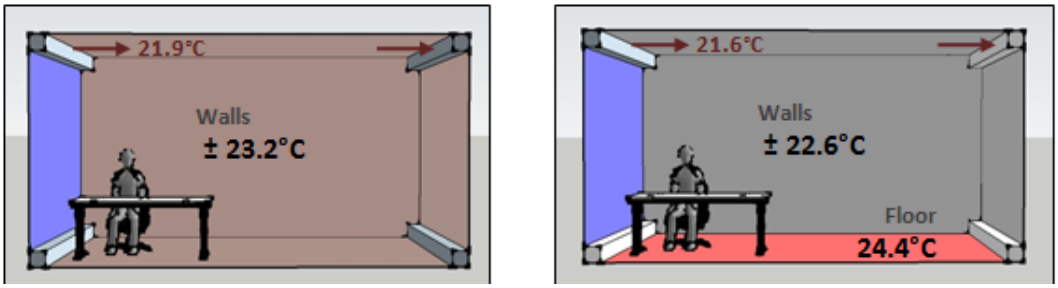

Figure 5.3 Measurement cases: Case I (left) & Case II (right)

Parameters and measurement instruments

During this research thermal comfort models are used with input from the CFD simulations. According to previous research by Timmers (2008) the most sensitive parameters of the models in ISO 7730 are air velocity, air temperature, radiant temperature and clothing. Skin temperature in ThermoSEM is mostly affected by air velocity and metabolism. From these parameters, air velocity and air temperature can be simulated with CFD. It is important to validate the CFD model on these parameters to indicate the reliability.

The air temperature is measured by NTC's and Dantec's are used to measure air velocity. The instruments are explained in paragraph 3.2.3 and Appendix 5. Only physical parameters are measured, because no human being is present in the room. To compensate the heat flow from a human being a thermal manikin is placed in the climate chamber. In figure 5.4 the manikin, made by Loomans (1998), can be seen. The output is fixed at 135 Watt (evenly distributed), to compensate for a human being with 1.2 met and a laptop.

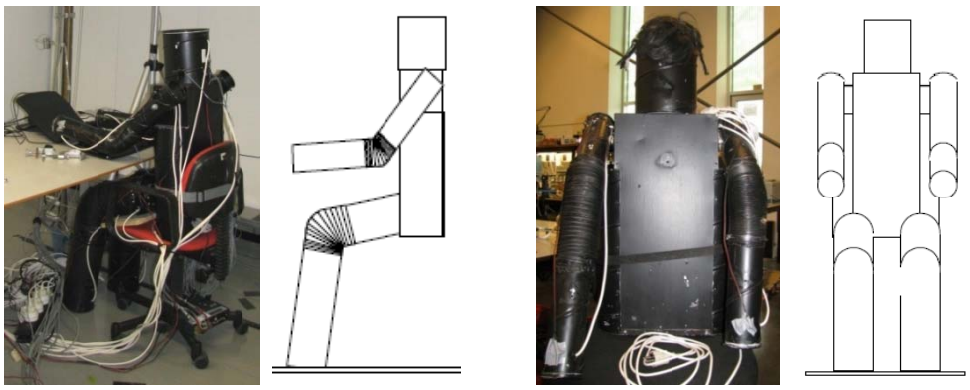

Figure 5.4 Thermal Manikin of Loomans (1998)

Table 5.1 Overview of measurement parameters and equipment

Variable	Unit	Range	Accuracy	Uncertainty	Interval [s]	Sensors
Air temperature	°C	10-40	±0.5	0.2°C	60	8 NTC
Air velocity	m/s	0.05-1.0	±(0.05+ 0.05v_a)	10%	1/10	8 Dantec
Surface temperature	°C	0-50	±1.0	0.2°C	60	54 U-therm.
Inlet profile						NTC + Dantec

Measurement grid and planning

In total, three calibration measurements are done. First Case I is measured to improve the measurement plan. Finally, Case I and Case II are measured to obtain the calibration data.

During the calibration measurements, one tripod is used and relocated. Seven hot sphere anemometers are combined with NTC's (to measure air temperature). The sensors are located at an interval of half a meter in height (0.1m – 0.6m – 1.1m – 1.6m – 2.1m – 2.6m)

and labeled from A (0.1m) to G (2.6m). One sensor (B) is placed at 0.2m because the ventilation boxes can influence the air flow at that height. When measuring close to the east wall the tripod has to be located between the ventilation boxes. Therefore, a tripod is needed with different measurements heights (0.3m – 0.6m – 1.1m – 1.6m – 2.1m – 2.4m) labeled from B to G, see figure 5.6. Air temperature and air velocity are also measured close to the inlet. At the chosen position (figure 5.5) the tripod influences the air flow the least. Finally, the reference point (at a height of 1.1 meters) is located close to the door to monitor the influence of opening and closing the door on the environmental conditions.

The measurement grid is shown in figure 5.5. Because measurement position 10 did not give additional information it is replaced by position 7*. The air flow due to downdraught with and without an obstruction (thermal manikin) can be compared this way. Eleven positions are spread over the room to calibrate the CFD model in x-, y-, and z-direction.
After relocating the tripod, a fifteen minutes stabilization period is used based on Loomans (1998) to let the air flow stabilize. This is followed by a five minute period in which data is gathered. For positions nine and eleven the tripod needed to be rebuilt. At those positions downdraught is measured without the surface temperature sensors at the cold wall to remove its influence to the airflow.

Measuring one case takes around four hours without the system setup time. To measure two cases in one day, the maximum number of positions is eleven. For the elaborated planning is referred to Appendix 17.

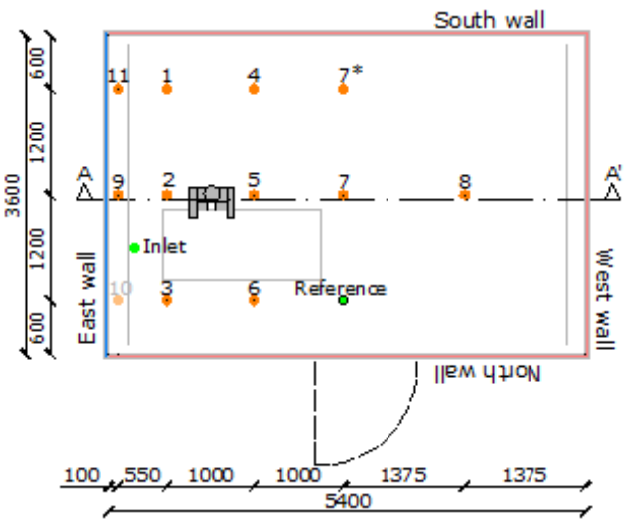

Figure 5.5 Floor plan of the measurement grid

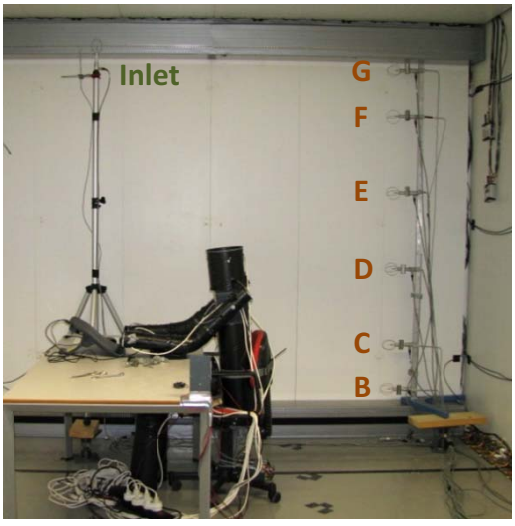

Figure 5.6 Calibration measurements

5.2.2 CFD simulations

In this subparagraph the simulation methodology is treated. The used model, boundary conditions and performed simulations are explained. The objective of the CFD simulations performed in this part of the research is to assess the reliability of the model and to obtain the correct input parameters for CFD. In this project, Fluent is used as the CFD software.

CFD model

In Gambit, the climate chamber is modeled (see figure 5.7 for dimensions). The details of the chamber like the ventilation boxes are implemented, but the lights are simplified to two beams. Also the human being, based on the dimensions of the thermal manikin, is built together with a chair and table. The legs of the chair and table are not included because it is expected that those will not influence the downdraught flow significantly.

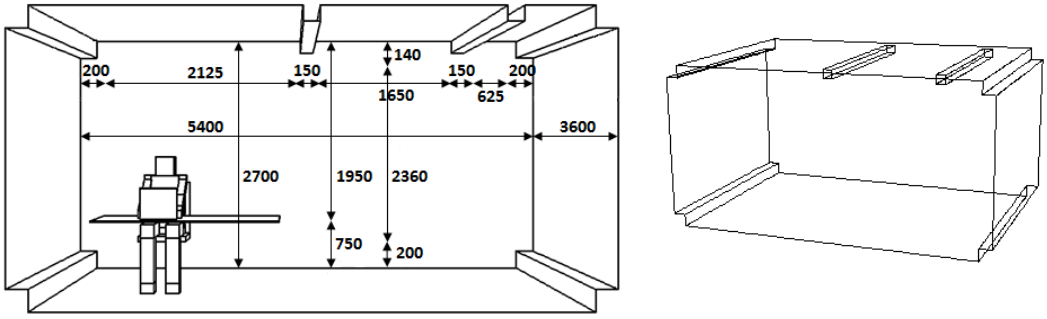

Figure 5.7 Computational domain – Climate chamber

Three different grids are created: one grid for the model with a human being and two grids for the empty climate chamber (coarse and fine). The advantage of an empty room is the decrease of the number of cells and in turn less computational time. For the model with a human being a hybrid grid is used, unstructured around the person and structured in the rest of the room. In table 5.2 and figure 5.8 all grids and related sizes are shown. To improve modeling of the natural convection boundary layer more cells are present close to the walls and around the human being to decrease the y^+ value. In Appendix 18 more information about the grid can be found.

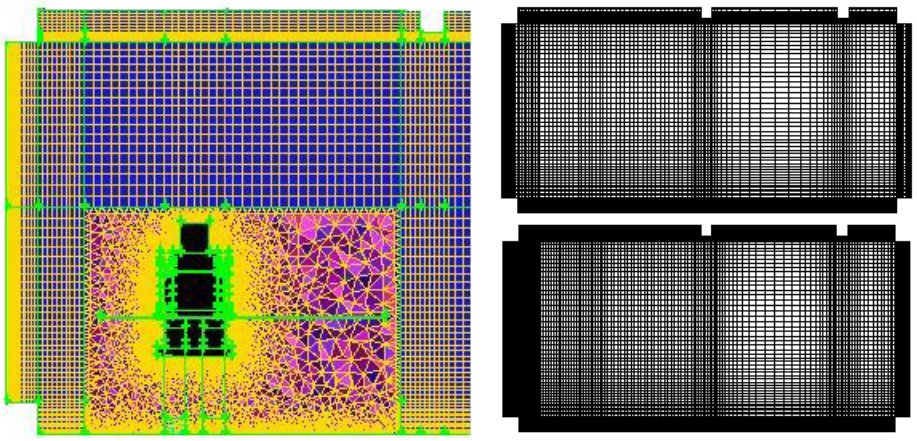

Figure 5.8 Hybrid grid (coarse) & structured mesh (above: coarse – below: fine)

Table 5.2 Grid sizes

Model	Number of cells	y^+ value - window	y^+ value - floor
Human being – coarse	1,350,579	10	10
Empty – coarse	511,599	10	8.5
Empty - fine	1,092,874	5	8

Fluent (solve) settings and boundary conditions

Before simulations can be performed, the solve settings have to be defined in Fluent. Some are constant for all simulations and some are case dependent.

In all cases, 3D transient RANS simulations are performed. Because of the RANS simulation method, a turbulence model has to be selected. From literature can be concluded that in case of natural convection and indoor air flow the RNG k-ε with enhanced wall treatment or the SST k-ω model can best be used. Also the boussinesq approximation has to be applied (natural convection problem) with a thermal expansion coefficient of 0.00341 K^{-1} and a gravitational acceleration of -9.81 m/s².
In case of the empty model has to be compensated for the heat flux of the human being. This is done by increasing the wall temperatures (+0.6°C for the climate chamber) or by implementing a User Defined Function (UDF) in Fluent (828.5W/m³ with 0.082m³). Finally, the specified boundary conditions are shown in table 5.3 and table 5.4.

Table 5.3 Constant boundary conditions

Boundary condition	Case I	Case II
Outlet	Outflow	Outflow
Light beam 1	75.2 W/m2	75.2 W/m2
Light beam 2	0 W/m²	0 W/m²
Human being	29.5 W/m²	29.5 W/m²
Laptop	41.7 W/m²	41.7 W/m²

Table 5.4 Measured boundary conditions (case dependent)

Boundary condition	Case I	Case II
North wall	296.25K (23.1°C)	295.85K (22.7°C)
South wall	296.35K (23.2°C)	295.85K (22.7°C)
East wall (window)	286.95K (13.8°C)	286.55K (13.4°C)
West wall	296.35K (23.2°C)	295.95K (22.8°C)
Floor	296.15K (23.0°C)	297.45K (24.3°C)
Ceiling	296.45K (23.3°C)	296.05K (22.9°C)
Inlet – Air temperature	295.15K (22.0°C)	295.15K (22.0°C)
Inlet – Air velocity	1.0 m/s	1.0 m/s
Inlet – Turb. length scale	TU: 7% – 0.0014	TU: 7% – 0.0014

After defining the model, the iteration process has to be started. A second order upwind discretization scheme is applied. The convergence criterion for every residual is 10^{-6} and several points are monitored. In the end, a heat balance has to be established.
To iterate, a time step of 1.0 second with ten iterations is used, resulting in 2700 time steps (45 minutes real time) for all simulations to obtain the results. For the total Fluent input is referred to Appendix 18.

Simulation planning

Several simulations are performed to compare the effect of for example input parameters on the model performance. It is started with a comparison between 2D and 3D simulations with a coarse and fine grid. In addition, several manipulations are done to increase the performance of the simulation like decreasing the underrelaxation factors, trying the PRESTO! solution, giving an initial value to the velocity components, or performing a steady state simulation with a lowered gravitational constant. This last solution is introduced by Neale (2006). All results are used to make simulation planning for calibration, as given in table 5.6. Next to those simulations, three types of special simulations, shown in table 5.5, are done to gain more knowledge about the performance of a model.

Table 5.5 Special simulations

Model	Grid	Specialty
2D - Empty	Coarse	Without ventilation boxes
3D - Empty	Coarse	Heat exchange
3D - Empty	Coarse	Time step size

Table 5.6 Calibration simulations

Model	Grid	Manipulation	Case	Ventilation
3D – Human being	Coarse	-	Case II	Yes
3D – Empty	Coarse	User Defined Function	Case II	Yes
3D – Empty	Fine	User Defined Function	Case II	Yes
3D – Empty	Coarse	Compensated by walls	Case II	Yes
3D – Empty	Coarse	Compensated by walls	Case II	No
3D – Human being	Coarse	-	Case I	No
3D – Empty	Coarse	User Defined Function	Case I	No
3D – Empty	Coarse	Compensated & SST-kω	Case I	No
3D – Empty	Coarse	Compensated & RNG-kε	Case I	No
3D – Empty	Fine	Compensated & RNG-kε	Case I	No

5.3 Results

The calibration measurement results are comparable to the physical measurement results of the experimental subjects, treated in paragraph 3.3.2. In this paragraph only the remarkable calibration measurement results are shown. The simulation results, which are compared to the calibration measurements, are also treated in this paragraph.

5.3.1 Calibration measurement results

All calibration measurement results of surface temperatures, air temperature, air velocity, and turbulence intensity can be found in Appendix 19. From the results can be seen that

downdraught occurs leading to higher air velocities and lower air temperatures at floor level. The air flow in the rest of the room is fluctuating, resulting in high turbulence intensities.
The differences between Case I and Case II are very small, mainly noticeable at the surface temperature level. The air velocities near the floor are also higher in Case II (0.02m/s). The intended surface temperature of 13°C for the east wall (window) could not be reached by the system during the calibration measurements.

Two other results that could not be observed during the subject measurements can be seen in figure 5.9 and figure 5.10.

Figure 5.9 shows the air velocity and air temperature at the reference point during one case. From the air velocity it is obvious when the door is opened and closed to relocate the tripod. It can be observed that the air velocity stabilizes very fast after closing the door. Around 200 minutes the tripod is rebuilt and therefore the disturbance in air velocity is larger than at the other times. The air temperature is not influenced by opening the door. Rebuilding also raises the air temperature with ± 0.2°C.

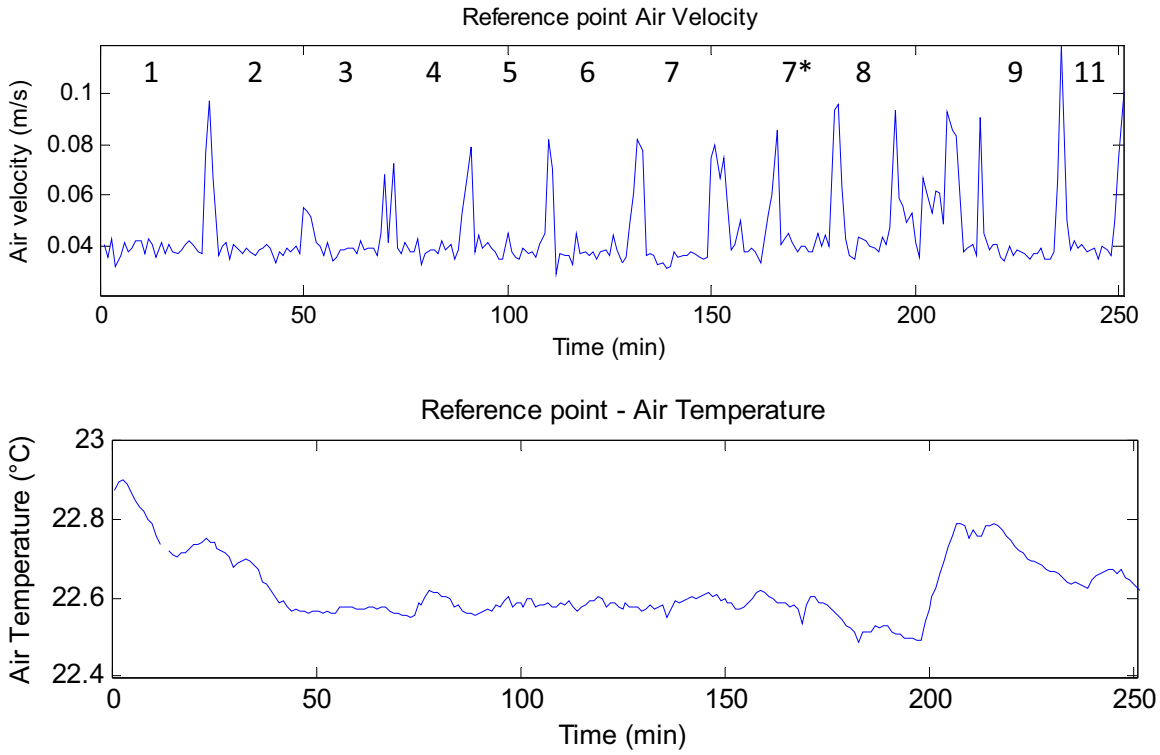

Figure 5.9 Air velocity and air temperature at the reference point during one case

In figure 5.10 the air flow pattern at 0.1 meter above the floor is given by the air velocity and the air temperature at measurement locations 9-2-5-7-8 and 11-1-4-7*. The blue line indicates an obstruction in the flow (thermal manikin) and the green line is an undisturbed air flow. The thermal manikin is located one meter from the window. It can be seen that the air temperature is not influenced by an obstruction, but the air velocity is higher in an undisturbed flow than when it is blocked by the thermal manikin.

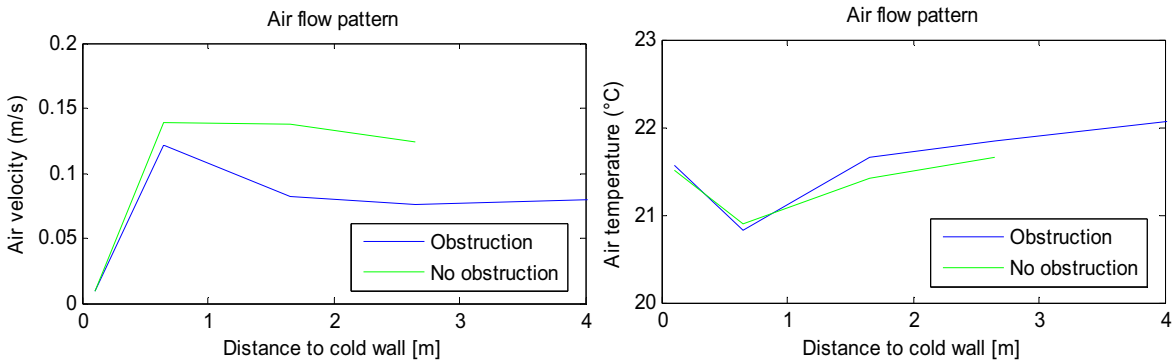

Figure 5.10 Air velocity and air temperature at 0.1m above the floor

To finish, the reproducibility is assessed because Case I is measured two times. The results of those two measurements can be seen in figure 5.11. The results show that the case could be reproduced. Also the accuracy is given in the graphs by error bars. The standard deviation is included in that bar with the instrument inaccuracy added.

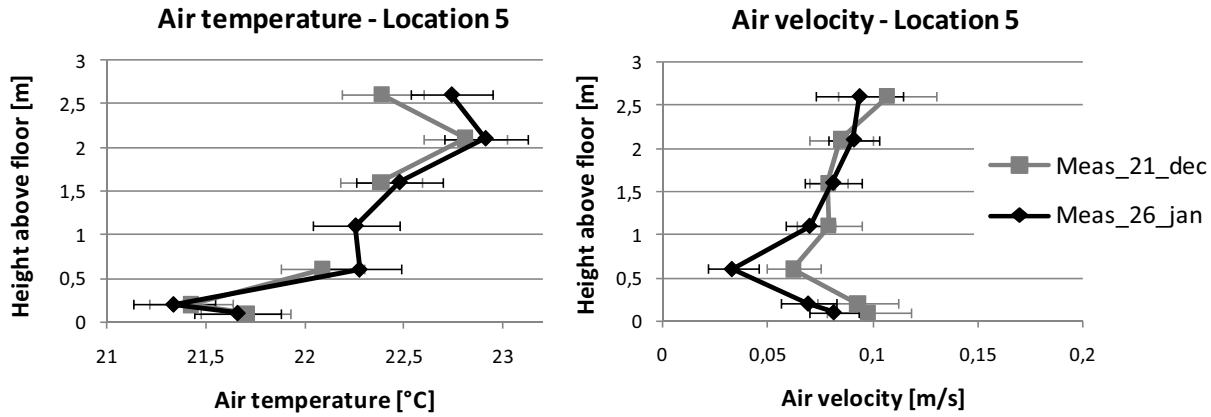

Figure 5.11 Reproducibility of the measurements

5.3.2 Simulation results

In Appendix 20 the first simulation results can be seen. From those results can be concluded that a 2D simulation underestimates the air temperature significantly. Adjustments like changing the underrelaxation factors or lowering the gravitational constant did not increase the convergence of the model. In this subparagraph the results for the three special simulations (no ventilation boxes, heat exchange, and time step size) are treated and the results of the calibration simulations are shown, with a comparison to the measurements.

Special simulations

With a 2D simulation is assessed what the influence of the ventilation boxes is on the air flow in the room. The results are shown in figure 5.12 and it turned out that from a distance of one meter from the window the results are comparable for both cases. Only the air velocity differs close to the ventilation boxes.

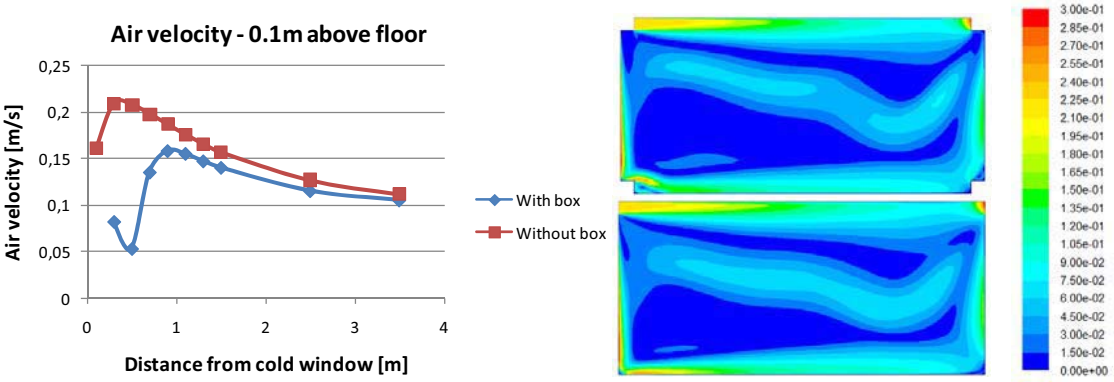

Figure 5.12 Comparison between a case with and without ventilation boxes (air velocity; m/s)

Also the heat exchange is researched. In Fluent, a surface can be given a temperature, heat transfer coefficient (with temperature) or heat flux. In one simulation all methods are applied to the floor and compared to each other and to measurements in the climate chamber. The results are shown in figure 5.13. The air temperature is better predicted with a heat flux, while the air velocity in that case is slightly overestimated.

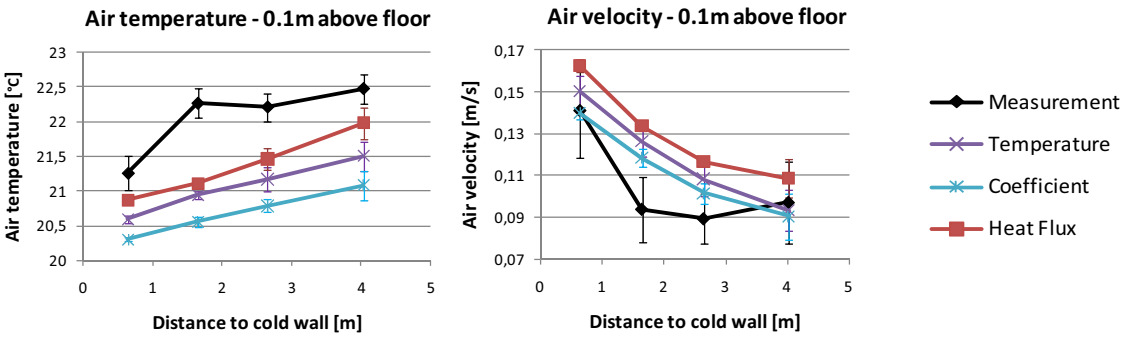

Figure 5.13 Heat exchange of the floor, compared with measurements

The other special simulation focuses on the time step size. Three simulations with time step sizes of 0.5sec, 1.0sec, and 1.5sec are performed with 10 iterations. This is done, because time step size is also a discretization parameter in those natural convection simulations. The results are shown in figure 5.14. The stability of air velocity is not influenced by time step size and the results do also not differ. Only the convergence of the residuals improves slightly when a smaller time step is used. The same results can be observed regarding the number of iterations, as shown by Van Harten (2011).

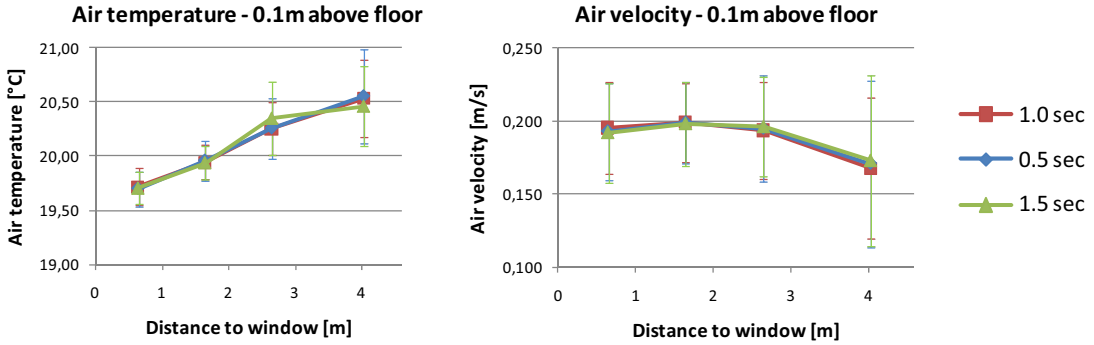

Figure 5.14 Effect of time step size on the air temperature and velocity

Calibration simulations

The input parameters for the calibration simulations are explained in paragraph 5.2.2. From the performed Case II simulations can be seen that they follow the measurement data quite well (figure 5.15). Also the difference between a compensated empty model, an empty model with a UDF and a model with a human being is very small.

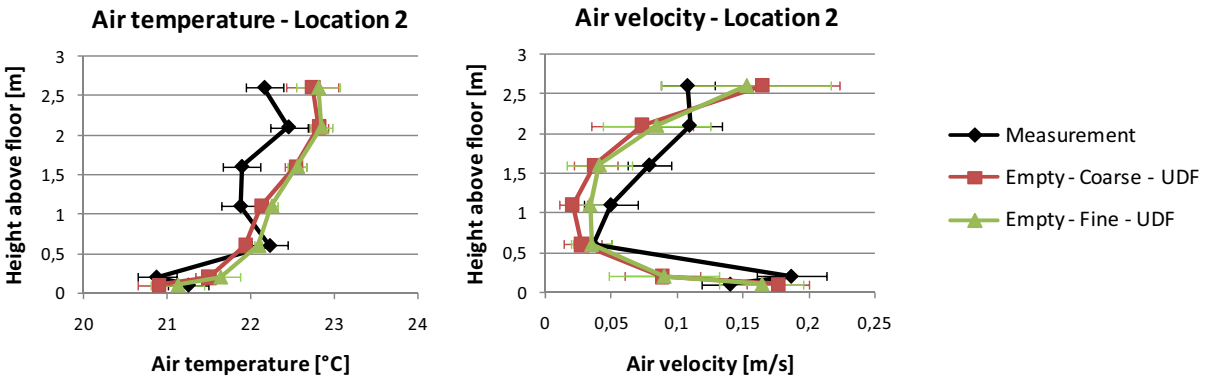

Figure 5.15 Comparison between the measured and simulated Case D

The only problem in all simulations is the convergence. Although a heat balance has been obtained, the residuals only converged to 10^{-3}(epsilon) and 10^{-7}(energy). Also the monitoring points are not stable. Figure 5.16 shows the results of a movie of the air velocity in the vertical cross section of the room. It becomes clear that the inlet disturbs the air flow in the room. Therefore, also a simulation without ventilation is performed. Those results can be seen in figure 5.17. The convergence of the model improved to 10^{-5} for the residuals of the epsilon and to a stable air velocity at the monitoring point. The results in figure 5.18 show that when no ventilation is implemented in the model the air temperature rises and the air velocity decreases at the top of the room, but the amount of downdraught is not affected by the ventilation. As a result, it is decided to perform all Case I calibration simulations without ventilation because the focus in this project is on downdraught.

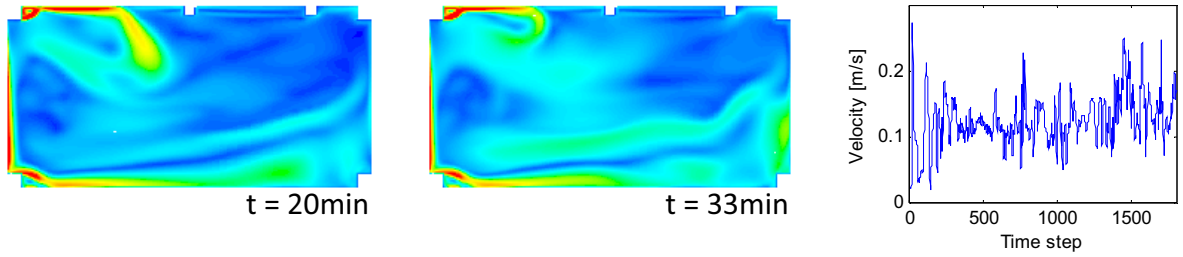

Figure 5.16 Two movie timeslots and the convergence of a monitoring point with ventilation

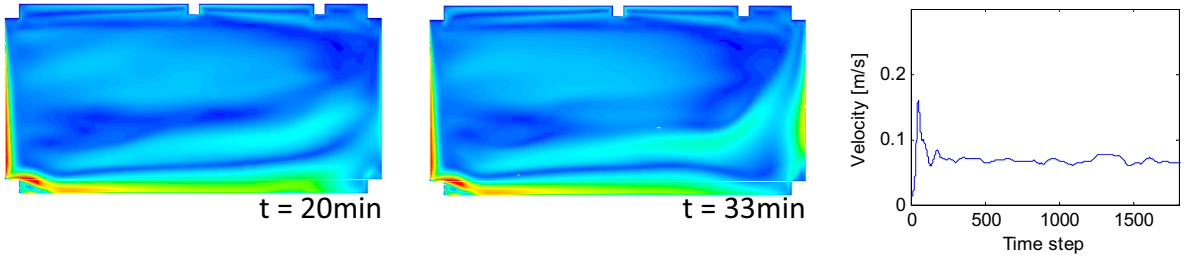

Figure 5.17 Two movie timeslots and the convergence of a monitoring point without ventilation

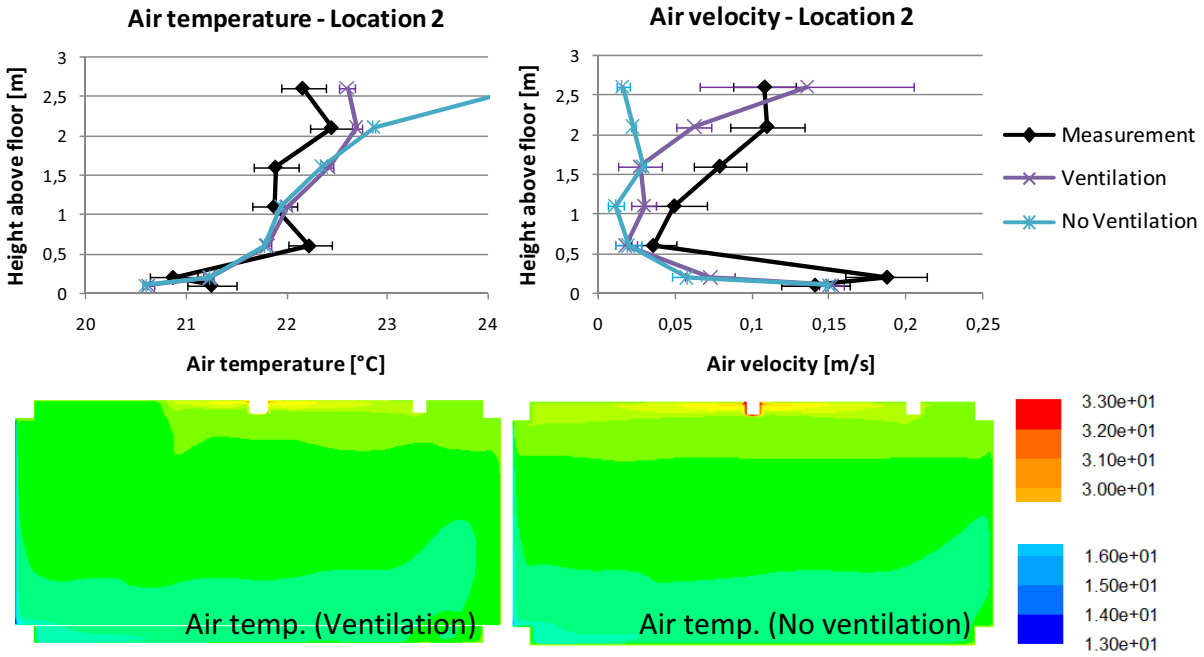

Figure 5.18 Comparison between simulations with and without ventilation

In table 5.6 the performed Case I simulations are shown and from all those simulations the results can be found in Appendix 21. The models are compared (figure 5.19) as well as the measurement and simulation results at every measurement location (1 to 11).

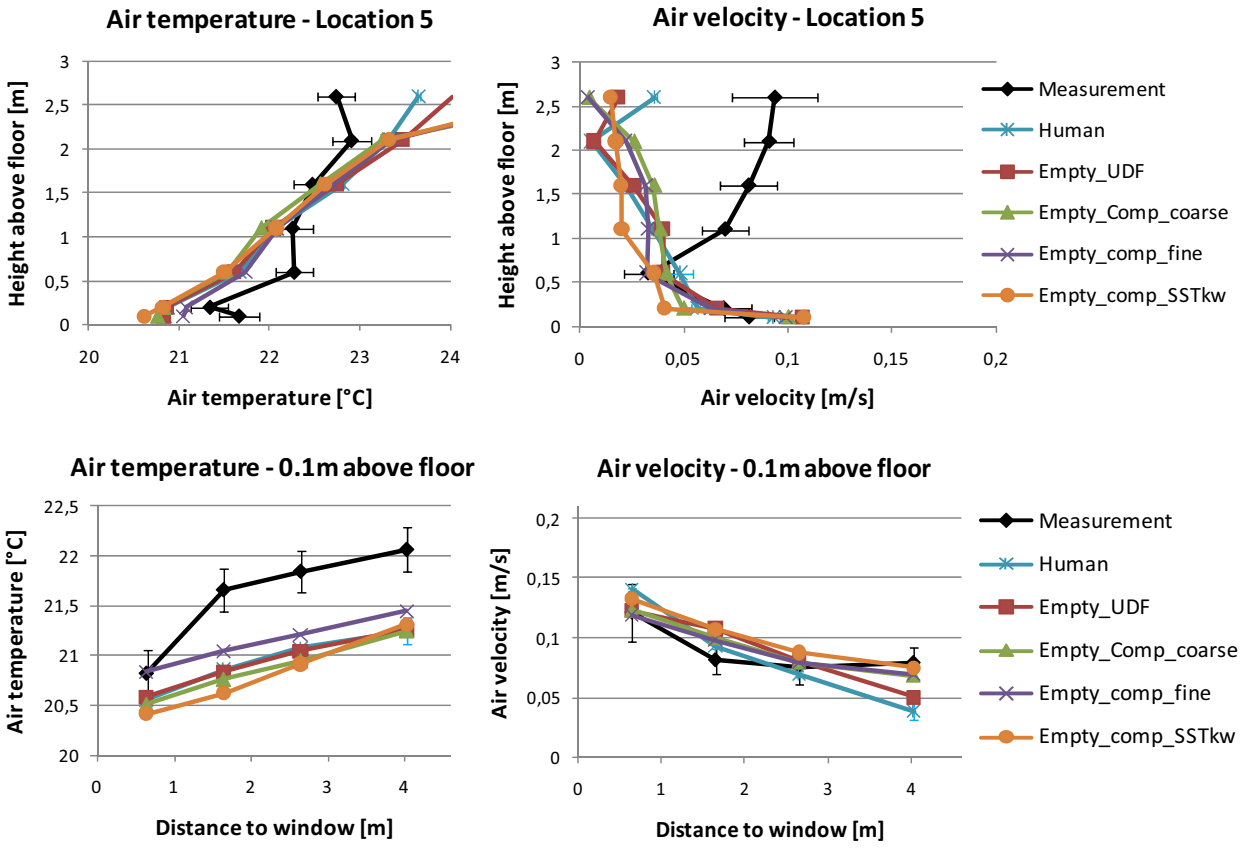

Figure 5.19 Calibration simulation results for two locations - Case I (No ventilation)

From figure 5.19 can be noticed that the difference between all models is very small. Air temperature is well predicted in the room, but less well close to the surfaces. A fine grid predicts the air temperature close to the floor slightly better. Contrary, the air velocity close to the floor is predicted very well, but in the rest of the room it deviates from the measurements due to the applied ventilation in the measurements. However, the simulated air velocity at the lower part of the room agrees with the measurements indicating that downdraught can be predicted with a model without ventilation.

In figure 5.20 the difference between the RNG-kε model and the SST-kω model close to the window (boundary layer) can be seen. The SST-kω model predicts the trend better, while the RNG-kε model is closer to the measured values.

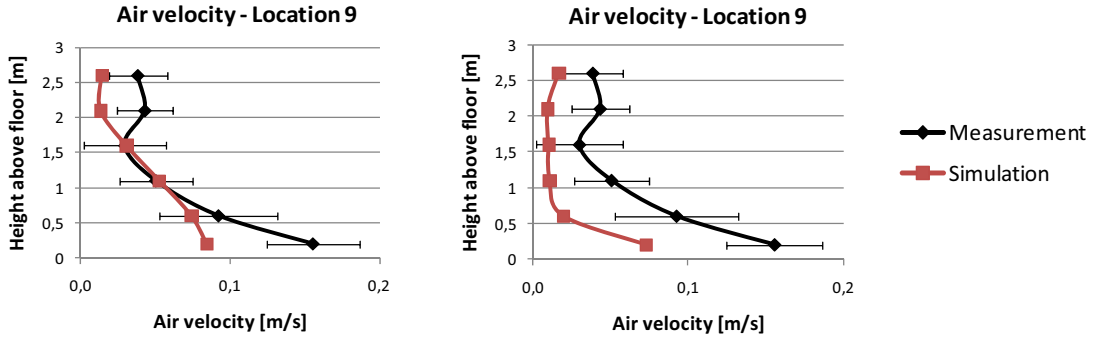

Figure 5.20 Results at location 9 of the RNG-kε model (left) and SST-kω model (right)

All cases are converged to 10^{-5} (epsilon), the monitoring points are stable, and a heat balance is obtained. The largest deviation in the heat balance is found in the case with a UDF. The most stable solution is found for the empty model with a fine grid and also in the simulation with the SST-kω model.

5.4 Discussion and conclusion

In this final paragraph the calibration and simulation results are discussed and a conclusion regarding the CFD model for the variant study is drawn.

Discussion

The CFD model of the climate chamber can be calibrated by air temperature and air velocity measurements. Air velocities below 0.05 m/s and above 1.0 m/s are not used because those are outside the measurement range of the Dantec. However, the air velocity of the downdraught flow is inside the range and can be used for calibration. The inlet velocity is above 1.0 m/s, but in the simulations 1.0 m/s is used because the influence on downdraught and the heat balance is considered very low. Additionally, during Case II the free floating wall temperature keeps decreasing, but very slowly with a maximum of 0.5°C over the whole case. In the CFD simulations the mean surface temperature of the case is used. The results also showed that measurements in the climate chamber can be reproduced.

In the CFD simulations, downdraught is unaffected by the ventilation system because the inlet temperature is close to room air temperature. In the model without ventilation both the airflow stability and convergence improved. However, it has to be borne in mind this is not realistic in practice. Based on these results, two new measurements can be proposed. First, to perform a correct calibration study, the calibration measurements should also be done without ventilation. In this calibration study is therefore focused on the obtained downdraught results. Second, it has to be discovered by a measurement period longer than five minutes whether fluctuations always occur in enclosed environments with low air velocities or this is due to the ventilation system. Research by Rees et al. (2001) indicates that with a gravity current from the inlet and buoyant plumes, complex quasi periodic fluctuations in the room can be observed.

Although differences in air velocity between an obstructed and free flow are measured, those did not appear in the simulation results. The results of all CFD calibration simulations are also comparable. For that reason, for the variant study an empty model is used to lower the number of cells and related computational time. With the CFD outcome the human response can be simulated using ThermoSEM. In the variants no compensation is needed, because the model is not compared to one with a human being present.
Literature shows that it is difficult to simulate natural convection flows (downdraught). The question is whether RANS is the right method to solve a natural convection problem or Large Eddy Simulation (LES) should be used. In addition, the maximum occurring turbulence intensity in the simulations is 7%, while in the climate chamber at least 20% is measured (based on the calculation method). This influences the outcome of for example the Draught Rate. Next to that, it is better to give the floor a heat flux instead of a fixed temperature, but it is hard to calculate this for the variants due to the unknown temperature difference. For that reason all walls are given a fixed temperature. In the end, the RNG k-ε model is used, because close to the walls this model is slightly better and the results in the room are comparable to the SST k-ω model.

Conclusion

Finally, the relevant research questions will be answered. First the definition of downdraught is given, followed by an overview of the simulation model that is going to be used for the variant study of next chapter.

- *How can downdraught be defined in terms of air velocity, air direction, air temperature, turbulence intensity and other parameters?*

From the measurements can be concluded that downdraught can be defined as increased air velocity and decreased air temperature close to the floor due to natural convection from a cold surface. The cold air starts moving downwards close to the cold wall until it reaches the floor and continues horizontally. The air velocity decreases with distance to the cold wall.

- *How accurate can downdraught cases be predicted with CFD?*

When only downdraught is considered, it can often be predicted within the inaccuracy of a measurement instrument. The only limitation is the heat transfer close to surfaces, resulting in lower simulated temperatures close to the floor compared to measurements. The results show that downdraught is not influenced by ventilation (as applied in the climate chamber) and therefore it can still be assessed by a CFD model without ventilation. Also with settings like a 1.0 second time step with 10 iterations, downdraught can be simulated correctly. In table 5.7 the final model that is going to be used during the variant study is explained.

Table 5.7 CFD model for the variant study

Parameter	Input
Model	3D empty
Grid	Coarse
Model specialties	No ventilation boxes No lighting equipment
Turbulence model	RNG k-ε
Boundary condition - Walls	Fixed temperature
Boundary condition - Floor	Fixed temperature
Boundary condition - Inlet	Wall (no ventilation)
Solution	Transient; 1.0 sec; 10 iterations

Chapter 6

Simulation of variants

Using the calibrated CFD model, variants can be simulated to assess the air flow and thermal comfort in downdraught situations. In this chapter, the composition of variants is treated as well as the simulation method. The number of variants depends on computational time. The last part of the chapter shows the simulation results followed by a discussion and conclusion.

6.1 Introduction

The interesting parameters during this project are window height, surface temperature, and floor temperature (low temperature heating system). In this introduction, the variables are explained in more detail. Parameters like internal heat loads, furniture, obstacles in a room, or the position of a person are not included in this project.

The conclusion regarding design guidelines will be drawn in the next chapter, but is based on the results explained in this chapter. The relevant research question in this chapter is:

- To what extent is the existing rule of thumb sufficient to predict downdraught

The window height is of special interest, because it is proven that higher windows cause more downdraught. [Jurelionis et al., 2008] Nevertheless, existing downdraught studies only take three meter high windows into account.

In addition, the surface temperature of the window is of importance because the larger the temperature difference between the window and the room air, the more downdraught occurs. [Heiselberg, 1994] The surface temperature depends on the outside temperature and on the U-value (heat transfer) of the glass. Only single glazing results in a surface temperature of 13°C and occurs more often in renovation projects than in new-built projects. It also causes more downdraught than one of 19°C (triple glazing). [Timmers, 2010]

The last parameter to research is floor heating, which is a Low Temperature Heating (LTH) system and saves energy compared to high temperature systems. According to NEN-EN 15377 the maximum allowed floor temperature is 29°C but according to Bruggema (2007) a floor temperature of 26°C is more realistic. Local denser floor heating will be studied as well. This is only allowed one meter from the window with a maximum temperature of 35°C.

Finally, the window frame is a variable of special interest. According to Heiselberg (1995) the structural system can contribute to a better indoor climate. One case will be simulated with a window frame to show the effect. A separate study is needed to investigate this further.

6.2 Methodology

Variants are composed based on the parameters described above. Due to time restrictions, the number of variants is limited. In this paragraph the variants, the comparison, but also the simulation method are treated shortly.

6.2.1 Cases

With the variables, eight variants are composed, as shown in table 6.1. The basic assumption during designing the variants is a constant temperature difference between the indoor air and the window and the floor. As indicated by Bruggema (2007) a realistic indoor air temperature during winter is 21°C. By using the theoretical heat balance (Appendix 1), the temperature of all walls is calculated, except for the window (constant at 13°C, 16°C, or 19°C) and floor (constant at 21°C or 26°C). All calculated values can be found in table 6.2.

Table 6.1 Overview of variants

	Surface temperature [°C]	13°C		16°C		19°C	
	Window height [m]	2.7m	5.4m	2.7m	5.4m	2.7m	5.4m
LTH system	No floor heating	**B**	**5**		**3**		**1**
	Floor heating	**A**	**4**		**2**		
	Local floor heating		**6**				

Besides the eight variants, two extra interesting cases are composed. First a window height of three stories (8.1 meter) is researched next to the 2.7 meter and 5.4 meter. Also the effect of an obstacle (20 cm) halfway a window of 5.4 m is assessed. According to Heiselberg (1995) this should improve the comfort conditions in the room. For all variants, the PMV and operative temperature are calculated as shown in table 6.2.

Table 6.2 Overview of variants

Var.	Room dimensions	Window temperature	Floor temperature	Wall temperature	PMV / Operative temp.
A	**5.4 x 3.6 x 2.7 m³**	**13°C**	**26.0°C**	19.6°C	0.06 / 21.3°C
B	**5.4 x 3.6 x 2.7 m³**	**13°C**	**21.0°C**	23.0°C	-0.02 / 21.0°C
1	**5.4 x 3.6 x 5.4 m³**	**19°C**	**21.0 °C**	21.6°C	-0.03 / 20.9°C
2	**5.4 x 3.6 x 5.4 m³**	**16°C**	**26.0°C**	20.3°C	0.11 / 21.5°C
3	**5.4 x 3.6 x 5.4 m³**	**16°C**	**21.0°C**	22.4°C	-0.03 / 20.9°C
4	**5.4 x 3.6 x 5.4 m³**	**13°C**	**26.0°C**	20.8°C	0.10 / 21.5°C
5	**5.4 x 3.6 x 5.4 m³**	**13°C**	**21.0°C**	23.2°C	-0.01 / 21.0°C
6	**5.4 x 3.6 x 5.4 m³**	**13°C**	**26°C+30°C**	20.6°C	-0.01 / 21.0°C
Ex1	**5.4 x 3.6 x 8.1 m³** Window height	**13°C**	**21.0°C**	23.3°C	-0.01 / 21.0°C
Ex2	**5.4 x 3.6 x 5.4 m³** Obstacle	**13°C**	**21.0°C**	23.2°C	-0.01 / 21.0°C

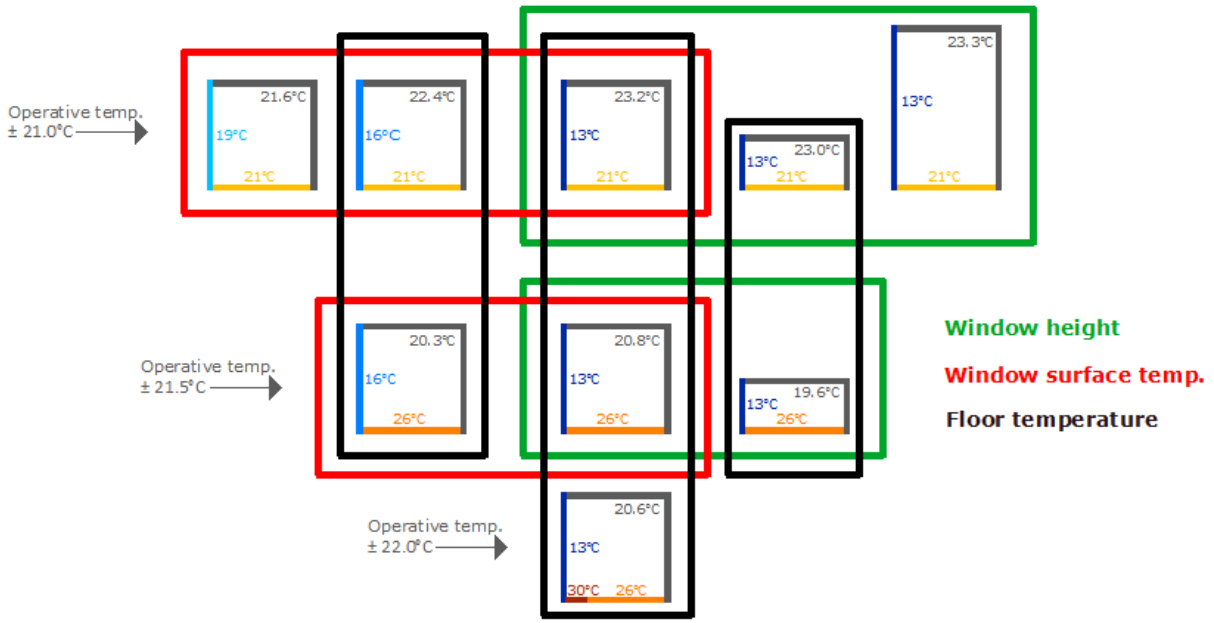

Figure 6.1 Comparison of variants, also on thermal comfort

In figure 6.1 a schematic cross section of all variants can be seen, as well as the way of comparing the variants in terms of window height, window surface temperature, and floor temperature. To draw conclusions about thermal comfort under different conditions the cases with an operative temperature of 21.5°C are going to be used. The PMV of all cases is between -0.03 and 0.21 which corresponds to a PPD smaller than 5% according to Fanger.

6.2.2 Simulation model

To obtain the simulation model for the variant study, the climate chamber model is only increased in height. The same grid is used with ten cells added at the x-axis close to the window. Furthermore, the ventilation boxes and light beams are removed. The grid for the different variants can be seen in figure 6.2.

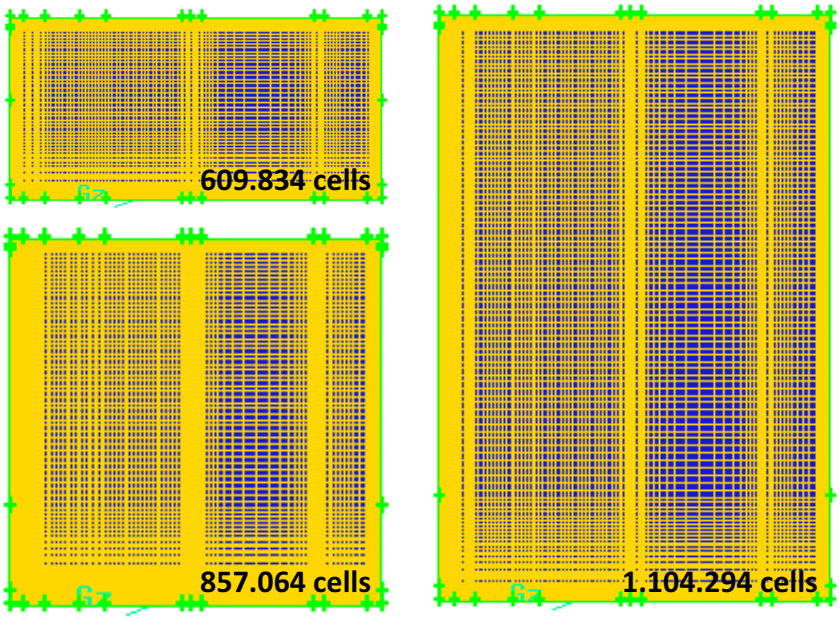

Figure 6.2 Different CFD models for the variant study (one, two and three stories)

To assess the performance of the new CFD model compared to the climate chamber model, three simulations are performed with the same boundary conditions of Variant A. The results are shown in figure 6.3. As can be noticed, air temperature and air velocity in the room are comparable, except for the region close to the floor. This can be explained by the presence of the ventilation boxes in the climate chamber model. The RNG-kε model predicts the air flow better close to the walls and this model is used during the variant study. It is also observed that the boundary conditions influence the stability of the simulation. When the (during calibration) stable climate chamber model is used for Variant A, the model only converges to 10^{-4} (epsilon) and the air velocity keeps fluctuating.

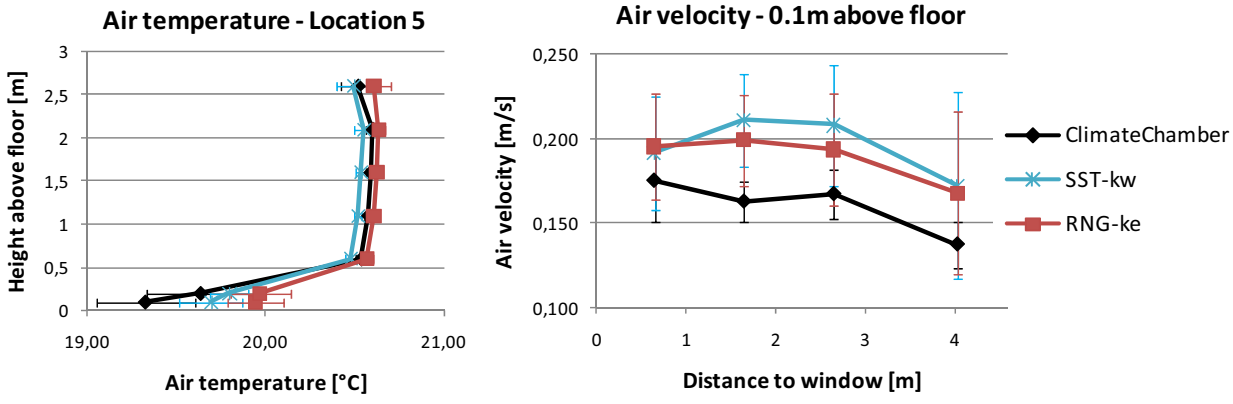

Figure 6.3 Simulation results of Variant A (climate chamber model and new variants model)

The same Fluent settings are used as during the calibration simulations, but this time with different boundary conditions of the variants. As indicated before, the RNG-kε model with enhanced wall treatment is applied. In total, 2700 time steps of 1.0 second with 10 iterations are used to obtain the simulation results. But because of the fluctuating results, also data sampling for time statistics is activated in Fluent.

6.3 Results

In this paragraph the simulation results are treated. The air flow pattern is shown as well as thermal comfort, based on ISO 7730. Additionally, the rule of the thumb is compared to the CFD outcome, eventually to answer the research question.

6.3.1 Simulation results – Air flow pattern

The variants are compared in three ways: window height, window surface temperature and floor temperature. For comparison, air temperature and air velocity are processed only at the height positions and floor positions shown in figure 6.4.

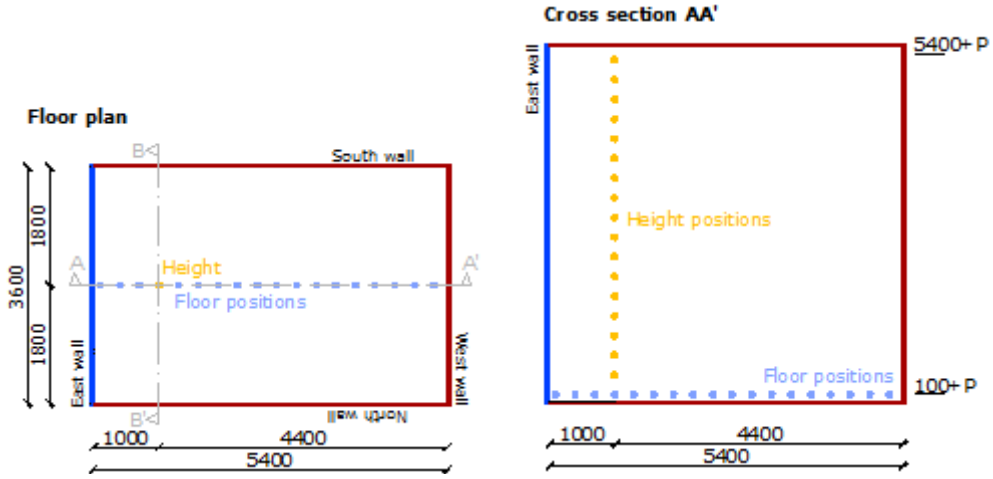

Figure 6.4 Positions at which air temperature and air velocity data is gathered

In Appendix 22 the simulation results for every case can be found. This paragraph mainly focuses on the occurring air velocity close to the floor. The biggest difference in results can be observed between the variants with a different floor temperature. Some of the air temperature and air velocity cross sections (AA') are shown in figure 6.5 en figure 6.6. All figures have the same scale (air temperature 16 °C - 22 °C and air velocity 0 m/s - 0.35 m/s)

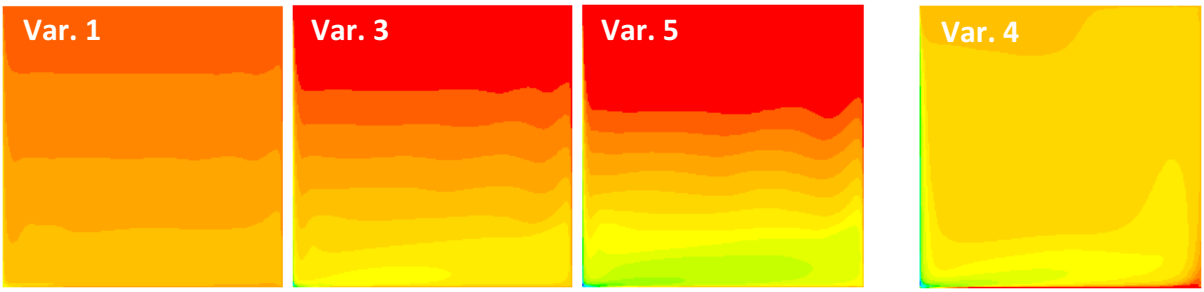

Figure 6.5 Air temperature distribution (three times 21°C floor temp. and one time 26°C floor temp.)

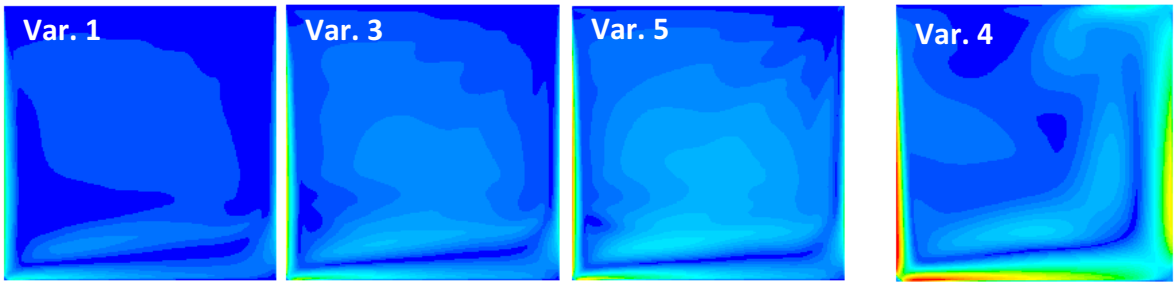

Figure 6.6 Air velocity distribution (three times 21°C floor temp. and one time 26°C floor temp.)

In the graphs of figure 6.7 the air temperature and air velocity are compared for different floor temperatures: variant 4 (26°C), variant 5 (21°C), and variant 6 (26°C+30°C). With floor heating the air temperate gradient is small, indicating more mixing of the air. Nevertheless, the mean air temperature in the room without floor heating is higher than with floor heating. Besides, the air velocity close to the floor is doubled when floor heating is applied.

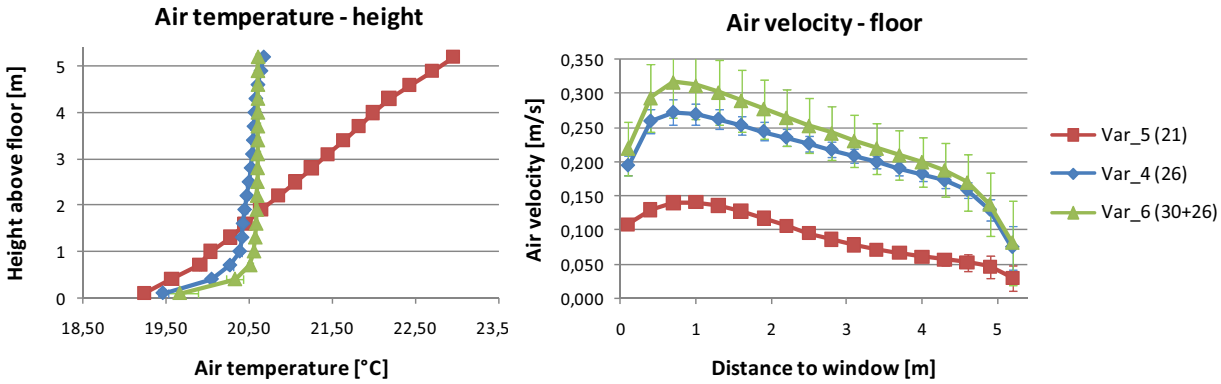

Figure 6.7 Effect of floor temperature (constant window height and window surface temperature)

The flow patterns of variant 4 (26°C) and variant 5 (21°C) are presented in figure 6.8 showing a difference between the cases. With higher floor temperatures the air circulates through the whole room where lower floor temperatures result in more horizontal air flows. This can explain the temperature gradient as found in figure 6.7.

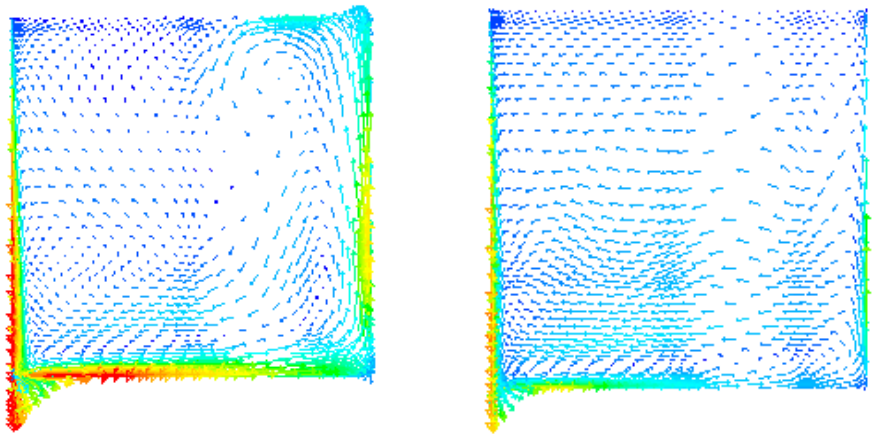

Figure 6.8 Flow pattern of Variant 4 (left) and Variant 5 (right)

The window surface temperature also influences the air flow in the room. In figure 6.9 can be seen that with a 19°C window (variant 1) no downdraught occurs. The coldest window of 13°C (variant 5) causes the most downdraught. In that case, the lowest air temperature and highest air velocity are found.

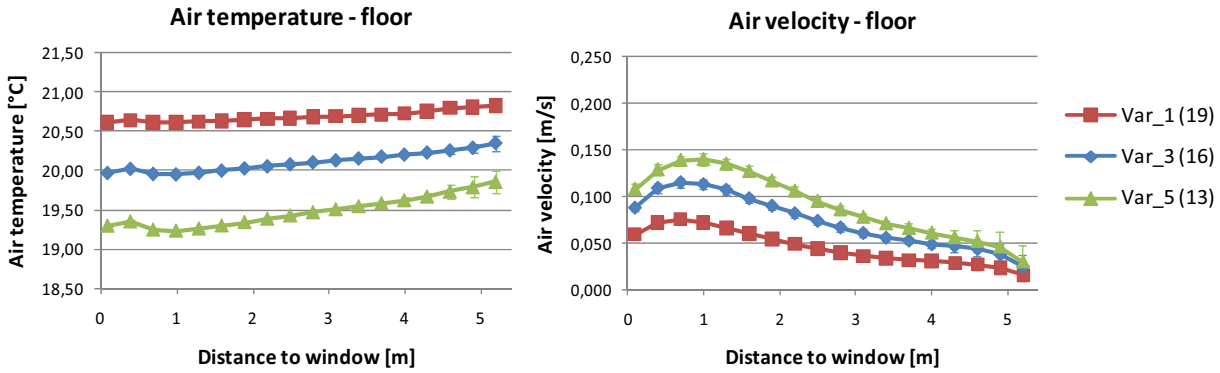

Figure 6.9 Effect of window surface temperature (constant window height and floor temperature)

Like the window surface temperature, also the window height increases the amount of downdraught. As shown in figure 6.10 the highest window of 8.1 meters causes the highest air velocity close to the floor. The maximum air velocity also occurs around one meter from the cold window.

Finally, one variant is researched with an obstacle. It turned out that the flow returns to the cold wall (coanda effect) and does not influence the amount of downdraught (see figure 6.10). Even with an obstacle of 40 centimeters the flow does not separate from the obstacle.

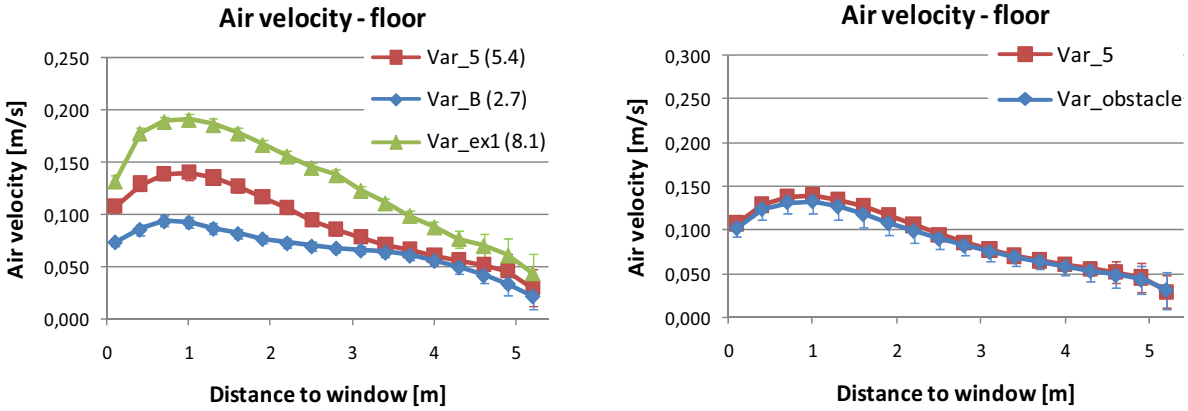

Figure 6.10 Effect of window height (left) and effect of an obstacle (right) on air velocity

6.3.2 Simulation results – Thermal comfort

All variants are assessed by ISO 7730. The whole body comfort index is calculated, as well as the local comfort indices (PD due to draught, temperature gradient, floor temperature, and radiation asymmetry). The Draught Rate is also considered for the area around the feet.

Furthermore, four variants (number 1, 4, 5 and 6) are assessed by ThermoSEM and the Comfort Zones graph to indicate the performance of the model in the different cases.

In table 6.2 the mean percentages dissatisfied for the room are shown. The variants with floor heating and related increased air velocity also have a higher percentage dissatisfied due to draught. The cases with a lower floor temperature have a higher PMV value, because the mean air temperature in the room is higher compared to the floor heating cases. According to the given limits in ISO 7730 all variants are comfortable, except when the maximum occurring Draught Rate is considered. The variants have an operative temperature around 21.0°C, which is also allowed by ISO 7730.

Table 6.2 Percentage dissatisfied due to whole body and local thermal discomfort

Var.	PMV	PPD	Draught Rate			Temp. gradient	Floor temp.	Radiation asymm.
			Mean	– Max.	– Ankles			
A	0.27	5.2%	5.0%	**32.2%**	14.8%	0.2%	6.8%	0.8%
B	0.38	5.4%	0.0%	**25.4%**	6.4%	0.1%	7.1%	1.1%
1	0.42	5.5%	0.0%	13.4%	3.8%	0.2%	7.1%	0.2%
2	0.32	5.2%	4.9%	**28.3%**	17.8%	0.2%	6.8%	0.5%
3	0.37	5.3%	0.0%	**21.9%**	8.8%	0.2%	7.1%	0.6%
4	0.26	5.2%	6.1%	**39.0%**	19.8%	0.1%	6.8%	1.0%
5	0.31	5.2%	2.4%	**31.0%**	11.8%	0.1%	7.1%	1.3%
6	0.33	5.3%	7.0%	**42.1%**	**23.1%**	0.1%	6.8%	0.7%
Ex1	0.29	5.2%	3.7%	**34.7%**	14.9%	0.1%	7.1%	1.3%
Ex2	0.34	5.3%	0.0%	**31.3%**	12.1%	0.1%	7.1%	1.3%

Figure 6.11 shows the Draught Rate for cross section AA' of Variant 4 (floor 26°C) and Variant 5 (floor 21°C). From the results can be seen that the risks with floor heating are higher than without floor heating. However, the area of risk is limited to the floor. In the rest of the room the percentages remain below 10%, see also Appendix 22.

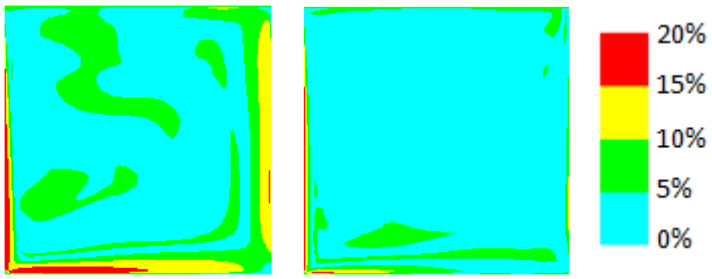

Figure 6.11 Draught Rate of Variant 4 and Variant 5

At last, the variants are simulated with ThermoSEM. The skin temperatures are unaffected by a cold window of 13.0°C. In the floor heating cases, the skin and equivalent temperatures are lower due to the increased air velocity and lower mean air temperature.
In figure 6.12 the Comfort Zones graphs of variant 1 (window of 19°C), variant 4 (window of 13°C and floor of 26°C), variant 5 (floor of 21°C), variant 6 (floor of 26°C+30°C) are shown. The comfort line differs for all cases, mainly for the feet and arms. The line of variant 1, having a window of 19°C and low air velocities, is fluctuating less than the more extreme variants. Nevertheless, all cases are predicted comfortable.

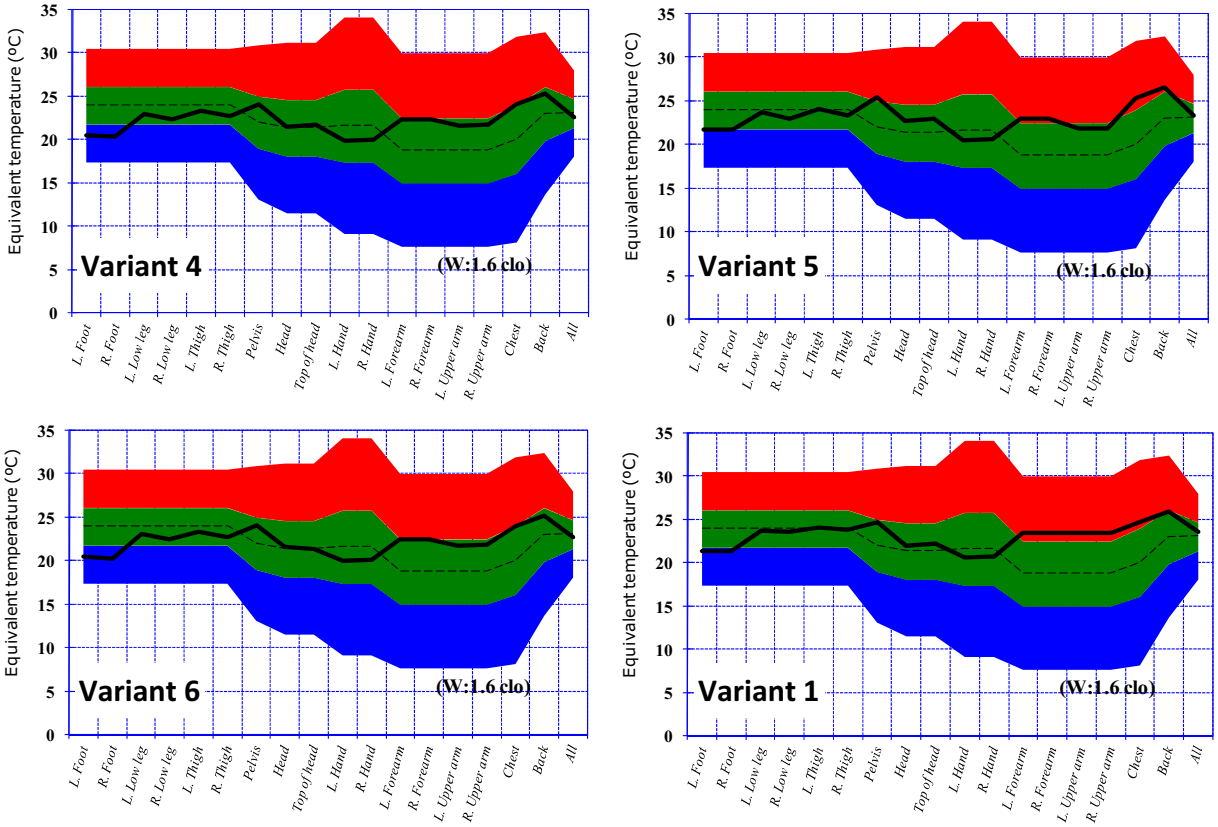

Figure 6.12 Comfort Zones Graph for four different variants

6.3.3 Rule of thumb

Finally, the existing rule of thumb of Olesen (1995) is applied to the cases. The rule of thumb, with a maximum allowed air velocity of 0.18 m/s, is:

- $U_{glass} \cdot h \leq 4.7$ with $U_{glass} = \frac{T_{air} - T_{surface}}{4.08}$

It is assessed whether the situation is allowed based on the rule of thumb. The results can be found in table 6.3, in which also the maximum occurring air velocity in the room is given.

Table 6.3 Results of the Rule of Thumb

Variant	$U_{glass} \cdot h$	Allowed	Max. Air velocity
A	4.9	No	0.33 m/s
B	5.3	No	0.26 m/s
1	2.7	Yes	0.18 m/s
2	6.0	No	0.34 m/s
3	6.6	No	0.26 m/s
4	9.5	No	0.42 m/s
5	10.4	No	0.33 m/s
6	9.7	No	0.45 m/s
Ex1	15.6	No	0.38 m/s
Ex2	10.4 / 5.3	No	0.33 m/s

With the rule of thumb, only variant 1 (window of 19°C) is allowed. The outcome of the rule of thumb is lower in the floor heating cases, indicating a better situation compared to cases without floor heating. However, the air velocity in those cases is higher. The contrast can be explained by the smaller temperature difference between the air and the surface in case of floor heating, which indicates less downdraught according to the rule of thumb.

6.4 Discussion and conclusion

The simulation results of the variants will be discussed in this paragraph, including the related comfort prediction. To conclude, the relevant research question about the rule of thumb will be answered.

Discussion

From the simulation results, parameters for design guidelines to prevent downdraught can be obtained. Window height and surface temperature influence downdraught, and the parameters are also implemented in the rule of thumb. The effect of floor temperature is not included, but proves to influence the air flow pattern in the room. A warm floor (+5°C) increases the maximum air velocity close to the floor by a factor two due to buoyant forces. Lower floor temperatures result in more horizontal flows that can explain the temperature gradient. However, in none of the existing downdraught studies, like those of Jurelionis et al. (2008) or Manz et al. (2003) floor temperature is studied. Furthermore, the floor heating variants have wall temperatures lower than room air temperature (cooling walls with max. $\Delta T = 0.9$°C) and the variants with a floor of 21.0°C have warmer walls compared to the room air (heating walls with max. $\Delta T = 2.5$°C) to obtain a heat balance. Even though this difference, the “cooling walls” do not result in extra downdraught and the air flow at these walls is still upwards. However, the wall temperature can influence the air flow in the rest of the room. The effect of floor heating on air flow is only researched by simulations and not available in literature. It is recommended to research this by means of experiments.
The effect of an obstacle is unobserved in this project, because the flow reattached to the surface. It can be useful to research this behavior to find a solution where the flow does not reattach. [Heiselberg et al., 1995] [Rueegg et al., 2001]

The calibrated CFD model without ventilation is used for the variant study because of its computational stability. However, in the cases with “cooling walls” the air velocity and air temperature keep fluctuating and the results have a larger inaccuracy than the “heating wall” cases. The wall temperatures also influence the convergence and stability in natural convection cases. A possible improvement can be the grid size because during calibration the RNG k-ε model performs slightly better with a fine grid, as shown in Chapter 5.
In all simulations a heat balance is obtained, but it differs from the theoretical balance. The CFD model can be improved in terms of heat release, because the heat flux from the floor was half the theoretical value. However, in the variants still an increase in air temperature above the floor can be noticed.

The variants also have to be assessed on thermal comfort level. The Comfort Zones graphs show differences between the variants, but the reliability is still undetermined (Chapter 4).
As shown in Chapter 4, ISO 7730 is found sufficient for downdraught situations. Using the limits of ISO 7730, all variants are comfortable. On the other hand, according to the rule of thumb all variants (except Variant 1) have a severe downdraught risk. This is based on the maximum occurring air velocity, which is in some variants around 0.45 m/s. However, these air velocities only occur within one meter from the window at floor level and decrease rapidly by distance. When the maximum occurring Draught Rate is considered, the same comfort prediction can be observed as with the rule of thumb, only Variant 1 with the 19°C window is comfortable (maximum Draught Rate < 20%). This method is very conservative, and perhaps it is better to look at the Draught Rate around the feet, to locate the problem. The remark is that the Draught Rate is designed for draught at the neck and therefore overestimates the Percentage Dissatisfied due to draught at foot level. Finally, the rule of thumb and the maximum Draught Rate show a different trend. Considering the rule of thumb, the temperature difference between the room and the glass surface decreases with floor heating (in the variants) indicating a lower maximum air velocity and a better situation. However, the Draught Rate predicts a higher PD in the floor heating variants. The effect of the heating system on the air flow pattern has to be included in the rule of thumb.

Conclusion

In the next chapter the composition of design guidelines related to downdraught will be explained. Based on the simulation results, important parameters are: window height, temperature difference between the window and indoor air, but also floor temperature. An increase in window height or a decrease in surface temperature results in higher air velocities close to the floor. However, the conclusion in this chapter only focuses on the existing rule of thumb and the related (thermal comfort) assessment.

- *To what extent is the existing rule of thumb sufficient to predict downdraught*

Together with the results of ISO 7730 and the subject results, it can be concluded that the rule of thumb is very conservative: when a situation is allowed by the rule of thumb, ISO 7730 and also the maximum Draught Rate are always allowing the situation. The rule of thumb is the most stringent measure for the situation. According to the rule of thumb, the climate chamber cases also had a downdraught risk ($2.1 \cdot 2.3 > 4.7$) but the subjects had no complaints due to radiation or increased air velocity around the feet.
The used limit in the rule of thumb (maximum of 0.18 m/s, no matter where it occurs) can be changed to prevent overdesigning because of fear for downdraught. The parameters in the rule of thumb influence downdraught, but also floor heating increases the air velocity close to the floor, which is not included in the rule of thumb.

Part IV

Practical applicability

The community Eindhoven has the ambition to be a zero-energy city by 2040. To achieve that ambition the existing buildings have to be renovated, but it is also important to maintain or create a comfortable indoor environment. Design guidelines to prevent downdraught can contribute to this. In this part of the report the possible design guidelines are composed and the link between the design guidelines and sustainability is given.

Chapter 7

Design Guidelines

Composing design guidelines needs elaborate research. Based on the available time and the number of variants in this project, no complete design guidelines can be created. The start in the first paragraph can be extended during future research. In the second paragraph is explained how the outcome of this research (design guidelines to prevent downdraught) can contribute to the zero-energy city ambition.

7.1 Possible design guidelines

In this paragraph the composition of possible design guidelines is shown. First is started with important parameters followed by a thermal comfort assessment. It is important that design guidelines are easy to use.

Parameters

An existing rule of thumb is still in use by engineers ($U_{glass} \cdot h \leq 4.7$). Based on the rule of thumb and the results in this project, the parameters that need to be included in the design guidelines can be indicated:

- Window height
- Indoor air temperature
- Window surface temperature
- Floor temperature

Assessment

With design guidelines it is desired to indicate whether a situation is acceptable or not. In the rule of thumb a maximum occurring air velocity of 0.18 m/s is allowed, but as explained in Chapter 6 it turned out to be conservative in downdraught prediction. More research is needed on the acceptability of air velocities.

For the possible design guidelines in this project, the Draught Rate and the mean air velocity around the feet at one meter from the window are calculated. This way, the maximum air velocity is excluded from the design guidelines, but the possible problem area is included (start of the living area and around the ankles). Also the PMV-model is used as assessment.

Design guidelines

The design guidelines are created in the form of graphs, with above parameters and assessment methods. The used data can be found in table 7.1.

Table 7.1 Data for composition of design guidelines

Var.	Window height	Window temp.	Floor temp.	ΔT	Air temp.	DR feet	v_{mean} feet
A	**2.7 m**	**13°C**	**26°C**	13°C	20.4°C	14.8 %	0.20 m/s
B	**2.7 m**	**13°C**	**21°C**	8°C	21.0°C	6.4 %	0.09 m/s
1	**5.4 m**	**19°C**	**21°C**	2°C	21.0°C	3.8 %	0.07 m/s
2	**5.4 m**	**16°C**	**26°C**	10°C	20.6°C	17.8 %	0.25 m/s
3	**5.4 m**	**16°C**	**21°C**	5°C	21.0°C	8.8 %	0.12 m/s
4	**5.4 m**	**13°C**	**26°C**	13°C	20.2°C	19.8 %	0.26 m/s
5	**5.4 m**	**13°C**	**21°C**	8°C	20.9°C	11.8 %	0.15 m/s
6	**5.4 m**	**13°C**	**26°C+30°C**	13.7°C	20.3°C	23.1 %	0.31 m/s
Ex1	**8.1 m**	**13°C**	**21°C**	8°C	20.9°C	14.9 %	0.19 m/s

The graphs are composed for an indoor air temperature of 20°C - 21°C, because in all simulation variants this temperature occurred. The temperature difference between floor and window is plotted against the assessment method. A linear correlation can be found between the data points of a 5.4m window. The other heights only have one or two simulation variants and are shown as points. A trend line is drawn as the design guideline, see figure 7.1 as an example. With the PMV no linear correlation can be found.

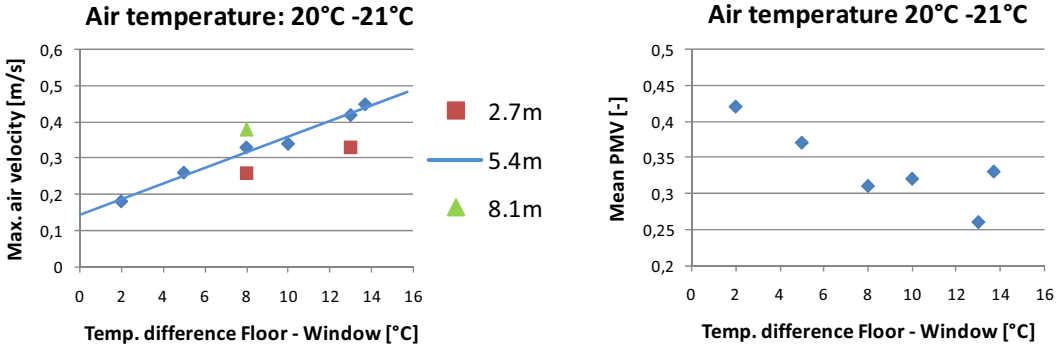

Figure 7.1 Composition of Design Guidelines & Non-linearity of the PMV

Two possible design guidelines for the mean air velocity and the mean Draught Rate around the feet are created with the data obtained in this project. Those are shown in figure 7.2.

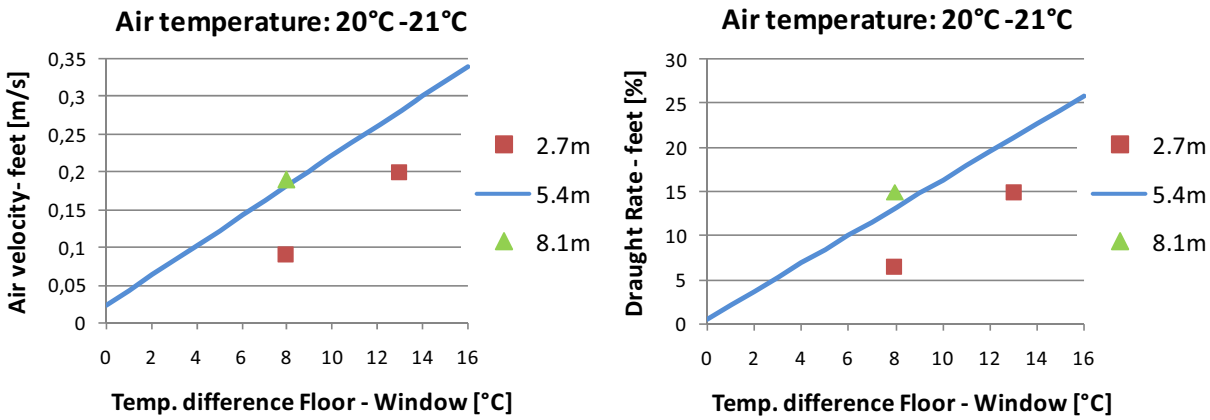

Figure 7.2 Design Guidelines based on mean air velocity and the Draught Rate around the feet

Future research

As indicated before, an easy to use equation or graph is needed. Therefore a surface plot can be very helpful in composing design guidelines. A surface plot of the rule of thumb is shown in figure 7.3. Too little data is obtained in this project to compose surface plots and it is not clear what is acceptable or not in downdraught situations. An example of a surface plot for future research can also be seen in figure 7.3.

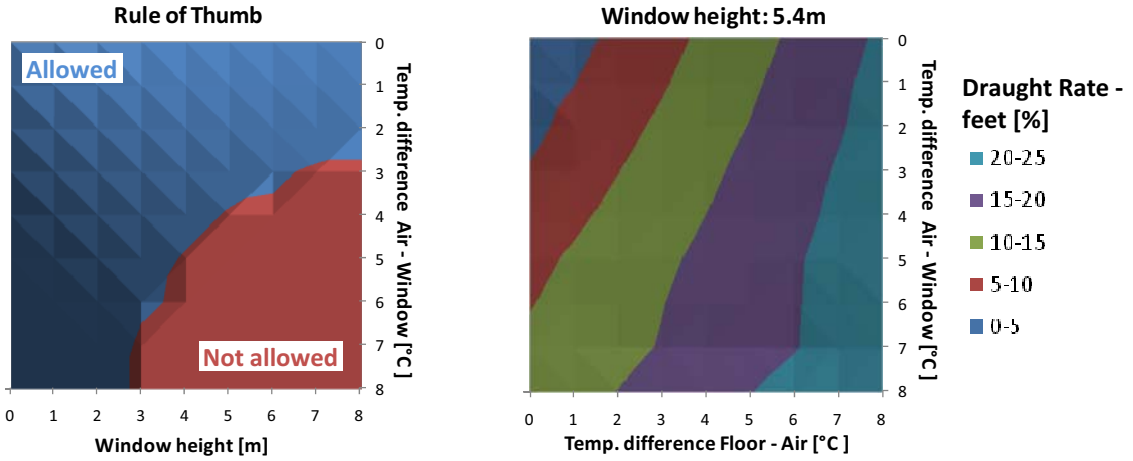

Figure 7.3 Surface plot of rule of thumb (left) and an EXAMPLE (right, not based on data)

7.2 Zero-energy city

Brainport, a region in Eindhoven, has the ambition to be a zero-energy region in 2040. The net energy use over the course of one year is zero: no more gas and electricity is used than generated by (local) sustainable sources. By a “Smart Grid” the energy is distributed to the users where it is used as efficient as possible. This project contributes to the last part. With design guidelines it must be prevented that designers put unnecessary heating elements in a building while still maintaining a comfortable indoor climate.

The buildings in the region have to be renovated to reach the goal of a zero-energy region. In renovation projects often single glazing is replaced by double glazing, but still (high temp.) radiators or convectors are placed beneath the window because of fear for downdraught. However, in this research no thermal comfort problems rise with a window of 13°C without radiators. Besides, Timmers (2010) showed that a 13°C window only occurs during 4% of the year with single glazing. It is expected that with double glazing in the Dutch climate no problems rise related to downdraught. It has to be noticed that also natural ventilation or air infiltration can cause draught complaints, but this is not researched during this project.

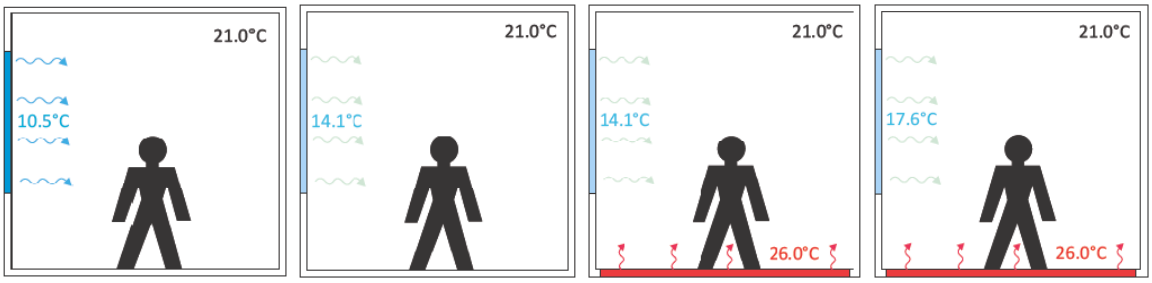

Figure 7.4 Examples of single glazing, double glazing and triple glazing with floor heating

Four examples with single (U = 5.7 W/m²K), double (U = 2.8 W/m²K), and triple (U = 1.1 W/m²K) glazing are shown in figure 7.4. An outdoor design temperature of -7.0°C is assumed and an indoor air temperature of 21.0°C. In two cases floor heating is take into account. The outcome of the composed design guidelines (figure 7.2) can be found in table 7.2.

Table 7.2 Outcome Design Guidelines (considering 5.4m window)

Variant	ΔT floor -window	Air velocity - feet	Draught Rate - feet
Single glazing	10.5 °C	0.23 m/s	17.2 %
Double glazing	6.9 °C	0.16 m/s	11.6 %
Double glazing - floor heating	11.9 °C	0.26 m/s	19.5 %
Triple glazing - floor heating	8.4 °C	0.18 m/s	14.2 %

Based on the Draught Rate around the feet, the high temperature heating systems can be removed below the window. Even with single glazing, no problems regarding downdraught occur. This way, energy and materials can be saved. However, heating systems are needed in dwellings to create a comfortable indoor environment (during winter). When chosen for low temperature systems, like floor heating, the downdraught flow can be become worse and almost reach the limit of a maximum Draught Rate of 20% (set by ISO 7730).
When the maximum allowed air velocity of the rule of thumb is considered (0.18 m/s) two cases are allowed: double glazing without floor heating or triple glazing with floor heating. This is based on the design guidelines for 5.4 meter high windows and with lower windows in dwellings both values will decrease. It can be concluded that energy and materials can be saved in the built environment (dwellings) by not fearing downdraught.

Part V
Conclusion

The focus in this research is on downdraught and effective measures to assure thermal comfort near glass façades. Measurements and simulations are done and the results are shown in the report. In this final part, the project is discussed with focus on downdraught and the conclusions regarding the main research questions are drawn. Finally, recommendations for future research are given.

Chapter 8
Discussion

In the discussion is focused on the different parts of the project. First is started with the main research objective: composition of design guidelines. This is followed by a discussion of the applied methods, consisting of measurements in the climate chamber, validation of thermal comfort models and calibration of the CFD model.

Design guidelines / Rule of thumb

A rule of thumb to prevent downdraught ($U_{glass} \cdot h \leq 4.7$) is still in use by engineers. Based on the results in this project, the rule of thumb is conservative, meaning that when a situation is allowed by the rule of thumb, ISO 7730 and the Comfort Zones graphs always predict a comfortable indoor environment. Also with the experimental subjects no problems related to downdraught occurred, although the rule of thumb indicated a downdraught risk. The rule of thumb is conservative because a maximum allowed air velocity is used as assessment, no matter where it occurs. Compared to the maximum Draught Rate in the downdraught flow the same comfort prediction is done. Compared with the rule of thumb the trend differs from that of the Draught Rate. In the floor heating cases, with increased air velocities at floor level, the Draught Rate becomes worse, while with the rule of thumb the situation improves. This indicates that the effect the floor temperature on downdraught is not correctly implemented in the rule of thumb.

For this reason, a start is made on the composition of new, possible design guidelines to prevent downdraught. The main parameters are window height, indoor air temperature, window surface temperature, and floor temperature. Also an assessment method is needed

to indicate whether a situation is acceptable, but more research is needed on that subject. For the design guidelines in this research is chosen to look at the mean Draught Rate and mean air velocity around the feet (one meter from the window and 0.1 meter above the floor). This way, the effect of a maximum occurring air velocity is excluded. With data obtained in the variant study, two possible guidelines to prevent downdraught are created. However, in this research is shown that many additional simulations are needed to compose design guidelines.

CFD simulations

To simulate the variants for the design guidelines, a calibrated CFD model is used. The model of the climate chamber is calibrated with air temperature and air velocity measurements. The results of all CFD calibration simulations, for example an empty room and with a person included, are comparable and follow the trend of the measurements.

In the climate chamber simulations with ventilation included, a transient flow occurred (fluctuating air velocities and air temperatures in time). Whether this is due to the simulation model or also happens in the climate chamber is unknown. At each position, only five minutes is measured and a longer measurement period is recommended. Research by Rees et al. (2001) indicates that with a gravity current from the inlet and buoyant plumes, complex quasi periodic fluctuations in the room can be observed. The stability and convergence of the model improved by removing the ventilation and the amount of downdraught is unaffected by that change since the inlet temperature is close to room air temperature. Therefore, the variants are simulated without ventilation. Two remarks are that ventilation will always influence the air flow pattern in the whole room and in practice a room without ventilation is not realistic.

With the variant study, parameters in design guidelines can be researched. From the results can be noticed that floor heating increases the air velocity in the downdraught flow. This can be accounted to the buoyant forces resulting from the warm floor. In addition, in the variant study the wall temperatures differ to obtain a heat balance and this can influence the air flow in the room. At least, it influences the transient behavior and convergence of the model. It is preferred to research the effect of floor heating by experiments, because in this project only simulations are used and the effect is not treated in literature.

Validation of thermal comfort models

As indicated before, a thermal comfort assessment is needed to compose design guidelines. For the researched downdraught cases, ISO 7730 with the PMV model of Fanger is the best prediction model. In Case II the Actual Mean Votes (AMV) are often lower than in Case I and in the statistical analysis the skin temperatures are also lower in Case II. The subjects are probably still being cooled by the cold wall over the course of four hours, indicating that time plays a role in thermal comfort prediction due to radiation asymmetry. Also the local thermal comfort models of ISO 7730 are assessed. However, the outcome of the local

thermal discomfort models is a percentage dissatisfied and this is hard to validate with a sample size of ten men. In this study, the Predicted Percentage Dissatisfied was low and also a low number of people voted for an uncomfortable situation. Next to that, it has to be researched what level of Draught Rate or air velocity can still be noticed around the feet, assuming socks, shoes, and trousers are worn during winter.

In ISO 7730, limits for every discomfort parameter are given. But according to Olesen and Parsons (2002) it is unclear how to predict thermal comfort in combined non-uniform situations. They also showed there is no method for combining the percentages dissatisfied people due to whole body and local comfort. Future research is recommended on this topic.

In case of the Comfort Zones graph it is possible to look at the effect of local stimuli which is an advantage regarding the Standards (ISO 7730). Nevertheless, an equivalent temperature is needed for every body part, based on a difficult calculation method. With the outcome the thermophysiological model ThermoSEM, these equivalent temperatures can be calculated. The model simulates the skin temperatures correctly within a RMS of 1.8°C and shows good results for downdraught situations. However, the calculated equivalent temperatures do not correspond to the voted comfort (around neutral) by the subjects.

Climate chamber measurements

The climate chamber is used for experimental subjects and calibration measurements. Two cases are designed, which differed only slightly due to two shortcomings of the climate chamber. Besides the aquifer system no additional cooling is present and not each wall can be given its own temperature. Despite these shortcomings, downdraught is measured in both cases with increased air velocity and decreased air temperature close to the floor.

According to the subjects no thermal comfort problems occur in case of a cold wall of 13°C and an indoor temperature of 22°C. It was not possible to indicate relations between body parts and whole body thermal sensation with the obtained data. This does not mean that those relations do not exist. Zhang et al. (2010-part II) observed a dominant influence of the back, chest, and pelvis on thermal sensation. In addition, Zhang et al. (2004) reported that overall thermal state of the body influences the sensitivity to local thermal stimuli.

During the calibration measurements for the simulation model it was found that the Dantecs are not sensitive to detect low air velocities (<0.05 m/s). In a natural convection case air velocities below the limit can occur. For CFD calibration those low air velocity regions should be measured, but such low air velocities will not play a role in thermal comfort prediction.

Chapter 9

Conclusion

Only the main three research questions are answered in this chapter, based on the results of all parts of the project. Every sub question is answered in Part II to Part IV.

- *What is the definition of downdraught?*

Downdraught can be defined as increased air velocity and decreased air temperature close to the floor due to natural convection from a cold surface. The cold air accelerates downwards close to the cold wall until it reaches the floor and enters the living area. The air velocity decreases with distance to the cold wall. An increased floor temperature increases the air velocities and decreases the vertical temperature gradient in the room.
It can be concluded that in the climate chamber with a cold wall (13.0°C), an air temperature between 22.0°C-22.5°C and a mean radiant temperature in the range of 21.0°C-21.5°C is accepted by the experimental subjects, positioned one meter from the window during a four hour exposure. Within this timeframe, it indicates that problems regarding downdraught are more related to draught which can increase due to window height than to radiation asymmetry (ΔT_{pr} = 6.0°C). However, in this study also no complaints occur due to draught (maximum air velocity 0.2 m/s around the feet). An increased floor temperature did not change the Thermal Sensation (neutral) and Thermal Comfort (comfortable) votes.

- *How can thermal comfort in relation to downdraught be predicted correctly?*

Based on the subject results can be concluded that the whole body stays comfortable, while some body parts like feet and hands are sometimes uncomfortable. Also a relation between thermal sensation and comfort is noticed. When thermal sensation moves to neutral, comfort increases. Comfort decreases when thermal sensation moves away from neutral. When thermal sensation remains constant, thermal comfort also remains constant.
The relevant, existing thermal comfort models for downdraught situations are ISO 7730 and the Comfort Zones graph of Nilsson. In the Comfort Zones graph comfort is assessed by the equivalent temperatures of 17 body parts. This way, it is also possible to look at the effect of local stimuli which is an advantage regarding the Standards. However, it is difficult to calculate the correct equivalent temperatures with environmental parameters. It has to be concluded that the method looks promising, but needs more research before it can be applied in the built environment. On the other hand, the PMV model of Fanger (ISO 7730) is a good predictor of whole body comfort in the researched cases. Also the local thermal comfort equations predicted comfortable cases, like the subjects voted. Within this project ISO 7730 has been used to assess variants for composing design guidelines.

- *What are possible design guidelines to predict downdraught?*

In this project downdraught variants are simulated with CFD. No ventilation is present in the CFD model, because the amount of downdraught is not influenced by ventilation (as applied in the climate chamber) while the model performance increases.
With the simulation results from the variants, important parameters for design guidelines can be indicated. Those are the same parameters as used in the rule of thumb: window height and the temperature difference between indoor air and the window. An increase in window height and temperature difference results in higher air velocities close to the floor. The heating system is an additional parameter. Floor heating increases the air velocity close

to the floor, which is not included in the rule of thumb. According to the rule of thumb, the situation with floor heating becomes better, but with the Draught Rate it becomes worse. From the results in this study it can be concluded that the rule of thumb is conservative. This is because it uses a maximum allowed air velocity, independent of its location.
With the (low) number of variants it is not possible to create full design guidelines. However, a start is made in Chapter 7 with inclusion of the floor temperature. More research is needed on a correct thermal comfort assessment method. In this project a graph is made for one indoor air temperature, which relates the window height and temperature difference between the floor and the window to a mean Draught Rate around the feet.

- *Overall conclusion*

No problems regarding downdraught (natural convection from a cold vertical surface) exist in a standard office, based on the experimental subject results. By not fearing downdraught, energy and materials can be saved in the built environment (such as dwellings). However, with calibrated CFD simulations it turned out that an increased floor temperature can worsen the occurring downdraught (increased air velocity). This indicates that radiators or convectors cannot simply be replaced by floor heating to prevent downdraught.
The outcome of the PMV model corresponds to the thermal sensation votes of the subjects. ISO 7730 is found best to assess downdraught situations, where the rule of thumb to prevent downdraught is very conservative. More research is needed to find the thermal comfort limit (i.e. maximum air velocity combined with radiation asymmetry) to compose design guidelines. Important parameters for the guidelines are window height, temperature difference between the window and indoor air, and floor temperature. To compose more extended design guidelines more simulation variants are still needed.

Chapter 10
Recommendations

In this final chapter of the report, the most important recommendations for future research are given. The recommendations are related to the thermal comfort and simulation part, both with respect to downdraught.

Thermal comfort

- Future research can focus on thermal comfort in downdraught situations. Until now, it is unclear what a correct thermal comfort limit is for design guidelines. Therefore, it has to be researched what is (un)acceptable in downdraught environments. From this project can be concluded that radiation asymmetry is not the main comfort problem (one meter from a 13°C window with $\Delta T_{air\text{-}window}$ of 9°C did not cause complaints). It can only influence thermal comfort in time because subjects keep cooling down. For that reason, the focus

in future research has to be on air movement. In the conservative rule of thumb one maximum allowed air velocity is used and perhaps that value has to be changed. More research is also needed for the Draught Rate (ISO 7730) and the Comfort Zones graph in downdraught situations.

- When working with subjects, the experiments have to be designed based on the chosen statistical method. It is also suggested to design two cases with one distinct manipulation. The climate chamber is a good facility to do measurements, but can be improved in two ways. The first enhancement is that all walls can be given a different temperature and also an active cooling system is required.
- Finally, in practice complaints related to downdraught exist. With the applied conditions in this project (indoor air temperature of 22°C) no comfort problems occurred according to the subjects. In the simulations the maximum air velocity does not exceed 0.45 m/s and it is questionable whether that local high air velocity is felt, wearing socks and shoes in the winter. Based on the existing complaints it is advisable to research situations in practice. Natural ventilation or other factors can influence the amount of downdraught and additionally thermal discomfort can be additive and raise the number of complaints.

Downdraught prediction (CFD)

- Downdraught can be predicted with CFD simulations and the CFD model can be calibrated with measurements in the climate chamber. Because very low air velocities (< 0.05 m/s) occur in downdraught environments is it advised to use instruments that are able to measure those air velocities. However, for one reason it is recommended to improve the calibration measurements; the CFD simulations showed a transient flow pattern. Whether this is model dependent or the actual occurring air flow can be investigated by a longer measurement period (>5 minutes). In future research, the CFD model can be improved as well because the model performs slightly better with a finer grid and this also influences the heat transfer from the floor.
- With the performed simulations (variant study) important parameters for downdraught prediction are determined. Besides the three parameters in the rule of thumb (air temperature, surface temperature and window height), also floor heating needs to be included in a future design guideline. An example can be found in chapter 7. The effect of the parameters on downdraught is visible from the results, but more simulations are required to compose actual design guidelines.
- In the simulations, the results show an increase in air velocity above the floor when floor heating is applied. Although slightly higher air velocities are measured in the climate chamber cases with an increased floor temperature of 1.2°C, measurements have to be done to validate those CFD variant results. Nevertheless, it is also recommended to measure (the stability of) the air flow under different boundary conditions.
- To finish, the effect of an obstacle like the window frame can be researched in the future. The obstacle assumed in this research did not show any effect. Theoretically it is a possible passive solution to decrease downdraught. [Heiselberg, 1994]

References

Aarts M.P.J., Bakker F.E., Schellen H.L., Hak C.C.J.M.: *Bouwfysisch ontwerpen 1*: Dictation Eindhoven University of Technology (Architecture) 2005;

Arens E., Zhang H.: *The skin's role in human thermoregulation and comfort*: University of California (Berkeley) 2006-1;

ASHRAE: *ASHRAE Handbook of Fundamentals*: American Society of Heating, Refrigerating and Air-conditioning Engineers 2004;

Baarda D.B., de Goede M.P.M.: *Basisboek methoden en technieken:* Wolters-Noordhoff (Groningen) 2006;

Berglund L.G., Fobelets A.P.R.: *Subjective human response to low-level air currents and asymmetric radiation*: ASHREA Transactions 1987; 93(1): 497-523.

Blocken B.: *CFD in building engineering – Fundamentals and applications in urban physics and wind engineering:* University of Technology (Eindhoven) 2008;

Boer T.L.J. den, Zeiler W.: *Transparantie en façade*: TVVL magazine 2008; 37(5): 4-13.

Bruggema H.M.: *Vergelijking van systemen: Betonkernactivering, klimaatplafonds, wand- en vloerverwarming*: TVVL magazine 2007; (3): 20-28.

deDear R.J., Arens E., Zhang H., Oguro M.: *Convective and radiative heat transfer coefficients for individual human body segments*: Int J Biometeorol 1997; 40: 141-156.

deDear R.J.: *Revisiting an old hypothesis of human thermal perception: alliesthesia:* Building Research and Information 2011; 39: 108-117

Eijdems H.H.E.W., Boerstra A.C., Op 't Veld P.J.M.: *Low temperature heating systems – Impact on IAQ, thermal comfort and energy consumption*: unpublished.

Fanger P.O.: *Thermal comfort: analysis and applications in environmental engineering*: Danish Technical Press 1970;

Fiala D.: *Dynamische Simulation des menschlichen Wärmehaushalts und der thermischen Behaglichkeit*: De Montfort University (Leicester) 1998;

Fiala D., Lomas K.J., Stohrer M.: *A computer model of human thermoregulation for a wide range of environmental conditions: the passive system*: Journal of Appl. Physiol 1999; 87: 1957-1972.

Field A.: *Discovering statistics using SPSS:* SAGE publication (London) 2009;

Fobelets A.P.R., Berglund L.G.: *Subjective human response to low-level air currents and asymmetric radiation*: ASHREA Transactions 1987; 93(1): 497-523.

Grant: *Temperature and humidity probes:* Grant data logging (Cambridge);

Griefahn B., Künemund C., Gehring U.: *Evaluation of draught in the workplace*: Ergonomics 2002; 45(2): 124-135.

Harten M. van: *Natuurlijke ventilatie toevoer in combinatie met een laag temperatuur verwarmingssysteem – de invloed van gecombineerde niet-uniforme omgevingscondities op het thermisch comfort and thermofysiologische respons:* University of Technology (Eindhoven) 2011;

Heijst G.J.F. van: *Fysische Transportverschijnselen voor W*: University of Technology (Eindhoven) 2007;

Heiselberg P.: *Draught risk from cold vertical surfaces*: Building and Environment 1994; 29(3): 297-301.

Heiselberg P., Overby H., Bjorn E.: *Energy-efficient measures to avoid downdraft from large glazed façades*: ASHREA Transactions 1995; 1127-1135.

Hensel H.: *Thermoreception and temperature regulation*: Academic Press (London) 1981;

de Heus P., van der Leeden R., Gazendam B.: *Toegepaste data-analyse*: Reed Business (The Hague) 2008;

Hsieh K.J., Lien F.S.: *Numerical modeling of buoyancy-driven turbulent flows in enclosures*: International Journal of Heat and Fluid Flow 2004; 25: 659-670

Huizenga C., Zhang H., Mattelaer P., Yu T., Arens E.: *Window performance for human thermal comfort*: University of California (Berkeley) 2006;

ISO/DIS 14505: *Ergonomics of the thermal environment – Evaluation of thermal environment in vehicles. Part 2: Determination of Equivalent temperature*: International Standards Organization (2005);

ISO/DIS 14505: *Ergonomics of the thermal environment – Evaluation of thermal environment in vehicles. Part 4: Determination of Equivalent temperature by means of a numerical manikin*: International Standards Organization (2005);

ISO 7726: *Ergonomics of the thermal environment – Instruments for measuring physical quantities*: International Standards Organization (2001);

ISO 7730: *Ergonomics of the thermal environment – Analytical determination and interpretation of thermal comfort using calculation of the PMV and PPD indices and local thermal comfort criteria*: International Standards Organization (2005);

ISO 9886: *Ergonomics – Evaluation of thermal strain by physiological measurements:* International Standards Organization (2004);

ISO 9920: *Ergonomics of the thermal environment – Estimation of thermal insulation and water vapour resistance of a clothing ensemble:* International Standards Organization (2009);

Jurelionis A., Isevicius E.: *CFD predictions of indoor air movement induced by cold window surfaces*: Journal of civil engineering and management 2008; 14(1): 29-38.

Lohman T.G., Roche A.F., Martorell R.: *Anthropometric standardization reference manual:* Human Kinetics book (Champaign) 1988;

Loomans M.G.L.C.: *Thermisch gedreven stromingen – Simulaties en metingen:* University of Technology (Eindhoven) 1994;

Loomans M.G.L.C.: *The measurement and simulation of indoor air flow*: University of Technology (Eindhoven) 1998;

Loomans M.G.L.C., van Schijndel A.W.M.: *Simulation and measurement of the stationary and transient characteristics of the hot sphere anemometer:* Building and Environment 2002; 37: 153-163.

Manz H.: *Numerical simulation of heat transfer by natural convection in cavities of façade elements:* Energy and Buildings 2003; 35: 305-311.

Manz H., Frank T.: *Analysis of thermal comfort near cold vertical surfaces by means of computational fluid dynamics*: Indoor and Built Environment 2003; 13: 233-242.

Marken-Lichtenbelt W.D. van, Frijns A.J.H., Fiala D., Janssen F.E.M., Ooijen A.M.J. van, Steenhoven A.A. van: *Effect of individual characteristics on a mathematical model of human thermoregulation*: Journal of Thermal Biology 2004; 29: 577-581.

Marken-Lichtenbelt W.D. van, Frijns A.J.H., Ooijen M.J. van, Fiala D., Kester A.M., Steenhoven A.A. van: *Validation of an individualised model of human thermoregulation for predicting responses to cold air*: Int J Biometeorol 2007; 51: 169-179.

Montgomery D.C., Runger G.C., Hubele N.F.: *Engineering statistics:* John Wiley & Sons, Inc. (Arizona) 2004;
Neale A.: *A study in computational fluid dynamics for the determination of convective heat and vapour transfer coefficients:* Concordia University (Montreal) 2006;

NEN-EN 1264-2: *Water based surface embedded heating and cooling systems - part 2: floor heating:* European Committee for standardization (2008);

NEN-EN 1264-5: *Water based surface embedded heating and cooling systems - part 5: Determination of thermal output:* European Committee for standardization (2008);

NEN-EN 15377-1: *Heating systems in buildings – Design of embedded water based surface heating and cooling systems: part 1:* European Committee for standardization (2008);

Nilsson H.O.: *Comfort climate evaluation with thermal manikin methods and computer simulation models*: Royal Institute of Technology (Sweden) 2004;

Nilsson H.O., Holmer I.: *Comfort climate evaluation with thermal manikin methods and computer simulation models*: Indoor Air 2003; 13: 8-37.

Olesen B.W.: *Vereinfachte Methode zur Vorausberechnung des thermischen Raumklimas*: HLH 1995; 46(4): 219-225.

OIesen B.W., Parsons K.C.: *Introduction to thermal comfort standards and to the proposed new version of EN ISO 7730*: Energy and Buildings 2002; 34: 537-548.

Parsons K.C.: *Human thermal environments: the effects of hot, moderate, and cold environments on human health, comfort, and performance*: Taylor and Francis (London) 2003;

Prendergast E., Leij H. v.d.: *Bouwkundige compensatie koudeval – Klimaatkameronderzoek naar het beperken van tocht met bouwkundige maatregelen*: Mobius consult 2004;

Rees S.J., McGuirk J.J., Haves P.: *Numerical investigation of transient buoyant flow in a room with displacement ventilation and chilled ceiling system:* International Journal of Heat and Mass Transfer 2001; 44: 3067-3080.

Richter W.: *Handbuch der thermischen Bahaglichkeit*: Bundesanstalt für Arbeitsschutz und Arbeidsmedizin 2003;

Rueegg T., Dorer V., Steinemann U.: *Must cold air down draughts be compensated when using highly insulating windows?*: Energy and Buildings 2001; 33: 489-493.

Schellen L.: *De invloed van een dynamisch binnenklimaat op thermisch comfort en productiviteit*: Eindhoven University of Technology 2007;

Schellen L., Loomans M., van Marken Lichtenbelt M., Frijns A., de Wit M.: *Assessment of thermal comfort in relation to applied low exergy system*: Proceedings Windsor (2010)

Sensor data bv.*: NTC thermistors: type DC95:* Sensor data bv (Rijswijk);

Stamou A., Katsiris I.: *Verification of a CFD model for indoor airflow and heat transfer:* Building and Environment 2006; 41: 1171-1181.

Timmers S.: *Thermische comfortindicatoren voor niet-uniforme omgevingscondities vaststellen en beoordelen*: Eindhoven University of Technology 2008;

Timmers S., *Design guidelines to prevent downdraught – part 1*: Technische Universiteit Eindhoven (2010);

Toftum J.: *Human response to combined indoor environment exposures*: Energy and Buildings 2002; 34: 601-606.

Toftum J., Nielsen R.: *Draught sensitivity is influenced by general thermal sensation*: International Journal of Industrial Ergonomics 1996-2; 18: 295-305.

Topp C., Nielen P.V., Sorensen D.N.: *Application of computer simulated persons in indoor environmental modeling:* ASHRAE Transactions 2002; 1084-1089.

Vries G. de , Silvester S.: *Bewonerservaring Lage Temperatuursystemen*: V&L Consultants 2000;

Wang D., Zhang H., Arens E., Huizenga C.: *Observations of upper-extremity skin temperature and corresponding overall-body thermal sensations and comfort:* Building and Environment 2007; 42: 3933-3943.

West B.T., Welch K.B., Galecki A.T., Gillespie B.W.: *Linear mixed model: a practical guide using statistical software:* Chapman & Hall (London) 2007.

Zhang H., Huizenga C., Arens E., Wang D.: *Thermal sensation and comfort in transient non-uniform thermal environments*: Journal of Appl. Physiol 2004; 92: 728-733.

Zhang H., Arens E., Huizenga C., Han T.: *Thermal sensation and comfort models for non-uniform and transient environments: Part 2: Local comfort of individual body parts*: Building and Environment 2010; 45: 389-398.

Zhang Z., Zhang W., Zhai Z.J., Chen Q.Y.: *Evaluation of various turbulence models in predicting airflow and turbulence in enclosed environments by CFD, Part 2:* HVAC&R research 2007; 13 (6): 871-886.

Nomenclature

A_D	Dubios surface area of the human body	[m²]
A_{glass}	Glass surface	[m²]
C	Convective heat exchange	[W/m²]
g	Gravitational constant (9,81)	[m/s²]
h	Height of the window / glass surface	[m]
h_c	Convective heat transfer coefficient	[W/m²°C]
h_r	Radiation heat transfer coefficient	[W/m²°C]
I_{cl}	Clothing insulation	[clo]
k	Turbulent kinetic energy	[m²/s²]
M	Metabolic rate	[W/m²]
Nu	Nusselt number	[-]
Q	Total heat loss	[W/m²]
R	Radiation heat exchange	[W/m²]
Re	Reynolds number	[-]
ΔT	Temperature difference indoor air – glass surface	[°C]
$\Delta T_{a,v}$	Temperature difference between head and feet	[°C]
ΔT_{pr}	Plane Radiant Temperature difference	[°C]
T_{air}	Air temperature close to the human being	[°C]
T_{eq}	Equivalent temperature	[°C]
T_f	Minimum temperature above the floor	[°C]
T_{fl}	Floor temperature	[°C]
T_{in}	Indoor air temperature	[°C]
T_o	Operative temperature	[°C]
T_{out}	Outside temperature	[°C]
T_r	Radiant temperature close to the human being	[°C]
T_{skin}	Skin (surface) temperature	[°C]
t_a	Ambient air temperature	[°C]
t_r	Mean radiant temperature	[°C]
t_s	Surface temperature	[°C]
t_{sk}	Mean skin (surface) temperature	[°C]
TU	Turbulence intensity	[%]
U_{frame}	Heat transfer coefficient of the frame	[W/m²K]
U_{glass}	Heat transfer coefficient of the glass	[W/m²K]
U_{window}	Heat transfer coefficient of the window	[W/m²K]

v_a	Air velocity (close to the human being)	[m/s]
v_{max}	Maximum air velocity	[m/s]
W	External work	[W/m²]
x	Distance from the cold surface	[m]
y^+	Dimensionless wall co-ordinate	[-]
δ	Boundary layer thickness	[m]
ε	Turbulence dissipation rate	[m²/s³]
ν	Kinematic molecular viscosity	[m²/s]
ω	Turbulence frequency	[rad/s]
ρ_T	Density at temperature T	[kg/m³]
σ	Stefan-Boltzmann constant ($5.67 \cdot 10^{-8}$)	[W/m²K]

Appendices